

**A strategy to optimize the arrangement of
multiple floating net cage farms to efficiently
accommodate dissolved nitrogenous wastes**

*Dissertation zur Erlangung des Doktorgrades
der Mathematisch-Naturwissenschaftlichen Fakultät
der Christian-Albrechts-Universität zu Kiel*

Vorgelegt von:

Simon Adriaan van der Wulp

Kiel, February 2015

**A strategy to optimize the arrangement of
multiple floating net cage farms to efficiently
accommodate dissolved nitrogenous wastes**

*Dissertation zur Erlangung des Doktorgrades
der Mathematisch-Naturwissenschaftlichen Fakultät
der Christian-Albrechts-Universität zu Kiel*

Vorgelegt von:

Simon Adriaan van der Wulp

Kiel, February 2015

Erste Gutachter

Prof. Dr. Roberto Mayerle

Zweite Gutachter

Prof. Dr. Federico Foders

Tag der mündlichen Prüfung: 26th of February 2014

Zum Druck genehmigt: 19^h of February 2015

gez.

Prof. Dr. Wolfgang J. Duschl, Dekan

To Collin and Arjen

Table of Contents

Table of Contents	i
List of Figures.....	iii
List of Tables.....	v
Abstract	vii
Kurzfassung	ix
Acknowledgements.....	xi
1 Introduction.....	13
1.1 Significance and statement of the problem	13
1.2 Objectives	14
1.3 Outline	14
2 Scientific background	15
3 Study area.....	19
4 Field measurements	23
4.2 Discussion	25
5 Setup of flow and wave models	27
5.1 Introduction.....	27
5.2 Set up of the flow model	27
5.3 Setup of the wave model	31
5.4 Results	32
5.5 Discussion	33
6 Quantifying temporal nitrogenous flux floating net cages	35
6.1 Introduction.....	35
6.2 Fish growth	36
6.3 Feed and nitrogen input	36
6.4 Metabolism, waste feed and nitrogen fluxes.....	37
6.5 Nitrogen flux from floating net cage farms culturing Tiger Grouper	38
6.6 Discussion	40

7	Modelling the fate of dissolved nitrogenous waste from floating net cage fish farms.....	43
7.1	Introduction	43
7.2	Water quality model setup	43
7.3	Water quality sensitivity	47
7.4	The fate of ammonia released from floating net cage farms in Pegametan Bay	51
7.5	Discussion.....	53
8	Physical carrying capacity for floating net cage farms.....	57
8.1	Introduction	57
8.2	Site suitability analysis	57
8.3	Discussion.....	62
9	A best practice strategy to optimize the arrangement of multiple floating net cage farms to efficiently accommodate dissolved nitrogenous wastes	63
9.1	Introduction	63
9.2	Farm placement scenarios	63
9.3	Results.....	66
9.4	Discussion.....	71
10	Environmental carrying capacity.....	73
10.1	Introduction	73
10.2	Determining the environmental carrying capacity	73
10.3	Model simulations	74
10.4	Discussion.....	77
11	Discussion.....	79
11.1	The physical carrying capacity for floating net cage farms.....	79
11.2	Optimizing farm arrangements.....	80
11.3	Environmental carrying capacity.....	82
11.4	Not only dissolved nitrogen	84
12	Conclusions and recommendations.....	85
	References	87
	Appendices.....	95

List of Figures

Figure 3.1. Pegametan Bay, Bali, Indonesia.	20
Figure 3.2. An example of a floating net cage farm as found in Pegametan Bay.....	21
Figure 4.1. Overview of the water sampling locations and points of interest.	23
Figure 4.2. Overview of the observed water levels as logged by the tidal gauge.....	25
Figure 5.1. The Bali Sea and Pegametan Bay model domains.....	28
Figure 5.2. Model sensitivity for a range of Manning bottom roughnesses.....	29
Figure 5.3. Model sensitivity for wind.....	30
Figure 5.4. Comparison of modelled and measured water level within Pegametan Bay	31
Figure 5.5. Simulated flow fields for Pegametan Bay for a period covering one neap-spring- neap tidal cycle.....	32
Figure 5.6. Worst case wave scenario for Pegametan Bay	33
Figure 6.1. Computed and observed growth-curve for cultured Tiger Grouper (<i>E. fuscoguttatus</i>).....	38
Figure 6.2. Calculated feed conversion ratios for cultured Tiger Grouper (<i>E. fuscoguttatus</i>)	39
Figure 6.3. Calculated Nitrogen flux distributed over the various sinks during the various life stages.....	39
Figure 6.4. Total ammonia nitrogen flux per unit farm volume.....	40
Figure 6.5. Approximated 24 hour post feeding nitrogen excretion rates per unit farm volume.....	40
Figure 7.1. A representation of a scaled farm and the corresponding numerical discharge cells.....	45
Figure 7.2. Warm up time of the water quality model	47
Figure 7.3. The effect of various diffusion settings on TAN concentrations	48
Figure 7.4. TAN enhancement effect due to post-feeding discharges.....	48
Figure 7.5. Nitrification fluxes and resulting TAN and NO ₃ -N concentrations for different maximum nitrification rates (K_{20nit}) ranging between 0 and 0.15 mg N l ⁻¹ d ⁻¹	49
Figure 7.6. Water quality model calibration of TAN concentrations.	50
Figure 7.7. Water quality model calibration for nitrate.....	51
Figure 7.8. Simulated TAN and nitrate concentration patterns during neap and spring tides in Pegametan Bay.....	52
Figure 7.9. Cross sections of simulated TAN and nitrate concentration along transect A- A'	53

Figure 8.1. Schematic overview of the site selection process exemplarily for minimum water depth criteria.....	59
Figure 8.2. Suitability maps for the considered parameters.	60
Figure 8.3. Combined suitability maps for floating net cage cultures	61
Figure 9.1: Spatial overviews of tide averaged and depth averaged current velocities (a) and tide averaged Reynolds numbers.	64
Figure 9.2. Scenarios for alternative farm arrangements within the suited domain.	65
Figure 9.3. Distribution patterns of time averaged vertical TAN and nitrate maxima in Pegametan Bay for model scenarios with equal farm sizes but different farm densities.....	67
Figure 9.4. Distribution patterns of time averaged vertical TAN and nitrate maxima in Pegametan Bay for model scenarios with farm sizes normalized according to current velocities at different farm densities.....	68
Figure 9.5. Distribution patterns of time averaged vertical TAN and nitrate maxima in Pegametan Bay for model scenarios with farm sizes normalized according to Reynolds numbers at different farm densities.....	69
Figure 9.6. Comparison of the overall impact of results from the different farm arrangements.	70
Figure 10.1. Carrying capacities for each suited domain according to the 1% nitrogen flux method	74
Figure 10.2. Farm distributions and simulated nutrient gradients for an environmental capacity of 116 tons.....	76
Figure 10.3. Farm distributions and simulated nutrient gradients for an environmental capacity of 161 tons.....	77
Figure 12.1: Assessment diagram to deal with efficiently accommodate dissolved nitrogenous wastes from floating net cage fish farms.	86

List of Tables

Table 4.1. Measured sea surface nitrogen concentrations, for reference and study area stations.....	24
Table 4.2. In situ measurements of sea surface temperatures, dissolved oxygen concentrations and salinity.....	24
Table 6.1. Comparison of calculated relative floating net cage nitrogen flux found by various studies.	41
Table 8.1. Site suitability parameters and criteria for floating net cages.	58

Abstract

Since the early seventies, the development of floating net cage mariculture has been of growing concern with respect to its environmental impacts. Floating net cage maricultures generate considerable amounts of effluent in the form of solids and dissolved nutrients. With the globally intensifying mariculture activities and improving feed technology, the direct release of dissolved nutrients from fish farming becomes of larger importance. However it is seldom taken into consideration during coastal planning procedures.

The present study focuses on impacts of dissolved nutrient loads from floating net cage mariculture. Numerical flow, wave and water quality modelling techniques provided the basis to develop a strategy to optimize the arrangement and sizes of multiple floating net cage farms in order to minimize dissolved nutrient enhancement in the area. Exemplarily, this study was done for Pegametan Bay, Bali, Indonesia.

The physical carrying capacity was determined using key physical parameters from flow and wave model results to identify those areas which provide favourable conditions for the practice of floating net cage farming.

A fish growth and mass balance model was set up to quantify nitrogen flux from Tiger grouper (*Epinephelus Fuscoguttatus*), the predominant reared species, concluding that of the total nitrogen input approximately 37% is excreted in the form of ammonia. Water quality model simulations of existing farms within the study area indicated a sub-optimal farm arrangement with excessive local enhancement of ammonium levels and accumulation of nitrate.

The water quality model was used to perform numerical experiments of alternative farm arrangement scenarios. From the simulated scenarios it was found that through a combination of suitability analysis and scaling of individual farm sizes according to the local dispersive character, defined by the Reynolds number, ammonium concentrations were reduced by 13% and nitrate concentrations were reduced by 41% when compared to a non optimized scenario. Furthermore the impacted area was reduced by up to 48%, relative to non-optimized scenario with identical fish standing stocks.

Even though the determination of the environmental carrying capacity remains a political and qualitative issue, it was concluded that optimizing the farm layout of multiple farms within a region can significantly reduce the enhancement of dissolved nutrients. The method described therefore offers a valuable addition to the development of sustainable floating net cage mariculture.

Kurzfassung

Seit den frühen Siebziger Jahren, ist das Bewusstsein für die Umweltauswirkungen im Zusammenhang mit der Entwicklung von Marikulturen gestiegen. Marine Fischzucht in Käfigen verursacht erhebliche Mengen an Nährstoffemissionen in Form von flüssigen und partikulären Substanzen. Mit weltweit zunehmender Intensivierung von mariner Fischzucht, gewinnen diese Emissionen an Bedeutung. Gegenwärtig werden sie jedoch noch selten im Planungsprozess berücksichtigt.

Die vorliegende Studie befasst sich mit den Auswirkungen von gelösten Stickstoffemissionen aus Zackenbarsch-Marikultur in Pegametan Bay, Bali, Indonesien. Ein numerisches Modell zur Simulation von Hydrodynamik, Wellen und Wasserqualität wurde verwendet, um eine Strategie zu entwickeln, welche die Anordnung von mehreren Fischfarmen hinsichtlich einer Minimierung der gelösten Nährstoffemissionen optimiert.

Unter der Verwendung von simulierten physikalischen Einflussgrößen wurde eine Eignungsstudie zur Bestimmung potentiell geeigneter Flächen für die Zucht von Zackenbarschen in Netzkäfigen durchgeführt.

Ein Wachstums- und Massenbilanzmodell wurde entwickelt, um den Stickstoffhaushalt der vorwiegend gezüchteten Spezies, *Epinephelus Fuscoguttatus*, zu quantifizieren. Ungefähr 37 % des Stickstoffes wird als Ammonia ausgeschieden. Simulationen der Wasserqualität mit dem bestehenden Farmbestand zeigen ein sub-optimales Farmarrangement mit lokal erhöhten Ammoniumkonzentrationen und Anreicherungen von Nitrat.

Mit dem numerischen Wasserqualitätsmodell wurden experimentell alternative Farmarrangements simuliert. Anhand der Szenarien konnte dargestellt werden, dass durch die Kombination von Machbarkeitsstudie und Anpassung der Farmgröße an den lokalen dispersiven Charakter, welcher über die Reynolds Zahl definiert wurde, im Vergleich zu einer nicht optimierten Situation die Ammoniumkonzentrationen um 13% und die Nitratkonzentrationen um 41% reduziert werden konnten. Die durch die Farmen beeinträchtigte Fläche konnte durch die Optimierung um bis zu 48% reduziert werden.

Obwohl die Festlegung der regionalen Tragfähigkeit für Marikultur meist eine politische und eher qualitative Angelegenheit ist, kann über die Optimierung in der Anordnung von mehreren marinen Fischfarmen in einer Region, eine signifikante Verbesserung hinsichtlich der Belastung durch gelöste Nährstoffemissionen bewirkt werden. Die dargestellte Methode bietet daher eine sinnvolle Ergänzung bei Planung und Umsetzung einer nachhaltigen Marikultur.

Acknowledgements

After obtaining my MSc. degree at the Coastal Research Laboratory, a sub division of the Research and Technology Centre (FTZ), I was given the opportunity to be involved in various projects and write this dissertation.

I would like to acknowledge my great appreciation to Professor Dr. Roberto Mayerle for his introduction into this specific field of work and the chance he offered me to successfully present this dissertation. Also, I would like to thank Professor Dr. Federico Foders for kindly co-revising my thesis. Special thanks are due to Dr. Karl-Jürgen Hesse for sharing his expertise and providing ongoing constructive feedback which has always motivated to think along various pathways.

On the Indonesian side I like to thank the late Dr. Adi Hanafi for providing the insights on Indonesian mariculture. This dissertation arose from the BMBF funded project: Science for the Protection of Indonesian Coastal Ecosystems, second phase (SPICE FKZ 03F0469A).

A special, warm and comforting thank you is directed to my girlfriend, Katharina Niederndorfer, for always being there and providing the manoeuvring space I needed even though it did not always come easy when sitting in the same boat. But the boat did not sink. I would like to thank my parents for bringing me there where I am now. Throughout the course of time I have come to meet many people who have supported me during both professional and personal activities. I would like to show my gratitude to these many people from many different nationalities for the many unique experiences.

Simon A. van der Wulp

1 Introduction

1.1 Significance and statement of the problem

With the rapid development of floating net cage culture in the mid 1970's, concerns grew with respect to its environmental impacts. Apart from the strain on protein resources for fish feed and escapes of non-indigenous farmed fish species, mariculture generates considerable amounts of effluent in the form of solid (waste feed, faeces) and dissolved substances such as nutrients, pesticides and pharmaceuticals which are released directly into the water column.

Most environmental impacts related to floating net cage mariculture were observed to affect the sea bed and to a lesser extent the water quality (Wu, 1995). The environmental impact of particulate waste released from floating net cage farms has been abundantly described since it proves to be the limiting factor the production capacity, i.e. the maximum carrying capacity of individual floating net cage farms as defined by Byron & Costa-Pierce (2013). Especially in shallow areas the deterioration of underlying sediments is clearly related to the above lying net cage farms (Hall et al., 1990, 1992; Wu, 1995; Yokoyama et al., 2004).

However, with ongoing improvement of feed technology and higher ingestion rates leads to a reduced wastage in the form of particulate organic matter, making substances a more important factor. So far, immediate large scale environmental impact by dissolved nutrients are only sporadically directly related to floating net cage practice since they tend to rapidly dissipate away from floating net cages (Gowen & Bradbury 1987; Aure & Stigebrandt, 1990; Karakassis et al., 2005; Pitta et al., 1998; Wu et al., 1994). Model studies indicate the importance of transport mechanisms as main driving force behind the resulting nutrient concentrations (Petihakis et al., 2012; Skogen et al. , 2009;). Concerns were expressed by Sara (2007) who found that nutrient discharges from floating net cages can trigger a biological response, even at larger distances.

So far, no clear link was laid between the placement of floating net cage fish farms and mitigation of dissolved floating net cage farm wastes. Since the degree of nutrient enhancement is related to the nutrient discharge of a given standing stock and the physical characteristics of a water body at both farm level and at greater distances away from the farm. Therefore, adequate farm placement and methods to optimize the distribution of cultured fish over multiple floating

net cage farms provides leverage to reduce potential impacts of the dissolved wastes which are directly released into the environment.

1.2 Objectives

The main objective is to develop strategic measures to optimize the arrangement of multiple floating net cage farms and the distribution of the standing stock to efficiently accommodate dissolved nitrogenous wastes into the direct environment and to minimize nutrient concentration enhancement and potential triggers of eutrophication effects.

In order to accomplish this objective it is intended to ...

- ✓ assess the behaviour of dissolved nitrogenous wastes released from floating net cage fish farms.
- ✓ study the relationship between the number of floating net cage farms, distribution of the standing stock and physical carrying capacity with respect to resulting nitrogen concentrations.
- ✓ assess the use of site specific indicators of flow characteristics to provide a strategy to optimize the arrangement of multiple floating net cages within a given domain.
- ✓ explore and test a method to determine the environmental carrying capacity of a region.

1.3 Outline

The following chapter will address the status of research towards floating net cage farms and the related environmental issues with dissolved wastes. Subsequently, the pilot study area will be introduced with a profile of the hydrographic structure and the existing floating net cage practices. The used field measurements will be described in chapter four. In chapters five through seven the set up of the numerical tools is described going from flow characteristics and waves to the quantification of nitrogen flux from cultured fish to the simulation of the fate of dissolved nitrogenous wastes. The determination of the physical carrying capacity is shown in chapter eight which provide the basis of a number of scenarios to study a strategy to optimize farm arrangements and reduce resulting impacts of dissolved nitrogenous wastes in chapter nine. A method to determine the Environmental carrying capacity is evaluated in chapter ten. Overall results and findings will be discussed and concluded in chapter eleven and twelve.

2 Scientific background

Wu (1995) has summarized the environmental impact of marine fish culture stating that 80-88% of carbon and 52-95% of nitrogen input into a marine fish farm as feed may be lost into the environment through feed wastage, fish excretion, faeces production and respiration. Even though improved feed technologies have led to a reduction of feed wastage, these numbers remain valid for mariculture in tropical regions where trash fish, i.e. commercially low value fish, is the common type of feed.

Solid farm wastes are dispersed by currents but generally tend to settle on the sea floor in the vicinity of the fish farm. Elevated levels of organic matter and nutrients leading to stimulated microbial production have mostly been observed underneath and in the close vicinity of floating net cage farms. Excessive amounts of deposited organic matter lead to increased oxygen demand if oxygen supply is insufficient to cope with this situation, resulting in methanogenesis and formation of hydrogen sulphide (Hall et al., 1990, 1992). In the worst case, at heavily impacted sites, azoic zones may occur (Yokoyama et al., 2004).

The direct release of dissolved nutrients from floating net cage farm activities, especially with high densities of cultured fish, may lead to elevated ambient nutrient levels. For marine environments it is mainly nitrogen which forms the limiting nutrient for potential biological responses in the form of elevated primary production. The abundance of nitrogen and changes of nutrient ratios in the water column may favour the growth of certain phytoplankton groups such as flagellates or cyanobacteria. Increased abundance of microalgae could lead to eutrophication when undesired effects occur. The EU defines eutrophication as “the enrichment of water by nutrients causing an accelerated growth of algae and higher forms of plant life to produce an undesirable disturbance to the balance of organisms present in the water and to the quality of the water concerned, and therefore refers to the undesirable effects resulting from anthropogenic enrichment by nutrients” (OSPAR, 2003). Undesirable consequences of eutrophication include an increased abundance of pelagic microalgae recognised as a bloom or “Red Tide”, changes in biodiversity and oxygen deficiency in deep water layers and sediments as a consequence of the sinking and decay of algal biomass which may again negatively affect the immediate response of organisms and finally result in mass mortality due to suffocation (Black et al., 2001).

Increased ammonium concentrations have been observed around floating net cage fish farms. Nonetheless, elevated primary production has only been directly associated with farm activities in poorly flushed regions (Gowen et al., 1989; Aure & Stigebrandt, 1990; Wu et al., 1994). Dissolved nutrients tend to rapidly dissipate away from floating net cages. At marine sites, where tidal currents may be considerable, increases in ammonium levels are often occurring during slack tides (Gowen & Bradbury, 1987).

Gowen et al. (1989) proposed a simple box model to estimate the equilibrium rise of concentration assuming a well mixed semi enclosed water body. By considering the flushing time of the entire water body the box model assumes that excreted nitrogen is fully dispersed and thus neglects the occurrence and severity of localized effects.

Gillibrandt & Turrell (1997) developed another simple box model to provide a more scientific and consistent basis for the assessment of the relative potential environmental impact of new and existing farms. The potential enhancement of nutrient levels within sea lochs due to fish farms was predicted to regulate compliance with environmental quality standards (EQS). Similar to the box model of Gowen et al. (1989) many simplifying assumptions were made about the underlying hydrography of sea lochs. However, it provided a first estimate of possible effects, and has proven to be a useful management tool.

Technical advances, however, have led to increased possibilities to utilize high resolution models to capture the fate and impacts of dissolved nutrients which could not have been observed with the previously mentioned box models or by field measurements. Model studies provide an improved view stating that fish farming does favour primary production even at larger distances and that the degree of impact is closely related to the local and regional hydrographic conditions, production intensity, farm locations and, for temperate regions, the seasonal physical variability.

Wu et al. (1999) applied two deterministic models to simulate hydrographic and water quality conditions within a sub-tropical marine fish culture site in Hong Kong, where trash fish is used as feed. The simulation predicted the extent of pollution and area affected under varying fish stock and pollutant loadings. It was shown that impacts of fish culture activities on water quality at the culture site were localized owing to strong advection by tidal residual flows.

Petihakis et al. (2012) created an ecosystem model capable of simulating nutrient diffusion and primary production for the Pagasitikos gulf ecosystem, Greece, and verified the impact of two farms at a well protected and an exposed site. Results showed little effects of nutrient inputs in the vicinity of the farm at the exposed site but revealed that these effluents affect more distant areas due to hydrodynamic transport where primary production was stimulated. Instead the

well protected site showed more localized and more intense nutrient enhancement in conjunction with higher primary productivity; these findings suggest that the effect depends, amongst others, on the location of the farm.

Skogen et al. (2009) has set up a coupled 3D physical, chemical and biological ocean model which has been applied for a fjord at the western coast of Norway. The main objective of the study was to investigate and document the environmental effects of fish farming on eutrophication. An environmental impact study with respect to both farm size (i.e., fish production) and location of the farms was performed. The experiments showed that increasing the production of fish in each farm resulted in a rather small increase in primary production, without any impact on the oxygen levels. The locations of the farms were of larger importance. The stimulating effect on primary production was strongest when the fish farms were located quite far inside the fjord. The best location of the fish farms with respect to eutrophication effects was found to be near the mouth of the fjord where water exchange with the open sea is largest.

Best Environmental Practice (BEP) and Best Available Techniques (BAT) are common terms to support the development of more sustainable practice of aquaculture including floating net cage cultures. Proposed BEP and BAT guidelines are under discussion among the European countries to unify and standardize licensing procedures. The Baltic Marine Environment Protection Commission (HELCOM, 2004) and the OSPAR Commission (OSPAR, 2009) described a number of BEP and BAT measures related to general aquaculture practice including the use of technologically advanced formulated feed types and feeding techniques. Together with the choice of fast growing (and indigenous) species, feed wastage and nutrient discharges per unit of production could be reduced to a minimum. The Baltic Marine Environment Protection Commission (HELCOM, 2004) has formulated thresholds for the discharge of nitrogen (50 g N kg^{-1}) and phosphorus (7 g P kg^{-1}) per unit of produced fish weight for the Baltic Sea Area.

Regional planning should be employed as an instrument for directing fish farming activities to suited areas mitigating conflicts between fish farming and other uses of the coastal area. Discharges from sites should be restricted by means of objective environmental impact evaluation methods in accordance with the holding capacity of the aquatic environment affected. A guideline for the accommodation of dissolved nutrients is generally rarely regulated. The Scottish Environmental Protection Agency (SEPA) estimates the equilibrium concentration enhancement (ECE) based on a box model from Gillibrand & Turrell (1992) which is assessed against environmental quality standards (EQS). The Oslo & Paris Commission assessment criterion for critical dissolved nutrient enhancement is 50% above natural background

concentrations (OSPAR 2009), but there is no statement on the allowable spatial extends of nutrient excess.

Recommended maximum levels of production of fish are stipulated for parts of Puget Sound, USA, defined by its hydrographical and geomorphologic properties (Weston, 1986). These levels are based on a tolerable increase in the flux of nitrogen into the area. Nitrogen flux was estimated from the flushing-rate of the area, using existing hydrographical information, and concentrations of nitrogen in surface waters. A 1% increase in the flux of nitrogen into an area was specified throughout the Sound as the maximum permissible effect of farming. In the absence of information on the ability of the waters of the Sound to assimilate additional nitrogen or to predict potential nutrient enhancement, this was considered to be small enough to avoid adverse environmental effects. Using published data on the release of nitrogen from cage-farmed salmon, the amount of nitrogen input was expressed in terms of production of fish. The existing flux, tolerable increase and maximum allowable rate of production of salmon were then calculated for each of the areas of the Sound (Gesamp, 2001).

From the above, I observe that dissolved nutrients is regarded as a minor aspect of the environmental issues but will contribute as a source of nutrients which affect a much larger area than for example, particulate wastes, which tend to have a more distinct and localized impact.

Treating dissolved nutrients from floating net cage fish farms as a matter which can be dealt with more systematically, a lack of solid guidelines is missing. Environmental impact assessments mostly deal with individual farms as well as other regulatory mechanisms (Bermudez, 2013). No attempt is made to consider optimized placement of multiple farms within a region of interest and define individual farm sizes to match a defined environmental carrying capacity.

The present study proposes a strategy to optimize the arrangement of multiple floating net cage farms to efficiently accommodate dissolved nitrogenous wastes and attempts to contribute to a tool for the appropriate selection of mariculture as developed by Mayerle et al. (2009).

3 Study area

This study area used to test the hypothesis was Pegametan Bay, situated at the northwest corner of Bali Island (114.6°E, 8.14°S), Indonesia (Figure 3.1). The bay covers approximately 540 ha and is characterized by a shallow coral reef in its centre which partly falls dry during low tides. Two main channels east and west of the main reef reach depths of 20 and 30 meters, respectively. The eastern channel is protected from the Bali Sea by a second reef. At the seaward edge of the bay water depths rapidly increase to several hundred meters. The area is dominated by a mixed diurnal tide with a tidal range of approximately 1.8 meters (Egbert & Erofeeva, 2002). The area is tide dominated with current velocities in the order of 5 cm s^{-1} and up to 40 cm s^{-1} in the main channels. Water temperatures in the area range between 26 and 30°C. Several minor small streams discharge water into Pegametan Bay during the rainy season between December to February. Salinity varies in the range of 28 – 30 PSU (Hanafi, 2008).

Prevailing wind directions undergo semi-annual reversing according to northwest and southeast monsoons. The northwest monsoon has wind speeds averaging approximately 5 m s^{-1} with maxima of up to 12 m s^{-1} . During the southeast monsoon wind reaches speeds of up to 6 m s^{-1} (Kalnay, 1996).

Bali island is heavily reliant on tourism. Even though Pegametan Bay itself does not have strong touristic activities, the northern coastline of Bali harbours tourist resorts a few kilometres east of Pegametan Bay onwards. The Bali Barat National park and marine reserve is located west of Pegametan. Within the bay, occupations consist of fishing, farming and aquaculture. Pegametan Bay is the largest aquaculture area on Bali. A large shrimp farm area is located west of Pegametan. Three additional shrimp farms are located along the shore. During this study, only a small number of the available ponds were stocked with Pacific White shrimp (*Litopenaeus vannamei*). A number of sea weed farms were situated in the more shallow areas of the western part of the bay culturing red sea weeds of the genus *Eucheuma*.

Floating net cage finfish mariculture has been established since 2001 and has grown to a total of 18 farms at the time of this study (Figure 3.1). The farms consist of wooden rafts equipped with 200 litre plastic drums to provide floatation for the net cages (Figure 3.2). Each individual cage typically measures 3×3×3 meters. This type of floating net cage farm is commonly found in Indonesia.

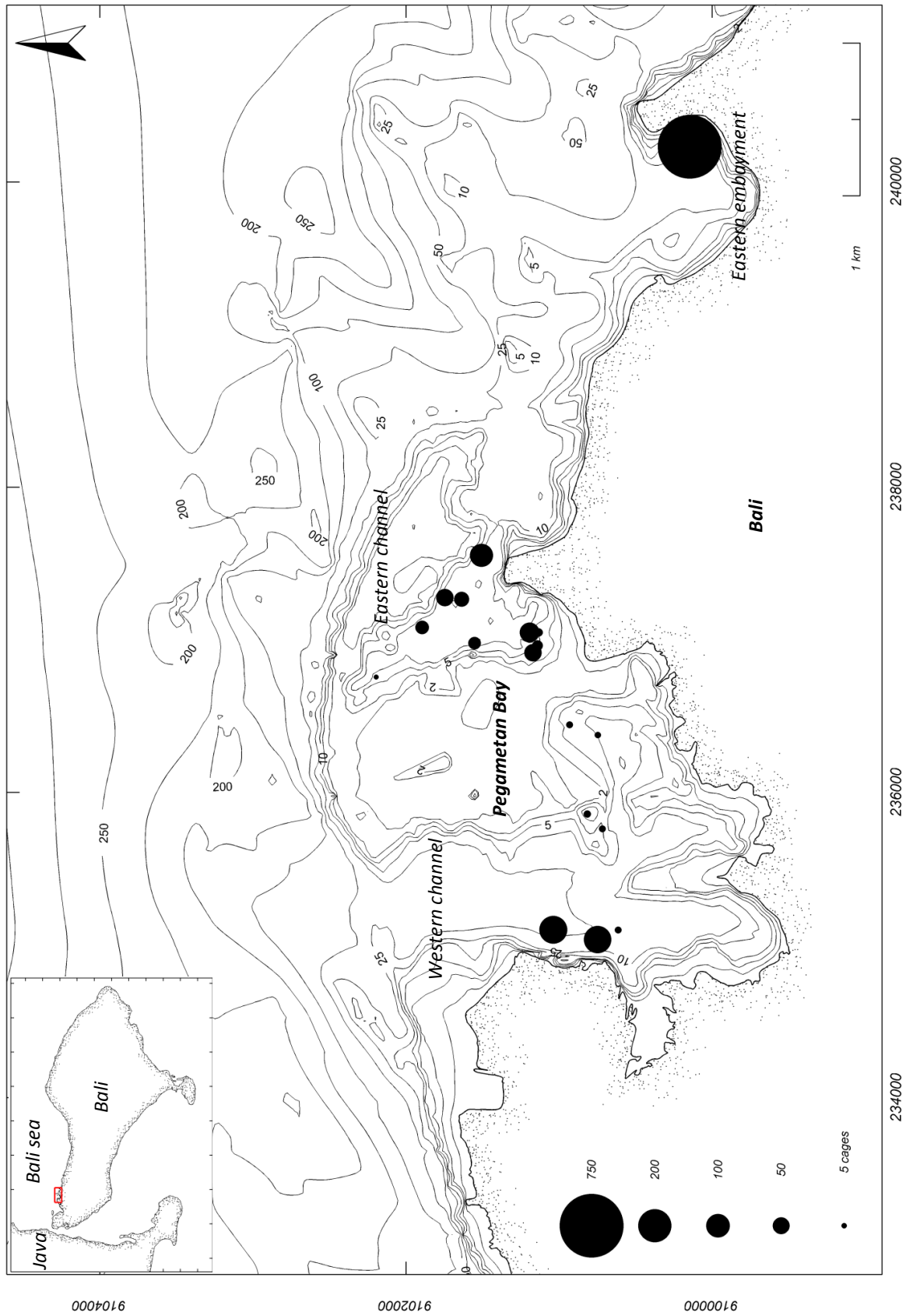


Figure 3.1. Pegametan Bay, Bali, Indonesia.
 In the period 2001-2008, 18 floating net cage fish farms have been established in Pegametan Bay. Farm sizes range from 4 to 750 cages.

A variety of fin fish species are cultured including: Asian Sea Bass (*Lates calcarifer*), Humpback Grouper (*Epinephelus altivelis*) and various species of ornamental fish. The bulk of standing stock consists of Tiger Grouper (*Epinephelus fuscoguttatus*) which is exported to the Chinese fish market. Individual farm sizes range from 7 to 750 cages in the eastern embayment. A total of 1478 cages was present. The maximum holding capacity is ~280 tons, when considering a typical stocking density of 7 kg m⁻³ for Tiger grouper at the end of the grow-out period (Hanafi, pers. comm.). At the time of inventory in December 2008 a total of 730 cages were stocked. Harvest is commonly scheduled around February (Chinese New Year) so cages were unlikely to be fully stocked. Assuming a stocking density of 3 kg m⁻³, as also observed by Alongi et. al. (2009), the standing stock was ~59 tons. A detailed overview of the observed farms is given in Appendix A.



*Figure 3.2. An example of a floating net cage farm as found in Pegametan Bay. Wooden rafts hold net cages measuring 3 x 3 x 3 meters. In Pegametan Bay, a total of 1478 cages were present divided over 18 farms, predominantly culturing Tiger Grouper (*Epinephelus fuscoguttatus*).*

4 Field measurements

4.1.1 Water quality

A number of water samples and in situ measurement were taken within the study area in December 2008, providing data which was used for the calibration of the water quality model. For each of the locations P_1 and P_2 , surface water samples were taken every two hours throughout an eight hour period. These locations were chosen according to the simulated flow field in the bay (see chapter 5) with the intend of capturing the accumulation of nitrogen from the existing multiple floating net cage fish farms within the area rather than influence from individual farms. Additionally, two reference locations (Ref_1 and Ref_2) situated outside the bay approximately two kilometres north of the area of interest, were sampled twice over the course of one day to obtain nutrient reference concentrations (Figure 4.1).

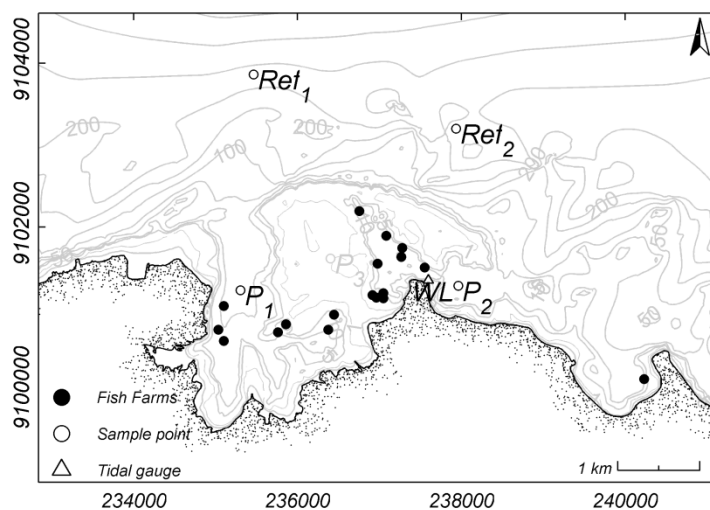


Figure 4.1. Overview of the water sampling locations and points of interest.

Along the sampling locations P_1 , P_2 , Ref_1 and Ref_2 , existing farms are indicated. In the center of the domain, a tidal gauge was installed.

Immediately after sampling, 200 ml subsamples were filtered and preserved with 0.4 ml of 3.5% mercury chloride solution ($HgCl_2$). Samples were routinely analyzed for dissolved nitrogenous nutrients i.e. ammonium, nitrite and nitrate and dissolved organic nitrogen using the calorimetric method according to Grasshoff et al. (2009) at the University of Kiel, Germany.

Table 4.1 provides an overview of mean concentrations and their standard deviations for reference stations $Ref_1 + Ref_2$ and stations P_1 and P_2 in the study area. Nitrogen concentration observed within the bay showed no significant difference ($p < 0.05$) with those observed at the

reference stations. Nitrogen flux from the existing farms and corresponding standing stock resulted in limited nutrient enrichment at the locations where water samples were taken. In contrast to the remaining nitrogen compounds, mean nitrate concentrations were 1.6 to 2.5 times higher than the mean reference concentration which could, despite its statistical similarity, indicate a possible tendency of nitrate accumulation.

Table 4.1. Measured sea surface nitrogen concentrations, for reference and study area stations. All concentrations are averaged (\pm standard deviation) in $\mu\text{g N l}^{-1}$.

Location	$\text{NH}_4^+ \text{-N}$	$\text{NO}_2^- \text{-N}$	$\text{NO}_3^- \text{-N}$	DON	TDN
<i>Ref₁ + Ref₂</i>	<i>2.1 \pm 0.7</i>	<i>0.14 \pm 0.02</i>	<i>1.99 \pm 0.54</i>	<i>130.5 \pm 41.1</i>	<i>133.7 \pm 42.2</i>
<i>P₁</i>	<i>1.8 \pm 0.3</i>	<i>0.17 \pm 0.09</i>	<i>3.25 \pm 1.73</i>	<i>131.4 \pm 31.7</i>	<i>135.0 \pm 30.3</i>
<i>P₂</i>	<i>2.0 \pm 0.7</i>	<i>0.24 \pm 0.08</i>	<i>5.02 \pm 3.29</i>	<i>125.1 \pm 49.7</i>	<i>132.4 \pm 49.7</i>
<i>Method Error</i>	<i>0.7</i>	<i>0.28</i>	<i>1.4</i>	<i>1.4</i>	<i>Σ of errors</i>

Along with surface water samples, in-situ readings of oxygen, salinity and water temperature were made using a handheld CTD-multiprobe (Sea + Sun Technology GmbH). In situ measurements (Table 4.2) show uniform conditions at both the reference and inner bay stations.

Table 4.2. In situ measurements of sea surface temperatures, dissolved oxygen concentrations and salinity. All readings are averaged (\pm standard deviation).

Location	Temp ($^{\circ}\text{C}$)	O_2 (mg l^{-1})	O_2 %	Salinity (psu)
<i>Ref₁ + Ref₂</i>	<i>30.5 \pm 0.3</i>	<i>6.9 \pm 0.08</i>	<i>108 \pm 1.3</i>	<i>28.9 \pm 0.4</i>
<i>P₁</i>	<i>30.5 \pm 0.3</i>	<i>7.0 \pm 0.1</i>	<i>106.4 \pm 4.0</i>	<i>29.1 \pm 0.5</i>
<i>P₂</i>	<i>30.3 \pm 0.3</i>	<i>6.6 \pm 0.4</i>	<i>106.6 \pm 3.0</i>	<i>28.7 \pm 0.6</i>

4.1.2 Tidal gauge

Due to the lack of current velocity field measurements a validation was done using the available water level field measurements, measured at observation point WL using a CeraDiver Pressure logger (Schumberger Water Services, 2010). Water pressure was logged every 10 minutes from the 16th of December 2007 until the 15th of April 2008.

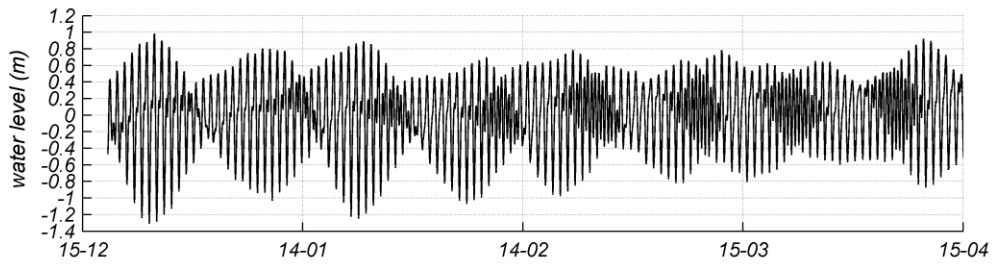


Figure 4.2. Overview of the observed water levels as logged by the tidal gauge.

4.2 Discussion

The measurements used for this study were taken during a dry period which provided the advantage that land based influences were reduced to a minimum. Observed nutrient concentrations were very low, common for tropical oligotrophic waters. Sample locations were chosen to capture the possible cumulative effect of the 18 floating net cage fish farms, rather than signals from individual farms. It was found that there is no significant difference between nutrient concentrations measured within the bay and at reference stations situated off shore. Nitrate concentrations however did tend to be slightly higher when compared to the reference stations.

Samples taken during the wet season as documented by Sulawestian (2008) were much higher with maximum ammonium and nitrate concentrations in the order of 20 and 18 $\mu\text{g l}^{-1}$. These high concentrations were attributed anthropogenic and natural land based sources such as shrimp farms, diffuse runoff and river discharge from one particular river.

It was chosen to adopt the nutrient measurements from the dry season since Pegametan Bay only functions as a pilot study area to address the behaviour of sole floating net cage farm effluents.

5 Setup of flow and wave models

5.1 Introduction

For this study, flow and wave modeling techniques are applied to provide spatial and temporal information of the physical parameters which are used as driving forces of the water quality model and for the determination of the physical carrying capacity which are discussed in chapters 7 and 8, respectively.

5.2 Set up of the flow model

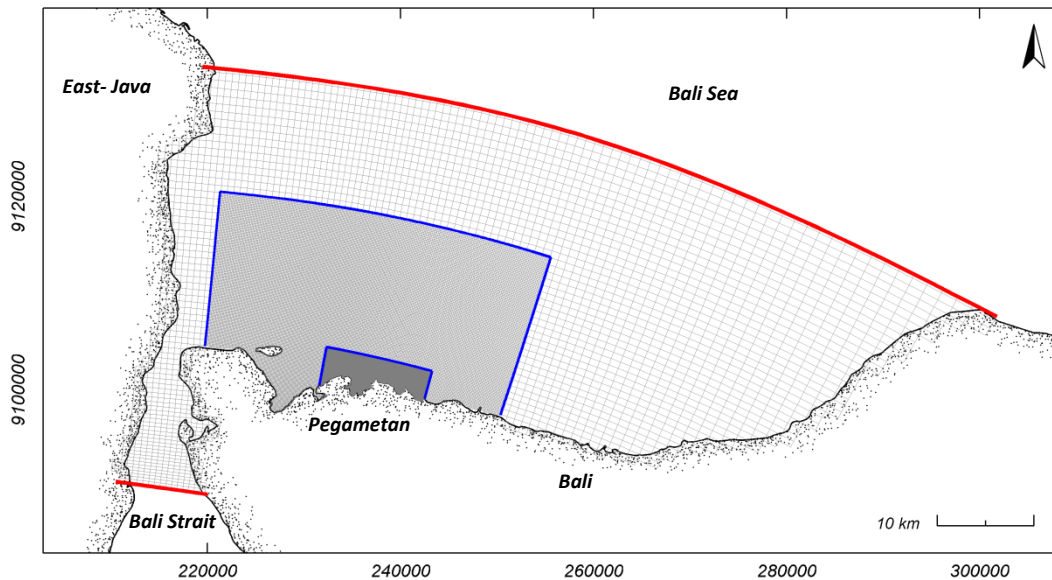
The flow model was set up using the Delft3D modelling software. This software allows the setup of, amongst others, numerical flow, wave and water quality models of any region of interest to simulate two-dimensional (depth averaged) and three-dimensional fluid flow resulting from tidal and meteorological forcing. Unsteady fluid flows are simulated onto boundary fitted grids by solving the shallow water equations consisting of the horizontal equations of motion and continuity (Deltares 2011a).

The model domain covers the Southern Bali Sea region between Bali Island, Java Island and the Bali Strait using three computation grids with increasing grid resolution towards Pegametan Bay as shown in Figure 5.1a. The coarsest domain has an average grid cell size of approximately 800 meters. An intermediate sub-domain along the north-western Bali coast was fitted with a grid resolution of approximately 200 meters. The finest domain covers the Pegametan Bay area with a resolution of up to 25 meters. The latter, in contrast to the two coarser domains was computed in three dimensions with five equally spaced vertical layers relative to the water depth (sigma-layers). Simulations were carried out using domain decomposition where computations of all grids are performed in parallel allowing smooth transitions between the refined sub-domains.

Tides were imposed at the northern and southern boundaries of the largest domain using 13 astronomical tidal constituents (M2, S2, N2, K2, K1, O1, P1, Q1, MF, MM, M4, MS4, MN4) extracted from the Global Tidal Model (Egbert & Erofeeva, 2002). Bathymetric information for the model domains were taken from three different sources. The General Bathymetric Chart of the Oceans (IOC, IHO & BODC, 2003) provided offshore depths at a 30 arc second resolution. Higher

resolution bathymetric information for the near coastal region was available from measurements taken by the Indonesian National Survey Authorities (Bakorsutanal, 2008). Additional field measurements were taken using a handheld echo sounder for the areas where bathymetric information was lacking. Space and time varying wind and pressure fields were taken from the NCEP/NCAR reanalysis database to incorporate the corresponding wind fields for the simulated periods (Kalnay, 1996).

a.



b.

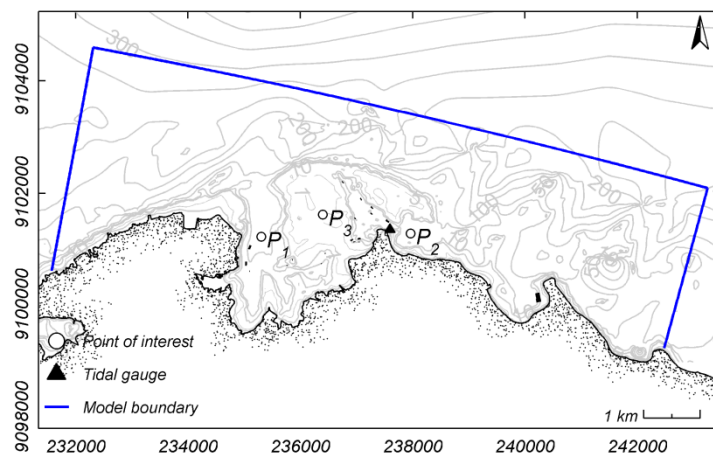


Figure 5.1. The Bali Sea and Pegametan Bay model domains
a. Three computational grids with increasing resolutions of 800, 200 and 25 meters towards Pegametan Bay. b. The Pegametan Bay model domain with the tidal gauge location and points of interest P_1 , P_2 and P_3 .

A sensitivity analysis was done for varying bottom roughness and wind magnitudes and compared for stations P_1 , P_2 and P_3 (Figure 5.1b).

The flow model proved to be most sensitive to bottom roughness settings and wind variations. Simulations were carried out for bottom roughness ranging $n = 0.02 \text{ s m}^{-1/3}$ to $n = 0.1 \text{ s m}^{-1/3}$ characterizing the range of a sandy plain bed to a strongly vegetated seabed by Chow, (1959). Model results of the imposed roughness as shown in Figure 5.2 demonstrates that current

velocities are affected considerably in areas with relatively high current velocities (P_2) in comparison to those with generally lower current velocities (P_1), indicating the importance of this parameter to the model results. Currents keep their principal flow directions apart from a minor influence. The roughness has no effect on In contrast to currents, water levels remain unaffected by the different bottom roughness settings.

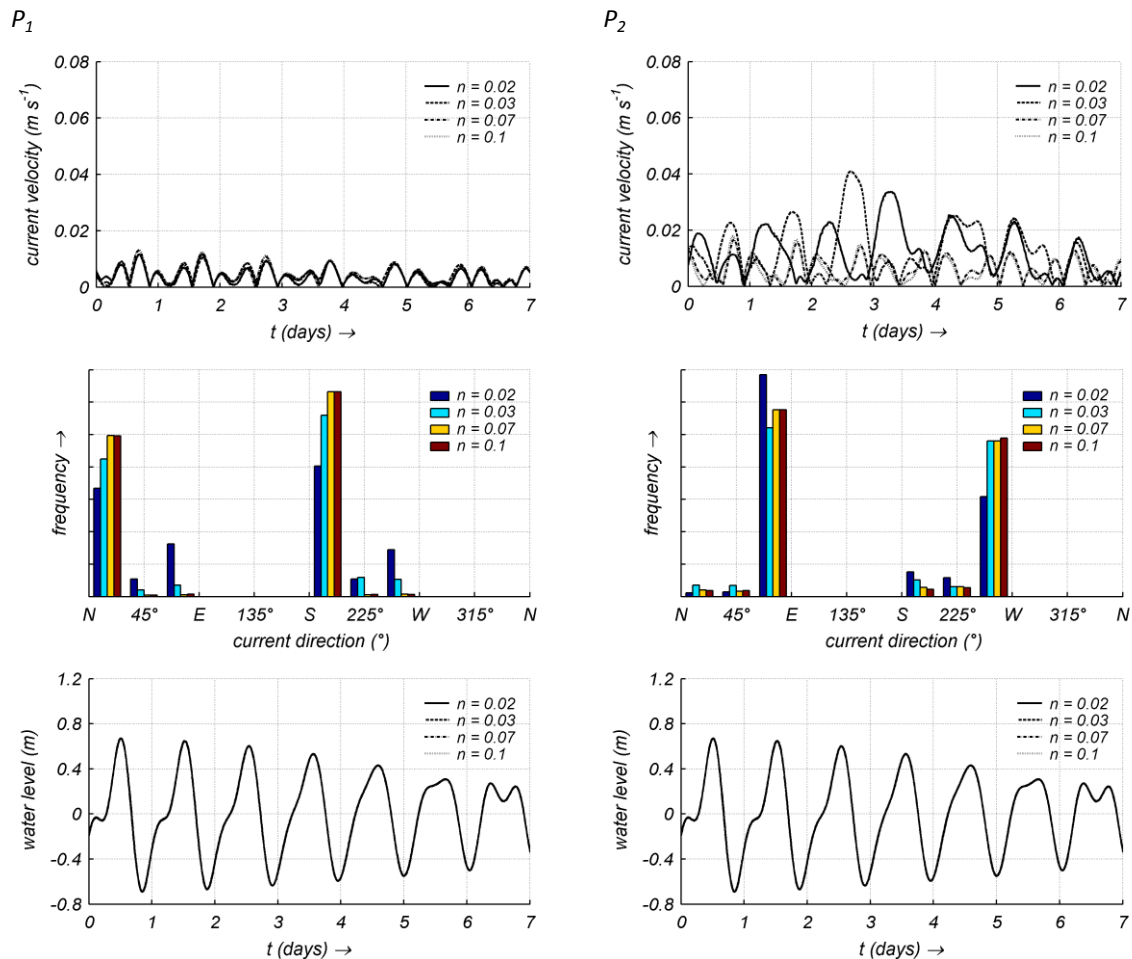


Figure 5.2. Model sensitivity for a range of Manning bottom roughnesses Ranging Manning roughnesses of 0.02, 0.03, 0.07 and 0.1 $m^{1/2} s^{-1}$ for observation points P_1 (left) and P_2 (right) (Figure 5.1b) with, from top to bottom, the depth averaged current velocities, current direction distribution and water levels. Current velocities are affected, principal current directions are kept and water levels show no reaction to the different settings imposed.

A variety of wind scenarios were imposed to the model. In addition to a no wind scenario, wind fields with magnitudes of $4 m s^{-1}$ and $8 m s^{-1}$ from predominantly north-north eastern direction were imposed. Model simulations indicate an increase in surface current magnitudes with increasing wind speeds as exemplarily indicated for observation points P_1 (left) and P_3 (right) in Figure 5.3. An impact of wind speeds on current directions is most obvious for locations with

limited water depth i.e. observation point P_3 , where currents are forced into south western directions with increasing wind speeds. Imposed winds did not affect the simulated water levels.

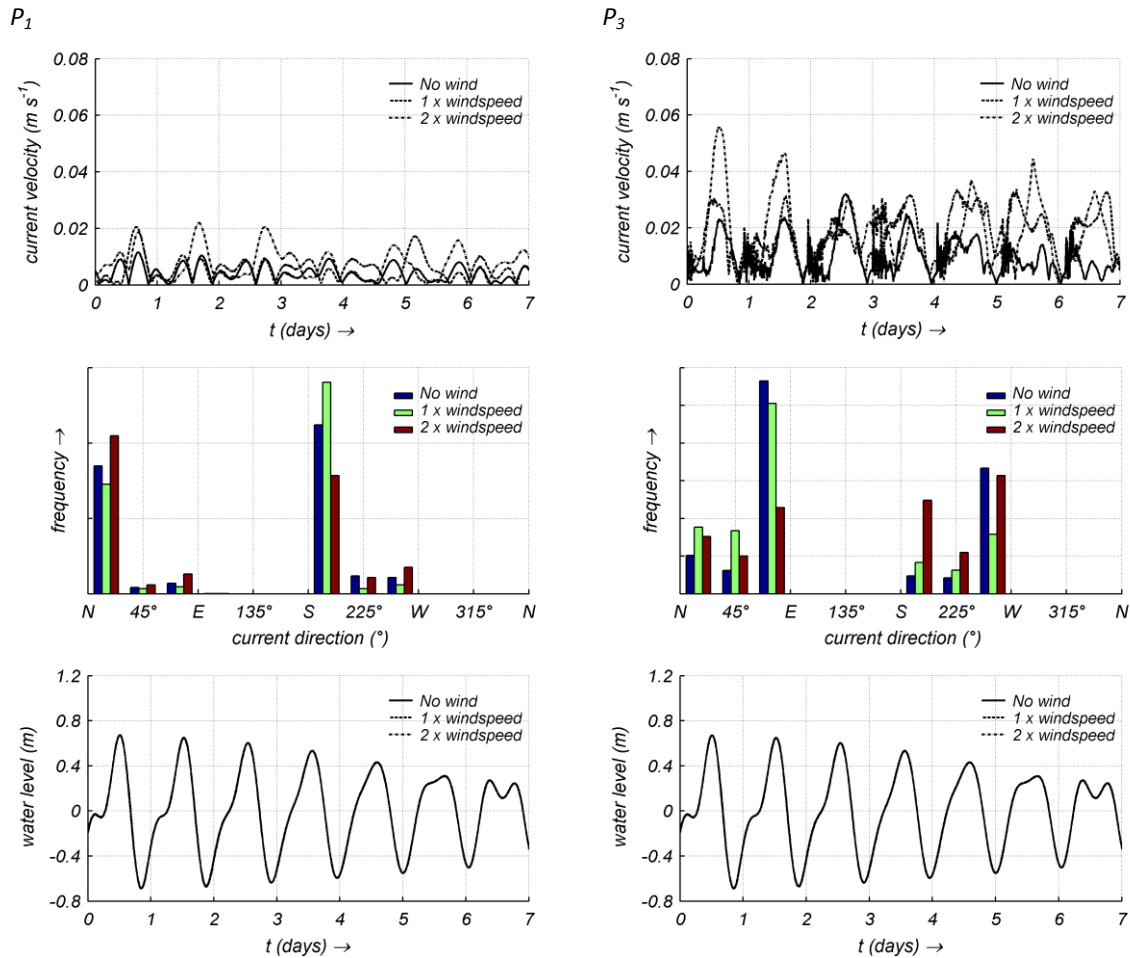


Figure 5.3. Model sensitivity for wind

Scenarios with no wind and winds with magnitudes of 4 and 8 m s^{-1} from north-north eastern direction shown for observation points P_1 (left) and P_3 (right) (Figure 5.1b) with, from top to bottom, the current velocity, current directions and water levels. Increasing winds affect both current velocities and directions. Shallow areas in the centralized reef are affected more.

According to the results obtained, the roughness has no effect on the water levels. Therefore, the bed roughness was selected based on values proposed by Chow (1959). A uniform Manning roughness of $0.03 \text{ s m}^{-1/3}$ is defined for a sandy, slightly vegetated, bottom (Chow, 1959) and was chosen to represent a coral reef environment with corals sand and moderate presence of corals. Wind was imposed on the model domain for the simulated periods as provided from the NCEP/NCAR reanalysis database (Kalnay, 1996). The water density was 1018 kg m^{-3} under the assumption that temperatures of 30°C and salinity of 30 psu were constant in space and time. A detailed overview of the model settings is given in appendix B.

Due to the lack of current velocity field measurements a validation was done using the available

water level field measurements, measured at observation point WL using a CeraDiver Pressure logger (Schumberger Water Services, 2010). Comparison of the model results with measured water level data provided a matching agreement with a mean absolute error of 6 centimetres (Figure 5.4). The analysis of the high and low water peaks indicated mean average errors of 9 and 5 centimetres, respectively. Phase shifts for high and low water level peaks were less than one minute.

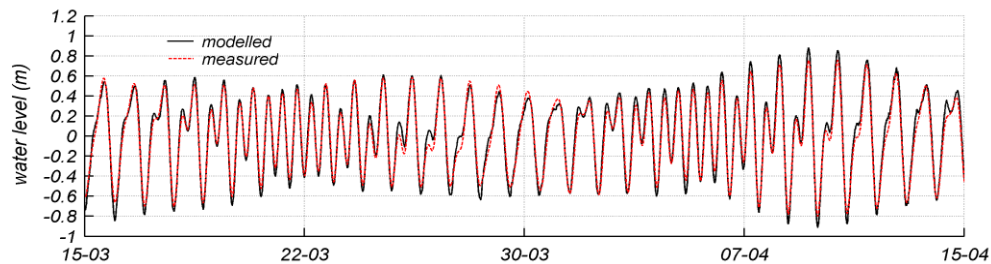


*Figure 5.4. Comparison of modelled and measured water level within Pegametan Bay
With a mean absolute error of 6 centimeters the simulated water levels are in good agreement with
field measurements observed at station WL.*

5.3 Setup of the wave model

An approximation of potential wave action affecting the Pegametan Bay shoreline was made using the Delft3D wave modelling software (Deltares, 2011b). The Delft3D wave module simulates the evolution of wind generated waves by computing wave propagation, wave generation by wind, wave dissipation and non-linear wave-wave interactions using the action-balance equation as described by Booij (1989).

For an analysis of the carrying capacity (See Chapter 8) a worst case wind forcing scenario was defined to identify those stretches of the north Bali coast which are vulnerable to wave exposure. Instead of one worst case event, the worst case conditions were defined by the predominant wind direction and the maximum wind speed of a represent period. In case of this study a 50 year reanalysis from the period 1960 to 2010 was taken. A 50 year period was assumed to provide a conservative representation of wind fields to identify wind driven wave fields at exposed areas which may cause excessive stresses on the floating net cages. This is done according to criteria which will be further discussed in chapter 8.

Wind information was extracted from the NCEP/NCAR reanalysis database. The dataset showed maximum wind speeds of $\sim 12 \text{ m s}^{-1}$. The predominant wind direction over the considered period was North-North-East (35°). Boundary conditions were specified with a significant wave height of 1.9 meters and a wave period of 6.25 seconds, determined from the nomogram for deep

water significant wave height predictions (US Corps of Engineers, 1984) using a fetch length of 100 km. An overview of the model settings and boundary conditions are given in appendix C.

5.4 Results

Current velocities generated from the model showed a magnitude of less than 0.05 m s^{-1} for both ebb and flood flows during neap tides in the confined regions of the model domain. During spring tides, ebb and flood flows were in the order of 0.2 m s^{-1} within the confinements of Pegametan Bay (Figure 5.5). Tide averaged current velocities are in the order of up to 0.1 m s^{-1} in a predominantly eastern direction through the bay.

Comparisons with water level measurements indicate that the model provides a good approximation of the volumes of water moving around within the domain. The sensitivity analysis has shown that different settings of bottom roughness significantly affect the current magnitudes. The approximation the bottom roughness is based on descriptive classifications according to Chow (1959).

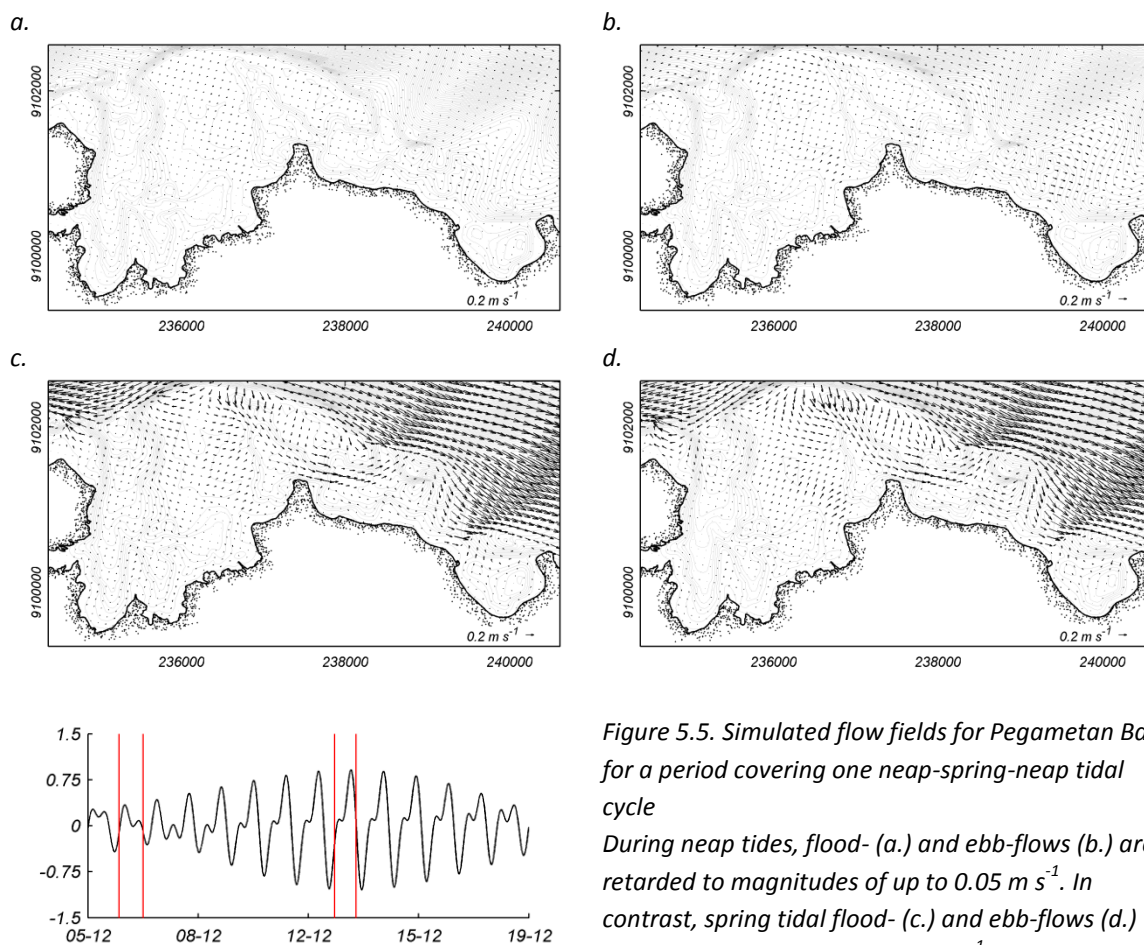


Figure 5.5. Simulated flow fields for Pegametan Bay for a period covering one neap-spring-neap tidal cycle. During neap tides, flood- (a.) and ebb-flows (b.) are retarded to magnitudes of up to 0.05 m s^{-1} . In contrast, spring tidal flood- (c.) and ebb-flows (d.) reach magnitudes of up to 0.2 m s^{-1} inside the bay.

The adopted worst case wind conditions generated a wave field with significant wave heights of approximately 1.6 meters when approaching the North Bali shoreline. Due to the considered processes of bottom friction, refraction and diffraction, energy rapidly dissipates to negligible wave heights within Pegametan Bay (Figure 5.6). The shallow reefs act as a barrier to shelter the inner bay.

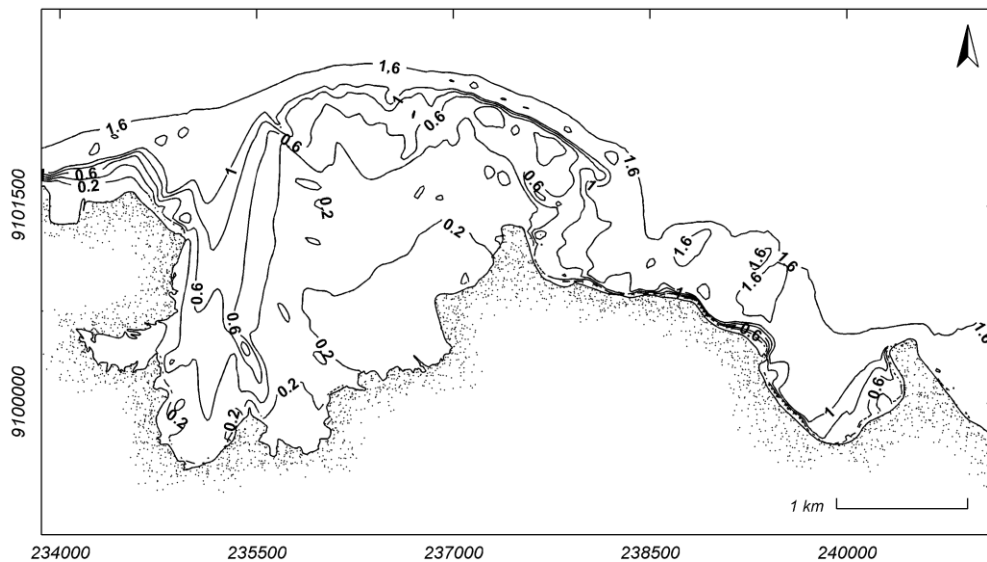


Figure 5.6. Worst case wave scenario for Pegametan Bay
Significant wave heights (m) of 1.6 meters approaching the Pegametan Bay shoreline under worst case conditions but quickly dissipate to negligible levels in the sheltered regions of the bay.

5.5 Discussion

Comparison with water level measurements indicate that the model provides a good approximation of water levels and hence, the volumes of water moving around within the domain. Optimally, a flow model is calibrated with current velocity measurements which were not available for this study. The sensitivity analysis showed that different settings of bottom roughness significantly affect the simulated current magnitudes. The approximation the bottom roughness is based on descriptive classifications according to Chow (1959) to provide the best possible approximation.

In case of the wave model, and "ad-hoc" setup was used where the model was not calibrated or validated. Model results however were able to show which shorted of the study area are subject to high wave impact and how wave energy dissipates leading to lower wave heights in the inner bay.

6 Quantifying temporal nitrogenous flux floating net cages

6.1 Introduction

An understanding and quantification of the nitrogen flux from floating net cage mariculture is a prerequisite to study the fate of nitrogenous wastes from floating net cage mariculture using a water quality model. However, direct assessment of floating cage fish farm emissions with field measurements are labour intensive and time consuming. Due to the open boundary conditions of marine cage fish farms, a complex measurement strategy is needed to capture all discharges. In contrast, a mass balance approach is easier to apply and can provide comparable results as described in this chapter.

Feed is the ultimate source of nutrients emitted from floating net cage farms. The type of feed is the major factor affecting the nutrient. Most investigations dealing with nutrient uptake and release in fin fish cultures are based on Salmonid farms operated with formulated feeds (Gowen et al., 1989; Hall et al., 1990; Holby & Hall, 1991; Hevia et al., 1996). Nevertheless, a major part of aquaculture, especially in South-East Asia, is practiced with non-Salmonid species, fed with trash fish (Wu et al. 1994; Wu, 1995; Wu et al., 1999; Alongi et al. 2003 & 2009). Moreover, according to Handy & Poxton (1993) juvenile fish have higher excretion rates than adult fish which hence illustrates the importance to assess the quantity of metabolic wastes from different life stages during the grow-out period.

In this chapter, a temporal growth and mass balance model for the quantification of the nitrogen fluxes from Tiger Grouper (*Epinephelus fuscoguttatus*) individuals is described. The mass balance model calculates fish growth and the fraction of nitrogen dedicated to the different pathways of growth, excretion, faecal discard and to feed wastage. In combination with floating net cage production properties, a quantitative estimate is made concerning the nitrogen flux and its temporal variations for a given farm volume. The results form the basis for modelling the fate of nitrogen emissions after being released into the water column.

6.2 Fish growth

Fish growth for Tiger Grouper was calculated using the weight based Von Bertalanffy Growth Model (VBGM) which is commonly used to calculate the growth of aquatic animals (Sparre & Venema, 1998). In particular, the daily growth rate ($\frac{dW}{dt}$) was computed using the first derivative of the VBGM with specification of the maximum or asymptotic wet fish weight (W_{∞}), the initial age (t_0) and a growth coefficient (K) according to Equation 6.1. The growth coefficient (K) was determined using culture properties regarding the age of the juveniles (t_0), the wet market weight (W_{market}) and the duration of the grow-out period (t_{market}) using Equation 6.2.

Equation 6.1.
$$\frac{dW}{dt} = W_{\infty} 3K [1 - e^{-K(t-t_0)}]^2 e^{-K(t-t_0)}$$

Equation 6.2.
$$K = \ln \left[1 - \left(\frac{W_{market}}{W_{\infty}} \right)^{1/3} \right] \frac{1}{t_{market} - t_0}$$

Tiger grouper fingerlings were estimated to be at the age of approximately 70 days. The maximum weight was assumed to be equal to the broodstock weight which was indicated to be in the order of 9 to 12 kg. Tiger Grouper reaches a market weight of 500 grams after a period of approximately 10 months (Hanafi, 2008). Fish growth was observed for one grow-out cycle by the Gondol Research Institute for Mariculture (Hanafi, 2008). 20 to 30 individuals were repeatedly weighed over the course of one grow-out period resulting in an average weight growth curve.

6.3 Feed and nitrogen input

For Indonesian grow-out cultures trash fish is commonly used. Feed is given manually according to fish appetite (*ad libitum*). Observed daily *ad libitum* feeding rates (R_t) were in the order of 20% of the fish body weight for fingerlings and decreased towards 4% for adult fish reaching a weight of 600 grams (Hanafi, 2008). Total feed input (I_t) was calculated using the fish weight (W_t) and the corresponding feeding rates (R_t) at time t according to Equation 6.3. The nitrogen input at a given time (N_t) was calculated according to Equation 6.4. The nitrogen content of trash fish (F_{Nfeed}) was adopted from findings at a comparable Tiger Grouper farm on Sumatra Island, Indonesia, and accounted for 3.96% of the wet weight (Alongi et al., 2009).

Equation 6.3.
$$I_t = R_t \cdot W_t$$

Equation 6.4.
$$N_t = I_t \cdot F_{Nfeed}$$

6.4 Metabolism, waste feed and nitrogen fluxes

The probability of feed ingestion is influenced by a number of factors such as fish appetite, the ability for the fish to detect the feed, to reach the feed and finally the decision of the fish to ingest the feed (Beveridge, 2004). Of the total amount of feed supplied to the fish, part will be ingested and part will be lost directly to the environment as waste feed. A fraction of the ingested organic nitrogen compounds in the feed is lost by the direct release of undigested nitrogen with the faeces. The catabolic part is absorbed across the gut, remineralised and excreted through gills and skin as ammonia and urea. Since grouper are ammoniotelic, the predominant nitrogenous excretion product is ammonia (Handy & Poxton 1993). The remaining fraction of nitrogen is assimilated and used for growth. In this study total nitrogen flux is divided over assimilation, excretion, faecal excretion and feed wastage according to the mass balance of Equation 6.5.

Equation 6.5.
$$N_t = N_{assimilation} + N_{excreted} + N_{faecal} + N_{wasted}$$

Leung et al. (1999) conducted nitrogen metabolism experiments with Areolated Grouper (*Epinephelus areolatus*) and found that 28.1% of the ingested nitrogen was assimilated, 63.9% was excreted as ammonia and 8.0% was excreted as faeces. In this study these rates were adopted for Tiger Grouper and represented as three empirical constants regarding assimilation ($M_{assimilation}$), excretion ($M_{excretion}$) and faecal excretion (M_{faecal}). The daily amount of assimilated nitrogen ($N_{assimilation}$) was computed from the growth rate ($\frac{dW}{dt}$) and the nitrogen content of the fish biomass (F_{Nfish}) according to Equation 6.6.

Equation 6.6.
$$N_{assimilation} = \frac{dW}{dt} \cdot F_{Nfish}$$

Nitrogen composition of cultured fish was taken to be in the same order as the feed composition i.e. 3.96% for wet weight (Alongi et al., 2009). The ingested, excreted and faecal nitrogen are determined by Equation 6.7, Equation 6.8 and Equation 6.9, respectively. The amount of nitrogen lost through feed wastage is used to close the mass balance (Equation 6.10).

Equation 6.7.
$$N_{consumed} = \frac{N_{assimilation}}{M_{assimilation}}$$

Equation 6.8.
$$N_{excreted} = N_{consumed} \cdot M_{excretion}$$

Equation 6.9.

$$N_{faecal} = N_{consumed} \cdot M_{faecal}$$

Equation 6.10.

$$N_{wasted} = N_t - N_{consumed}$$

Ammonia is excreted at different rates throughout the day, strongly regulated by the time at which feed is given (Handy & Poxton, 1993; Dosdat et al., 1996; Sumagaysay-Chavoso, 2003). Maximum post feeding ammonia excretion rates occur between four and six hours after feeding for various cultured species (Sumagaysay-Chavoso, 2003; Dosdat et al., 1996). Such excretion peaks may have a significant effect on the water quality as further discussed in chapter four. Hourly ammonia fluxes were approximated from the normalized temporal post feeding excretion pattern as found by Dosdat et al. (1996) which were adapted to the daily averaged values from the mass balance model.

Once released into the water, a major fraction of ammonia (NH_3) is rapidly ionized to ammonium ions (NH_4^+). The major factor that determines the proportion of ammonium in water is the pH. In the following, farm flux, once released into the direct environment is thus expressed as Total Ammonia Nitrogen (TAN), the sum of non-ionic ammonia and ammonium ions, or simply ammonium.

6.5 Nitrogen flux from floating net cage farms culturing Tiger Grouper

Computed Tiger Grouper growth was compared to field observations as shown in Figure 6.1. With a mean absolute error of 3.5 grams, fish growth was accurately reproduced. Specific growth rates were in the order of 4.7% of its body mass per day for juvenile fish and decreased to approximately 1% at the end of the grow out period.

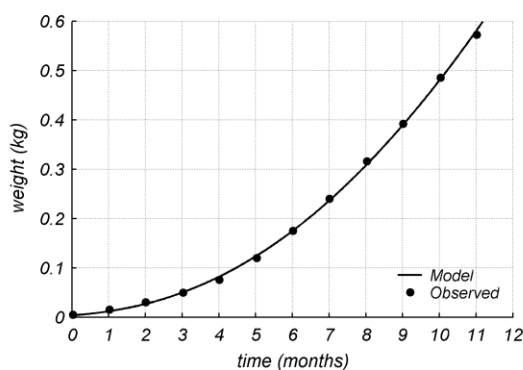


Figure 6.1. Computed and observed growth-curve for cultured Tiger Grouper (*E. fuscoguttatus*) The use of the VBGM with physical grow out-culture parameters yielded a good agreement with observed fish growth.

Feed efficiency was highest in the early life stages with feed conversion ratios in the order of 4 kg feed per kg of biomass yield (wet weight). At later life stages, feed conversion ratios increased

towards 7 as indicated in Figure 6.2. Daily nitrogen input per kilogram of fish produced, decreased over the duration of the grow-out period from 7 to 1.75 g N kg⁻¹ d⁻¹ (Figure 6.3). Of the supplied nitrogen approximately 1.8 to 0.25 g N kg⁻¹ d⁻¹ was assimilated by the fish for growth. Faecal excretion was in the range of 0.53 to 0.07 g N kg⁻¹ d⁻¹. Metabolic nitrogen excretion rates for ammonia were in the order of 4.3 – 0.6 g N kg⁻¹ d⁻¹. The remaining 1.6 – 0.34 g N kg⁻¹ d⁻¹ was considered to be lost to the environment as waste feed.

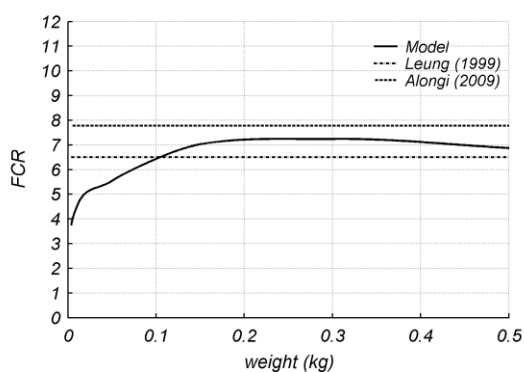


Figure 6.2. Calculated feed conversion ratios for cultured Tiger Grouper (*E. fuscoguttatus*) The various FCR's along the computed life stages reach the order of magnitude of those described by studies for similar fish cultures feeding trash fish feed.

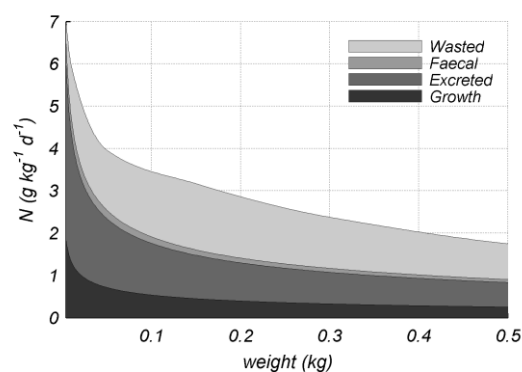


Figure 6.3. Calculated Nitrogen flux distributed over the various sinks during the various life stages Feed wastage is the largest sink of nitrogen followed by the excretion of ammonia.

Optimal stocking densities for Tiger Grouper cultures are indicated to be in the range of 3 kg m⁻³ for younger fish and up to 7 kg m⁻³ for market weight fish as indicated by the Gondol Research Institute for Mariculture (Hanafi, 2008) which is in agreement with stocking densities found by Alongi et al. (2009) in a comparable Tiger Grouper farm. Dissolved nitrogen farm fluxes per unit farm volume are shown in Figure 6.4. Ammonia excretion flux expressed as Total Ammonia Nitrogen (TAN) were in the order 12.8 – 1.7 g TAN m⁻³ d⁻¹ for a stocking density of 3 kg m⁻³ and 29.9 – 4 g TAN m⁻³ d⁻¹ for a stocking density of 7 kg m⁻³. Assuming a stocking density of 3 kg m⁻³ for averaged weight fish (170 grams) and 7 kg m⁻³ for adult fish (500 grams), 2.91 g TAN m⁻³ d⁻¹ and 4.05 g TAN m⁻³ d⁻¹ are released into the water column, respectively. Hourly post feeding excretion rates were in the range of 61.2 to 199.7 mg TAN m⁻³ hr⁻¹ for average weight fish and 85.2 to 277.9 mg TAN m⁻³ hr⁻¹ for adult fish as shown in Figure 6.5.

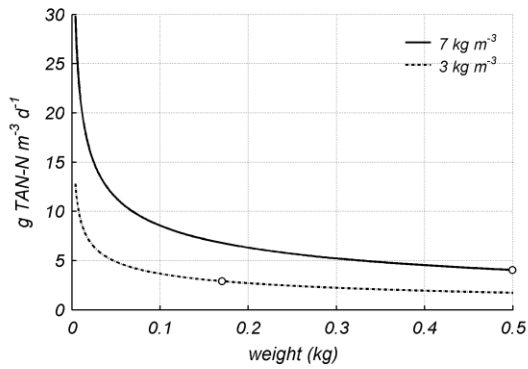


Figure 6.4. Total ammonia nitrogen flux per unit farm volume
TAN fluxes are indicated for two stocking densities of 3 and 7 kg m⁻³ at mean and maximum fish body weight, respectively, as indicated by the white dots

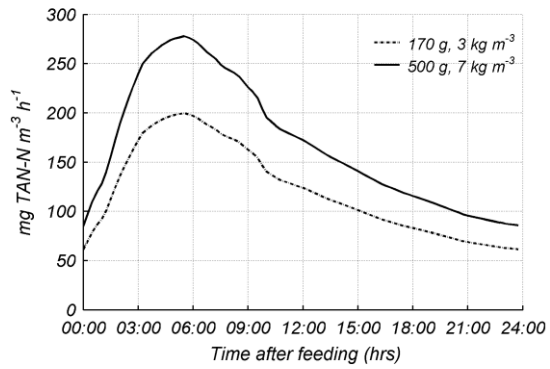


Figure 6.5. Approximated 24 hour post feeding nitrogen excretion rates per unit farm volume
Two stocking densities were applied with mean and maximum fish weights.

6.6 Discussion

The temporal growth and mass balance model quantifies the nitrogen flux from Tiger Grouper cultures over the course of its grow-out period. The computed growth curve provided a reasonable reproduction of the observed growth indicating that the VBGm can be used to approximate growth of cultured fish species based on their production properties with good accuracy.

Total feed input was calculated based on recorded feeding rates relative to the fish bodyweight and formed an empirical approximation of ad libitum feeding of Tiger Grouper. Resulting feed conversion ratios (FCR) were in the order of 4 – 7 demonstrating the amount of feed required per unit of biomass produced. Leung et al. (1999) found a feed conversion ratio in the order of 6.5. Tiger groupers cultured on Sumatra, Indonesia, had feed conversion ratios in the order of 7.78 (Alongi et al., 2009). Wu et al. (1994) summarized feed conversion ratios in the range of 4 to 9 for mixed species fed with trash fish. Compared to the available studies computed FCR's are in good agreement with those found for comparable farms utilizing trash fish as the primary feed source.

The relative percentage distribution of nitrogen over the different somatic pathways and sinks i.e. assimilation, ammonia excretion; faecal excretion and feed wastage were compared to similar studies as shown in Table 6.1. Both nitrogen assimilation through growth and total loss to the environment fall within the order of magnitude as found for the Tiger Grouper culture studied by Alongi et al. (2009) and for other tropical species studied by Wu et al. (1994).

Table 6.1. Comparison of calculated relative floating net cage nitrogen flux found by various studies.

	<i>Species</i>	<i>Feed</i>	<i>FCR</i>	<i>Growth (%)</i>	<i>Excreted (%)</i>	<i>Faeces (%)</i>	<i>Wasted (%)</i>	<i>Total loss (%)</i>
<i>Wu et al. 1994</i>	<i>Mixed</i>	<i>Trash fish</i>	4-9	20	52		20 – 47	52 – 95
<i>Alongi et al. 2009</i>	<i>Tiger grouper</i>	<i>Trash fish</i>	7.78	12.8				87
<i>This study</i>	<i>Tiger Grouper</i>	<i>Trash fish</i>	6.5	16.3	37.1	4.7	41.9	83.7

Handy & Poxton (1993) reviewed nitrogen toxicity and excretion and found that maximum hourly post feeding ammonium fluxes fall within a range of 6 – 140 mg TAN-N kg⁻¹ hr⁻¹ equivalent to 18 – 420 mg TAN-N m⁻³ hr⁻¹ and 42 – 980 mg TAN-N m⁻³ hr⁻¹ for stocking densities of 3 and 7 kg m⁻³, respectively. These ranges cover the hourly rates found by the mass balance model when a post feeding distribution was imposed.

Confined species are susceptible to adverse conditions which may affect growth and metabolism. Constant nitrogen compositions for both feed and fish biomass were assumed which in reality change over the course of the grow-out period (Hall et al. 1992). During its development, fish require different amounts of energy to maintain various bodily functions which may affect the assimilation and excretion of nitrogen over time (Stigebrandt, 1999). Such processes were not considered in the model.

7 Modelling the fate of dissolved nitrogenous waste from floating net cage fish farms

7.1 Introduction

In chapter four it was concluded that approximately 37% of the total nitrogen input given to Tiger Grouper (*Epinephelus fuscoguttatus*) is excreted as ammonia. Such discharges may contribute to the enhancement of ammonium concentrations in the water column. Concerns have been expressed about the fate of dissolved nutrients released which appear to have no immediate large scale effects (Karakassis et al., 2005) but could affect biological processes at larger distances from the farm depending on the temporal relation between nutrient diffusion and nutrient uptake (Sara, 2007). Various model studies have dealt with the diffusion of dissolved wastes to perform environmental impact assessments and were able to clarify that the accommodation of dissolved nitrogen is strongly regulated by the dispersive character of a farm site and region (Wu et al., 1999; Skogen et al., 2009; Petihakis, 2012).

In this chapter the set up of a water quality model for Pegametan Bay is presented. Simulations of ammonium fluxes from existing floating net cage farms were compared to field measurements to provide an insight in model performance. Results from model simulations are analysed to identify the main controlling mechanisms that contribute to the resulting ammonium and nitrate concentrations in this semi-enclosed area.

7.2 Water quality model setup

The fate of dissolved nitrogenous farm discharges was simulated using the Delft3D-WAQ water quality modelling software (Deltares, 2011c). The water quality model was coupled to the flow model results as described in Chapter 8 and solves the advection-diffusion-reaction equation (Equation 7.1).

Equation 7.1

$$\frac{\partial C}{\partial t} = D_x \frac{\partial^2 C}{\partial x^2} - \frac{\partial uC}{\partial x} + D_y \frac{\partial^2 C}{\partial y^2} - \frac{\partial vC}{\partial y} + D_z \frac{\partial^2 C}{\partial z^2} - \frac{\partial wC}{\partial z} + S + f_R(C, t)$$

The advection-diffusion-reaction equation is divided into separate terms of advection and diffusion describing concentration change due to mass transport of a substance. The reactive term captures the decay or generation of a substance as a function of the concentration and the reaction rate over time. Additionally, discharges of a substance are considered as a concentration change.

7.2.1 Advection and diffusion

Advective mass transport results from the unidirectional flow in which a dissolved substance is present. It is incorporated in the water quality model using the coupled current velocities u , v and w from the flow model flowing in x , y and z directions. Diffusion refers to the movement of mass due to random water motion causing mixing and minimizing concentration gradients. Even though mass transport is broken down into the two idealized forms of advection and diffusion an overlap of the two processes is considered where diffusion numerically takes into account all motion not captured by the flow model. Diffusive mass transport was computed in both horizontal and vertical directions using diffusion coefficients D_x , D_y and D_z . Time and space varying horizontal diffusion coefficients ($D_{x,y}$) were computed for the water quality model as a function of depth (d) and current velocity (u) incorporating a number of calibration indices a , b and c as shown in Equation 7.2 (Deltares, 2011c). Due to the reduction of the vertical momentum equation which assumes only gravitational influences, the vertical diffusion coefficient (D_z) was considered to be in the order of molecular diffusion.

Equation 7.2
$$D_{x,y} = a \times u^b \times d^c + D_{background}$$

7.2.2 Ammonium discharges

Discharges of ammonium from floating net cage cultures are imposed to individual grid cells and are numerically incorporated as a change in concentration (S) determined from the discharged load and the volume of the computational cell at a given time. Discharges of the eighteen existing farms were imposed to the model grid. Discharge cells were selected to match individual farm sizes as illustrated in Figure 7.1.

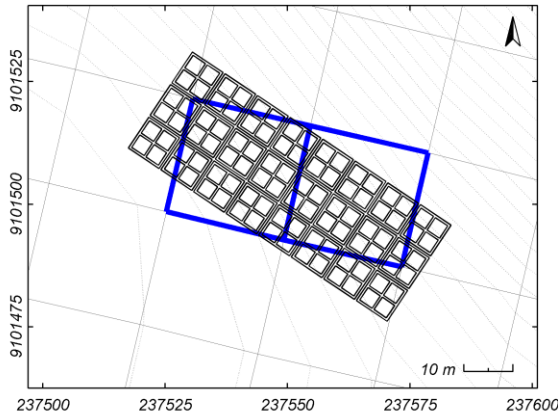


Figure 7.1. A representation of a scaled farm and the corresponding numerical discharge cells.

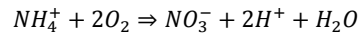
Coarser resolution of the model grid requires an approximation of discharge cells which resemble the realistic scenarios as found in the field.

Ammonium discharges per model grid cell were specified in accordance with the individual floating net cage farm sizes. The ammonium discharge per floating net cage farm was determined from the farm volume and the approximated discharge per unit volume as described in section 6.5. Daily TAN emissions accounted for $2.91 \text{ g TAN m}^{-3} \text{ d}^{-1}$ under the assumption that cultured fish had an average weight of 170 grams and that average stocking density accounted for 3 kg m^{-3} . The daily discharge and incorporated post feeding peak as described in section 6.5 resulted in a distribution of hourly discharges in the range of $61.2 - 199.7 \text{ mg TAN m}^{-3} \text{ hr}^{-1}$. Of the 1478 cages present in the study area at the time of the simulated period, 730 were stocked with fish, predominantly with Tiger Grouper (*Epinephelus fuscoguttatus*). The stocked volume corresponds to a cage volume of 19710 m^3 made up by individual cages measuring $3 \times 3 \times 3$ meters. According to these findings, the total holding capacity during the simulated period accounted for 59.1 tonnes which would emit approximately $57.4 \text{ kg TAN d}^{-1}$.

7.2.3 Nitrification

Apart from physical transport, biochemical transformation processes play an important role on the fate of nutrients in the environment. The individual processes are incorporated into the model as reactive terms $f_R(C,t)$. Nutrient transformation may constitute a source or sink to dissolved inorganic nutrients. In the present study it been assumed that phase transfer processes such as mineralisation and uptake of nutrients are balanced. Due to the well oxygenated water ideally denitrification was considered to be negligible. Instead, nitrification of ammonium was considered as a main transformation process.

The oxidation of ammonium to nitrate (NO_3) occurs in two steps through various genera of ammonium oxidizing and nitrite oxidizing bacteria (*Nitrosomonas*, *Nitrosococcus*, *Nitrobacter*, *Nitrospira* and *Nitrococcus*) and can be summarized as:



The nitrification process is controlled by ammonium ($C_{ammonium}$) and oxygen (C_{oxygen}) concentrations and follows the Michaelis-Menten kinetics. Half saturation concentrations for ammonium and oxygen ($K_{mammmonium}$, $K_{moxygen}$) were used to numerically induce limitation of nitrification and determine the nitrification rate (R_{nit}) according to Equation 7.3. The reaction rate is strongly temperature sensitive. The maximum nitrification rate (k_{nit}) was calculated using the temperature dependent nitrification variables (Equation 7.4) where k_{nit20} represents the nitrification rate at a temperature of 20°C and kt_{nit} is the corrected nitrification rate at temperature T .

Equation 7.3.
$$R_{nit} = k_{nit} \times \left(\frac{C_{ammonium}}{K_{mammmonium} + C_{ammonium}} \right) \times \left(\frac{C_{oxygen}}{K_{moxygen} + C_{oxygen}} \right)$$

Equation 7.4.
$$k_{nit} = k_{nit20} \times kt_{nit}^{(T-20)}$$

7.2.4 Boundary conditions

Boundary conditions and initial ammonium concentrations were taken to be equal to the mean observed ammonium concentration of $2.1 \mu\text{g N l}^{-1}$ as observed in the surface waters at the reference locations Ref_1 and Ref_2 situated at the open boundary. Similarly, a nitrate concentration of $1.99 \mu\text{g N l}^{-1}$ was taken at the open boundaries. To account for the mass transport of the dissolved substance across the open boundaries from the domain and its potential return into the model domain, boundary conditions are corrected using the Thatcher-Harlemann time-lag (Equation 7.5). The Thatcher-Harlemann time-lag uses the defined boundary condition (C_{Bt}) and the last modelled concentration (C_{t0}) of a substance leaving the domain to define a corrected value of boundary conditions (C_{t0+t}) as function of time (t) according to the time-lag (T_h).

Equation 7.5
$$C_{t0+t} = (C_{t0} - C_{Bt}) \times \cos\left(\frac{\pi}{2T_h}\right) + C_{Bt}$$

7.3 Water quality sensitivity

7.3.1 Warm up time

Water quality model runs were coupled to flow model results in multiples of a neap-spring-neap tidal cycle simulated for the period of the 5th until the 19th of December 2008. A sequence of this cycle reached an equilibrium depth averaged concentration pattern after one neap-spring-neap tidal cycle with constant discharges from the selected discharge points. A 14 day warm up time for the water quality model should thus be kept in consideration (Figure 7.2).

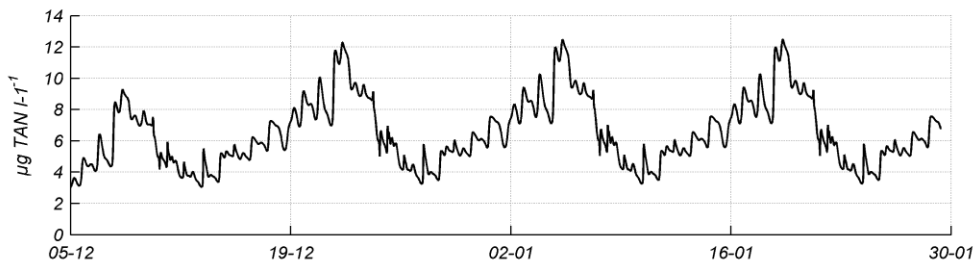


Figure 7.2. Warm up time of the water quality model

An equilibrium ammonium concentration pattern is reached after a simulation period of one neap-spring-neap tidal cycle as illustrated for location P₂.

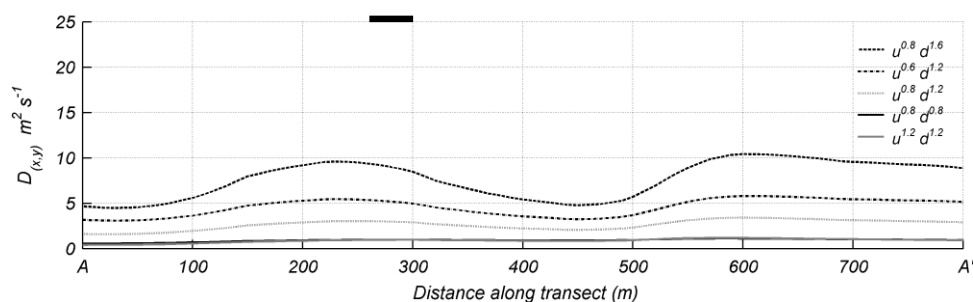
7.3.2 Diffusion coefficients

Based on the default dispersion settings ($a = 1$, $b = 0.8$ and $c = 1.2$; see also section 7.2.1) given by Deltares (2011c), different simulations were conducted altering the influence of current velocities and water depth for the calculation of the diffusion rate. Numerically, it was the influence of depth which had a greater effect on the computed diffusion rates. Increased diffusion coefficients (Figure 7.3.a.) led to a more rapid spreading of the released substance which results in a decrease of concentrations close to the discharge point (Figure 7.3.b.). The influence of settings for the calculation of the diffusion greatly affects the ambient TAN surface water concentrations.

7.3.3 Time of feeding

In addition to constant discharges, approximated post-feeding peaks were considered with “feeding-times” at 6:00, 10:00 and 14:00. Maximum TAN concentrations along transect A-A’ were higher for peak discharges than for constant discharges in the vicinity of the discharge location. The degree of enhancement was also dependent on the time at which peak discharges occurred, indicating the relevance of temporal variations in feeding times and of the flow situation occurring during peak discharges (Figure 7.4).

a.



b.

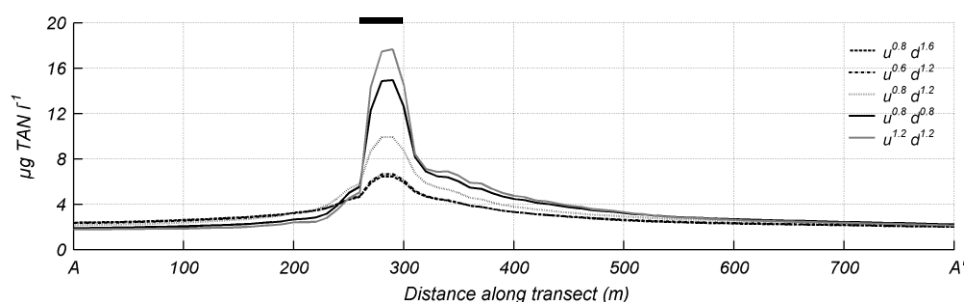


Figure 7.3. The effect of various diffusion settings on TAN concentrations. Time averaged diffusion coefficients (a.) and surface water TAN concentrations (b.) along transect A-A' under different influences of depth (d) and current velocity (u). Indices leading to a higher diffusion resulted in a more rapid spreading and a subsequent local decrease of the simulated TAN concentration. The farm location is indicated by the short bold line.

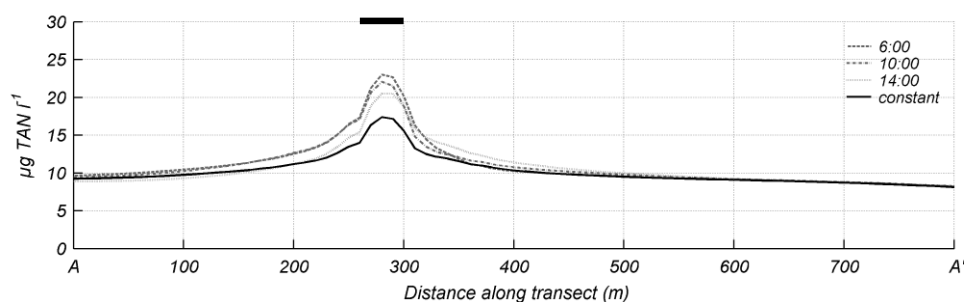


Figure 7.4. TAN enhancement effect due to post-feeding discharges. Maximum TAN concentrations after 14 day period along transect A-A' for post-feeding peak discharges induced by different "feeding times". A time shift of discharge peaks in contrast to a constant release of the same amount of substance results in different local TAN enhancements. The farm location is indicated by the short bold line.

7.3.4 Nitrification rates

Variation of maximum nitrification rates (0, 0.05, 0.1 and 0.15 mg N l⁻¹ d⁻¹) leads to differences in time averaged nitrification fluxes along transect A-A' in the order of several micrograms per litre

and day. Along with increasing nitrification intensity simulated TAN concentrations were reduced by up to 30% at the water surface for the range of settings while simulated nitrate concentrations were enhanced. Due to the time span required for the conversion of TAN to nitrate and the mass transport at which these substances are exposed, nitrate is equally distributed in space as indicated by time averaged concentrations along transect A-A' (Figure 7.5).

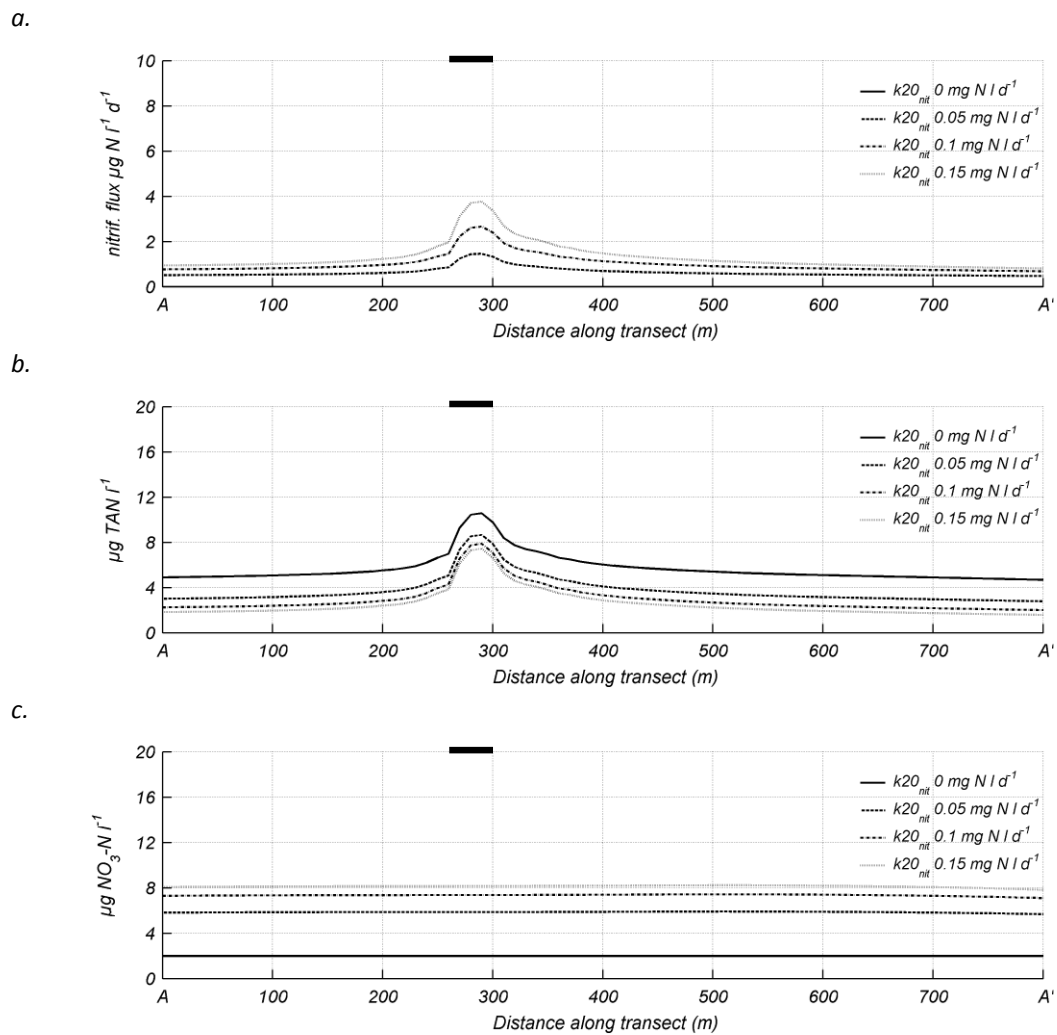


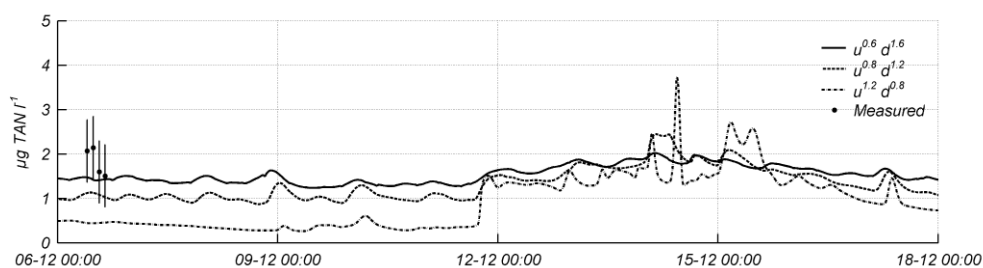
Figure 7.5. Nitrification fluxes and resulting TAN and $\text{NO}_3\text{-N}$ concentrations for different maximum nitrification rates ($K_{20\text{nit}}$) ranging between 0 and $0.15 \text{ mg N l}^{-1} \text{ d}^{-1}$. Simulated nitrification fluxes (a.) increase at higher maximum nitrification rates and are dependent on the availability of ammonium. Along with an increase of nitrification rates TAN concentrations (b.) are reduced and subsequently nitrate concentrations are enhanced (c.). The farm location is indicated by the short bold line.

7.3.5 Water quality model calibration

Simulations for calibration of the water quality model were conducted in 3D with five vertical layers each of which representing 20% of the local water depth. A 14 day warm up period covering one neap-spring-neap tidal cycle was taken in consideration for each simulation. Post-feeding discharge variability was adopted based on the local average feeding times at 10:00 every day resulting in daily peak discharges of TAN at approximately 15:00. A default maximum nitrification rate ($k_{20\text{nit}}$) of $0.1 \text{ mg l}^{-1} \text{ d}^{-1}$ was taken to account for the nitrification of ammonium in the water column (Deltares, 2011c; Boderie & Ouboter, 1997). Diffusion settings were used for calibration.

Simulated surface TAN concentrations were compared to those observed at the corresponding time and locations P_1 and P_2 (Figure 7.6). Diffusion settings of $a = 1$, $b = 0.6$, $c = 1.6$, $a = 1$, $b = 0.8$, $c = 1.2$ and $a = 1$, $b = 1.2$, $c = 0.8$ indicated an overall agreement in the order of magnitude and error ranges of the measurements. Settings of $b = 0.6$ and $c = 1.6$ for diffusion indices for velocity and water depth, respectively, resulted in the best agreement with mean absolute errors of 0.40 and $0.42 \text{ } \mu\text{g TAN l}^{-1}$ equal to mean absolute percentage errors of 19.9 and 17.4% for both locations P_1 and P_2 . Surface nitrate concentrations were reproduced with mean absolute errors of 3.5 and $5.25 \text{ } \mu\text{g NO}_3\text{-N l}^{-1}$ and mean absolute percentage errors of 99.9 and 99.8% (Figure 7.7). A detailed overview of the final water quality model settings is given in Appendix D.

a.



b.

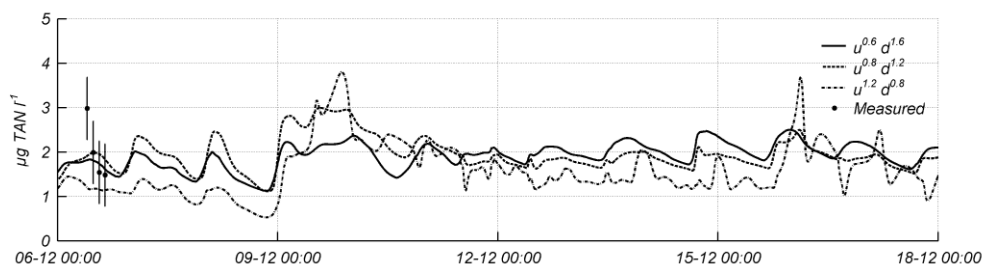
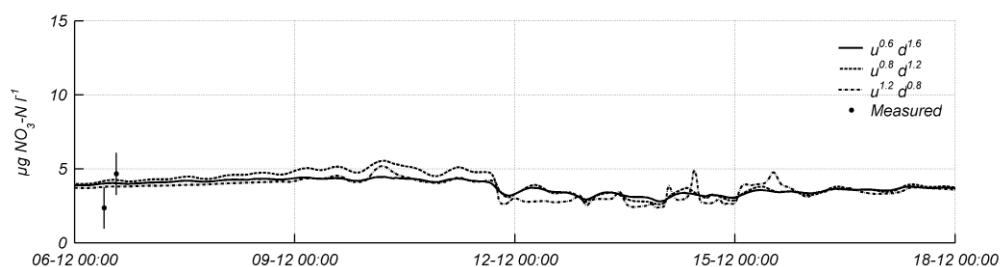


Figure 7.6. Water quality model calibration of TAN concentrations.

Comparison of measured and simulated TAN concentrations for different calibration simulations at locations P_1 (a) and P_2 (b).

a.



b.

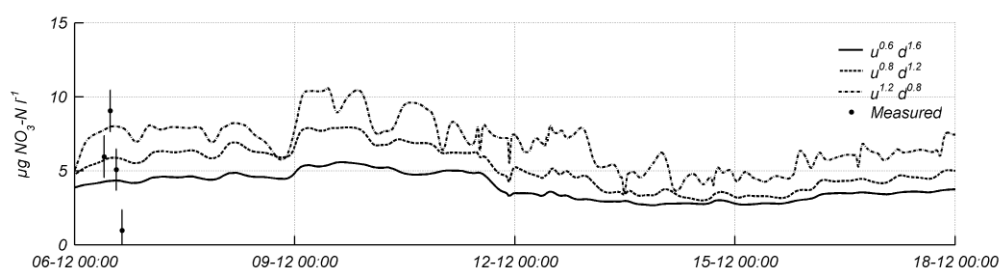


Figure 7.7. Water quality model calibration for nitrate.

Comparison of measured and simulated nitrate concentrations for different calibration simulations at locations P_1 (a) and P_2 (b).

7.4 The fate of ammonia released from floating net cage farms in Pegametan Bay

Water quality model results indicate that ammonium enhancement occurs locally in the vicinity of the floating net cage farms (Figure 7.8 a and b). In the far eastern bay where one individual farm accounts for 46% of the total emission in the study area, TAN concentrations were $31.8 \pm 11.5 \mu\text{g TAN l}^{-1}$ and $46.5 \mu\text{g TAN l}^{-1}$ for time averaged mean (\pm standard deviation) and maximum values, respectively. In the center of the domain, where 30% of the total emission is divided over 12 farms, TAN concentrations were in the order of $7.7 \pm 5.0 \mu\text{g TAN l}^{-1}$ and a maximum of $40.8 \mu\text{g TAN l}^{-1}$ was reached locally. In the western part where the remaining 24% of all emissions were released, ammonium concentrations were in the order of $4.8 \pm 1.4 \mu\text{g TAN l}^{-1}$ with maximum concentrations of $14 \mu\text{g TAN l}^{-1}$. During neap tides, TAN concentrations increase in the direct vicinity of sites where one or more farms are located. When tidal amplitudes increase during spring tides and corresponding ebb and flood flows are strongest, ammonium is dispersed more efficiently resulting in reduced localized impacts (Figure 7.8 a and b).

Nitrification, as implemented by the model, occurs at a rate of approximately 0.3 d^{-1} corresponding to a nitrification flux in the order of $2 \mu\text{g N l}^{-1} \text{ d}^{-1}$, but varied over the domain according to the presence of ammonium. Since the amount of time required for the biological oxidation of ammonium to nitrate is much longer than the diffusion rate it is subjected to

causing the signal of individual farm on nitrate concentrations to be faded. Nonetheless, elevated nitrate concentrations were found around sites where fish farms are present governed indirectly by accumulation of multiple farm ammonium discharges. Nitrate is accumulated during neap tides and partly flushed away from the domain during spring tides (Figure 7.8 c and d). The pockets of the western and far eastern embayment remain affected by elevated nitrate concentrations. Maximum time averaged nitrate concentrations within the domain were in the order $10.5 \pm 1.7 \mu\text{g NO}_3\text{-N l}^{-1}$ and $16.0 \mu\text{g NO}_3\text{-N l}^{-1}$.

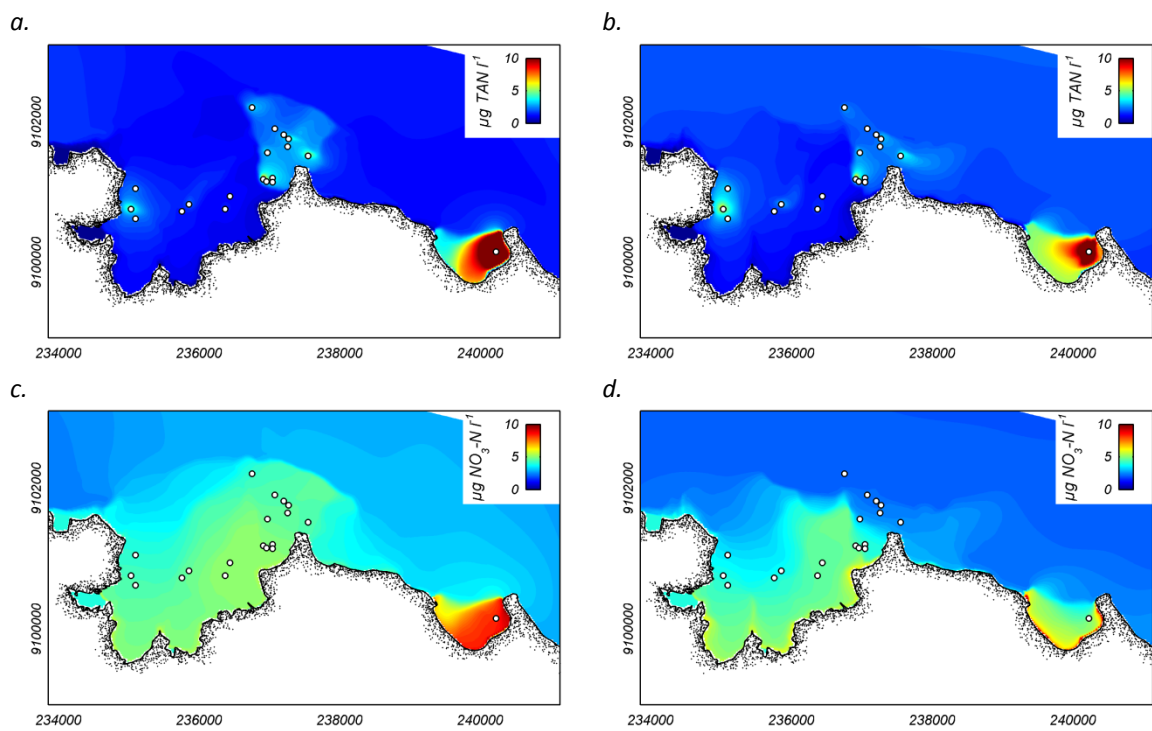


Figure 7.8. Simulated TAN and nitrate concentration patterns during neap and spring tides in Pegametan Bay. Ammonium patterns during ebb flows for neap (a) and spring (b) tides illustrate the enhanced dispersion during spring tides. Nitrate patterns during neap tide (c) are accumulated and partly flushed away during spring tides (d).

Highest ammonium concentrations were restricted to the surface layers of the water column where the floating net cages were present (Figure 7.9 a) and were gradually diluted with increasing distance from its source. Due to the temporal delay at which nitrification occurs in relation to turbulent mixing, nitrate is more uniformly distributed over the water column (Figure 7.9 b).

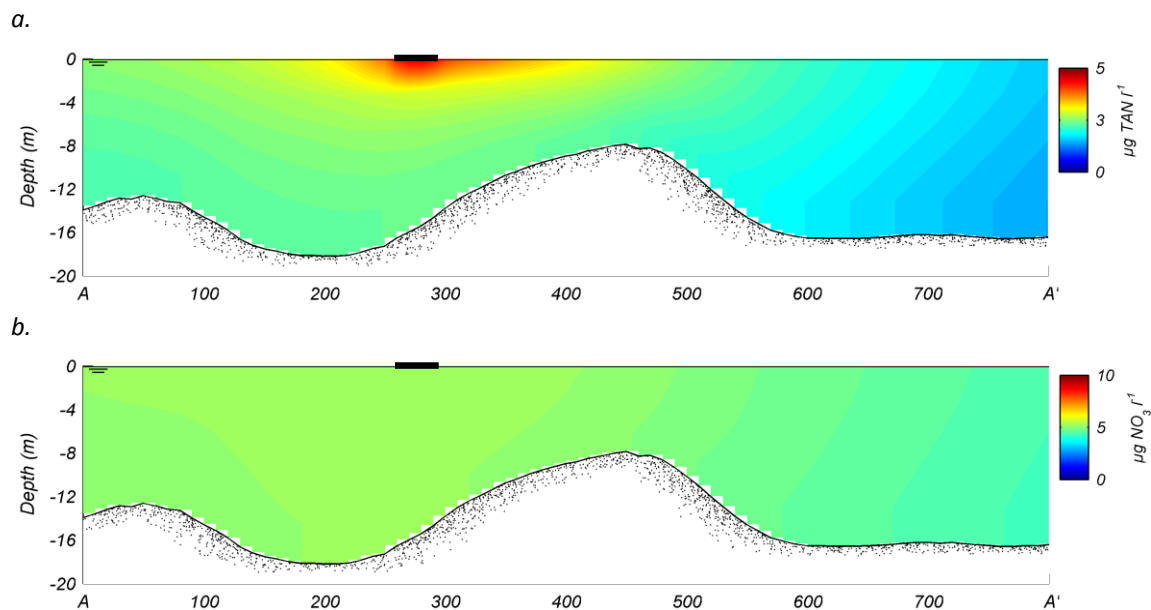


Figure 7.9. Cross sections of simulated TAN and nitrate concentration along transect A- A' TAN (a) and nitrate (b) during neap tide. The farm location is indicated by the bold line.

An attempt is made to assess the environmental impact status of the domain, based on the deviation of TAN and nitrate concentrations from background levels. Potential problem areas were defined as the areas where both ammonium nitrogen and nitrate concentrations are exceeding the natural background levels by more than 50%. This definition is adopted by the Oslo & Paris Commission responsible for the control of eutrophication in its member states (OSPAR 2008). For the assessment, tide averaged concentrations were taken. The 50% threshold was exceeded over an area of 66.9 hectares with average concentrations of $7.2 \pm 1.7 \mu\text{g TAN l}^{-1}$ and $7.2 \pm 2.2 \mu\text{g NO}_3\text{-N l}^{-1}$. Compared to reference background values at the boundaries of the domain, these concentrations represent an enhancement of 252% for ammonium nitrogen and 264% for nitrate.

7.5 Discussion

A water quality model was set up for Pegametan Bay to simulate the fate of dissolved nitrogenous waste from existing floating net cage farms. The nitrogen flux per individual farm was imposed at the corresponding locations. Coupling with the output of the flow model results allowed the simulation of advection and diffusion of inorganic dissolved nitrogen. Grid resolution on both horizontal and vertical were chosen to be in the order of individual farm dimensions. As the main transformation process, nitrification was considered to account for the conversion of ammonium to nitrate.

The used measurements were taken during a dry period, with limited influence of land based discharges or runoff. It should be kept in consideration that land based discharges from rivers and diffuse runoff could have a significant effect on water quality in the bay during the wet season as described by Sulawestian (2008). Adopted samples taken in December 2009, prior to the beginning of the wet season, were more likely to capture the signal of the floating net cage farms. The sampling locations were deliberately chosen at some distance of the farms to eliminate the influence of individual farms. The only difference between the reference stations and the inner bay sampling stations was found for nitrate where mean nitrate concentrations were $1.99 \mu\text{g NO}_3\text{-N l}^{-1}$ for the reference station and $3.25 \mu\text{g NO}_3\text{-N l}^{-1}$ and $5.02 \mu\text{g NO}_3\text{-N l}^{-1}$ for locations P_1 and P_2 , respectively. Even though elevated nitrate levels were not statistically supported when compared to reference levels ($p > 0.05$) it may indicate the enhancement of nitrate rather than ammonium.

Model results reproduced the order of magnitude which was observed by the field measurements taken during a neap tide period at some distance of the farms. These concentrations, however, were in the same order of those found at the model boundaries, i.e. the reference concentrations. Given the limited number of available field data and the assumptions taken regarding the nitrogen flux, the approximated standing stock, time of feeding, water quality model simplifications and measurement errors, model results approach the order of magnitude and will be used to study the general tendencies with respect to the dispersion of dissolved nitrogenous fish farm waste.

Adopting the model settings, it was found that ammonium is enhanced at a local scale and was rapidly dispersed at increasing distance from its source. Mean modeled nitrification fluxes were in the order of $2 \mu\text{g N l}^{-1} \text{d}^{-1}$ and resulted in a rapid conversion from ammonium to nitrate. According to the model results, it is nitrate which is abundantly present within the bay and accumulated in those regions where flushing rates were lowest, i.e. the western and eastern embayments.

The overall impact defined at the area at which 50% of the background level is exceeded for both ammonium and nitrate was adopted from the threshold set by the Oslo-Paris Commission, responsible for the control of eutrophication in its European member states (OSPAR 2008). The affected area of about 67 ha covered a substantial part of the bay.

Even though the enrichment of biologically reactive nutrients is indicated, the magnitude of its biological impact remains uncertain. Although the availability of dissolved inorganic nitrogen (DIN), i.e. ammonium + nitrate, was assumed to be the limiting factor for primary production in the area, no adverse effects of nitrogen enhancement in the water column are known for

Pegametan Bay. Due to the relatively short time scale considered, nutrient uptake through primary production and promotion of phytoplankton growth is not included in the water quality model. From studies in other coral reef systems including the Caribbean, Indian Ocean, the Great Barrier Reef and Red Sea it has been concluded that inorganic nitrogen levels (DIN) chronically exceeding the range of $14 \mu\text{g DIN l}^{-1}$ may lead to increased algal dominance (Lapointe, 1997). In the present study average DIN (ammonium + nitrate) levels within the affected domain did not exceed this threshold.

8 Physical carrying capacity for floating net cage farms

8.1 Introduction

A site suitability analysis identifies the sites which physically allow the placement of floating net cage farms. It provides the physical carrying capacity in terms of the available perimeter which provides favorable conditions to practice a culture of a given species and cage type.

The verification of key physical parameters to predefined suitability criteria is a common method to assess whether a site is suited for floating net cage cultures or not. Such analysis can be conducted for a single farm site through the interpretation of measurements as done by Halide et al. (2009) but proves more effective when applied to a spatial domain with the usage of geographical information systems (GIS) as done by Pérez et al. (2002), Hargrave (2002) and Silvert (1994). The disadvantage of spatial domains is the difficulty to achieve full coverage of the required data in both space and time. This problem has been partly resolved through the application of high resolution numerical flow and wave models which are able to provide required physical information and significantly improve the degree of detail considered in the suitability analysis (Mayerle et al., 2009; Windupranata & Mayerle, 2009). This chapter describes the application of a numerical flow model and wave model for Pegametan Bay. Model results serve the purpose of a site suitability analysis for Pegametan Bay to narrow down the region of interest to the available areas which allow the placement of floating net cage.

8.2 Site suitability analysis

The site suitability analysis was done using physical parameters of water depth, current velocities and waves provided by the numerical models. Criteria for the key parameters adopted for this study as shown in Table 8.1, were previously used for similar purposes by Windupranata & Mayerle (2009) and originate from recommendations for South East Asian floating net cage types (FAO, 1988; FAO, 1989).

Floating net cage cultures require a clearing from the bottom of approximately three to five meters to prevent any contact with the sea bed. Sufficient clearing maximizes water exchange

and prevents the build up of noxious gasses such as H₂S generated by anaerobic decomposition of deposited organic wastes which may affect fish stock health (Beveridge, 2004). Accordingly, for cage depths of three meters, local minimum water depths should thus be at least six to eight meters. In contrast to the minimum depths, maximum depths preferably should not exceed 20 meters, otherwise investment and maintenance costs will be higher as longer anchoring ropes and heavier anchor blocks are required (FAO, 1989). Current velocities should be in the given range to guarantee sufficient exchange of water in the fin fish cages for the supply of oxygen and the flushing of harmful excretory products from the standing stock. However, to prevent excessive strain on the farm structure and fish stress, current velocities should not exceed the range of 0.5 to 1 m s⁻¹. Worst case wave action, corresponding to the acceptable time of occurrence may cause damage to the farm and additionally stress to the fish stock and hence should remain below significant wave height in the range of 0.6 to 1 m.

Table 8.1. Site suitability parameters and criteria for floating net cages.

Parameter	Units	Allowable	Optimum
<i>Minimum water depth</i>	<i>m</i>	<i>> 6</i>	<i>> 8</i>
<i>Maximum water depth</i>	<i>m</i>	<i>< 25</i>	<i>< 20</i>
<i>Maximum current velocity (cage flushing)</i>	<i>m s⁻¹</i>	<i>> 0.05</i>	<i>0.2 - 0.5</i>
<i>Maximum current velocity (exposure)</i>	<i>m s⁻¹</i>	<i>< 1</i>	<i>< 0.5</i>
<i>Worst case significant wave height (exposure)</i>	<i>m</i>	<i>< 1</i>	<i>< 0.6</i>

The necessary statistics for water depth and current velocities were calculated from a 14 day period to provide a representation of flow characteristics which cover the tidal amplitude during a neap-spring-neap tidal cycle for tide dominated areas.

The resulting spatial grids were reclassified, as schematically shown in Figure 8.1, indicating suitability for each grid cell to be allowable (1) or optimal (2) for floating net cage culture. The remaining values, outside of the specified ranges, were classified as unsuited (0). The final suitability for the domain was obtained by a grid overlay of the reclassified grids where the final suitability consists of the average score of all parameters. Each grid cell which did not reach the score “allowable” for one or more parameters was classified as unsuited.

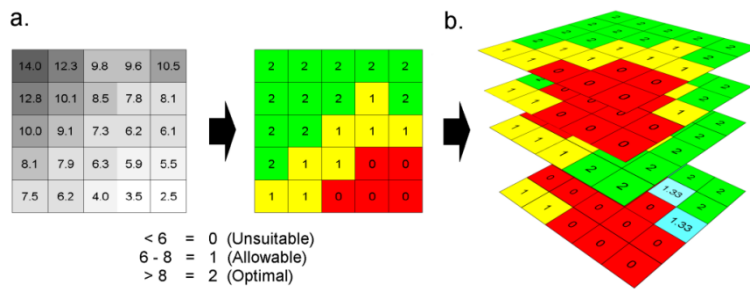


Figure 8.1. Schematic overview of the site selection process exemplarily for minimum water depth criteria. Parameter information is reclassified (a.) followed by an overlay (b.) which yields the averaged suitability score.

Identification of the selected physical parameters for the suitability analysis each resulted in an overview of the domain specifying the unsuited, allowable or optimal perimeters. Critical minimum water depths were found at the reefs and shoreline, leaving suited regions within the two main channels located in the western and centre part of the domain. Additionally, part of the eastern embayment is deep enough to house floating net cage farms (Figure 8.2a). The offshore area and part of the eastern channel is limited by exceeding maximum water depths (Figure 8.2b). In several near shore parts of the study area, current velocities are beyond the range required for the flushing of the farms as defined by the adopted criteria (Figure 8.2c). In particular, current velocities are insufficient in the "pockets" of the western channel as well inside the eastern embayment. Current velocities inside the bay do not reach magnitudes which exceed the maximum allowable strain on the farms (Figure 8.2d). By contrast, in parts of the offshore area currents exceed the permitted magnitudes. The confined nature of the area between the reefs protects the bay from harmful wave action as visible in Figure 8.2e, but shorelines east and west of the area of interest prove to be unsuited due to wave exposure with exception of a small stripe in the eastern embayment.

For the existing farms locations in Pegametan Bay were mostly based on trial-and-error practice with water depth and wave actions as factors observable with the naked eye of the farmers. Similarly, water depth and wave information was used for a first overall site suitability analysis. Here, a total area of 216 hectares covering 6.2% of the entire domain was found to be suited for the common type of floating net cages, ranging between allowable to optimal (Figure 8.3a). The existing farm locations are in good agreement with the identified suited perimeter where most farms are located within or on the edge of the identified suited perimeter.

In a second analysis current velocity was included. Lacking current velocities in the western embayment and in the far most eastern embayment resulted in a reduction of the suited area to 89.2 hectares equal to 2.6% of the entire domain (Figure 8.3b). According to the analysis, four existing farms are located in unsuited areas.

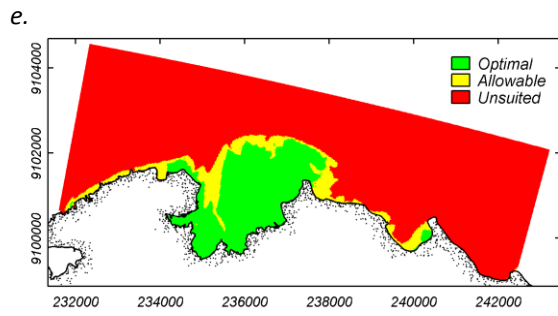
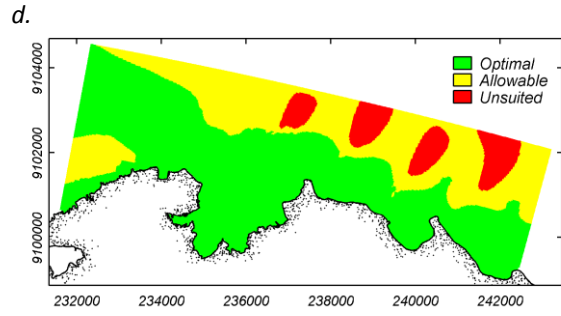
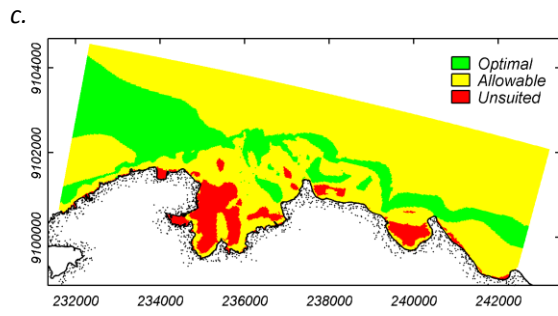
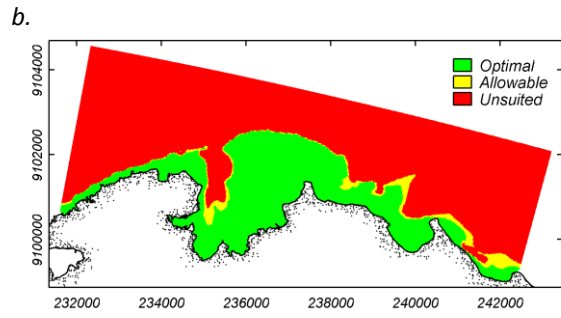
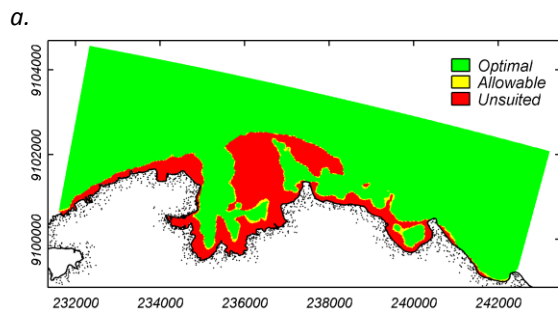


Figure 8.2. Suitability maps for the considered parameters. Minimum water depth (a.), Maximum water (b.), Maximum current velocities for flushing (c.) and Maximum current velocities (d.) during the considered 14 days neap-spring-neap period and wave exposure (e.) during extreme wind conditions based on a 50 year period.

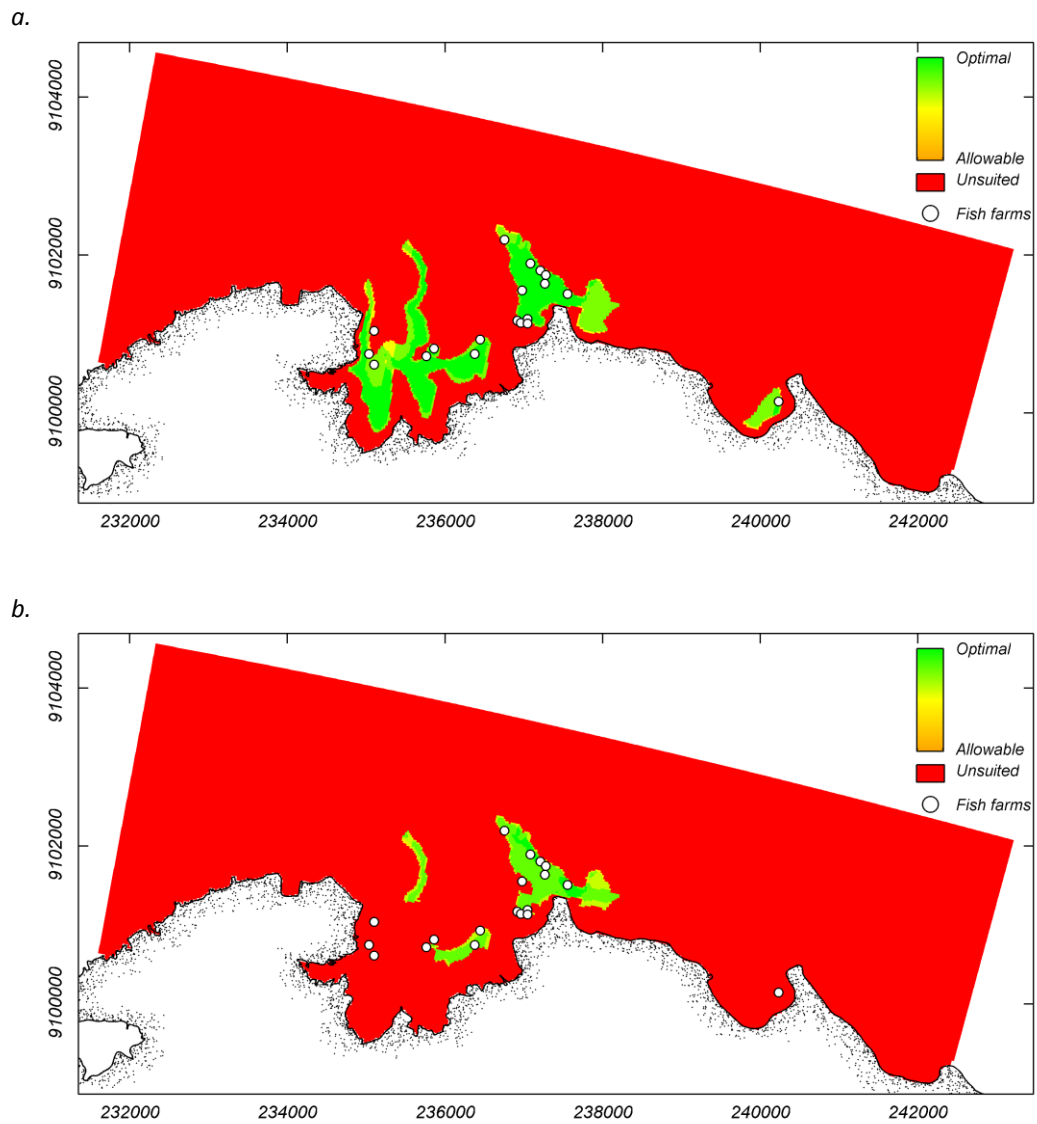


Figure 8.3. Combined suitability maps for floating net cage cultures considering water depth and wave exposure (a) and the additional incorporation of current velocities (b) which narrow down the suited perimeter of the domain. The locations of existing farm (white dots) coincide with suitable depths and waves, however, three farms are situated in low current velocity areas classified as unsuited.

8.3 Discussion

With the use of flow and wave model results, the areas which provided the basic environmental needs for floating net cage farming in terms of the key physical parameters were identified.

From the classification of the individual parameters it became obvious that apart from water depth, the consideration of current velocities with respect to cage flushing and potential wave impact results in a reduced physical carrying capacity of areas which are exposed to the open sea. According to the adopted criteria and the information provided by the flow model, insufficient current velocities dominate the western and far most eastern embayment making them unsuited for the placement of floating net cage farms. The physical carrying capacity found for Pegametan Bay is in good agreement with the locations of existing fish farms when current velocities are not considered. These farms were placed by trial and error since 2001, the year when floating net cages were introduced to Pegametan Bay. When current velocities are considered for determination of the physical carrying capacity, three of the existing farms were situated at sub-optimal sites where reduced current velocities may affect water exchange within the cages and increases risks on fish wellbeing. Lacking current velocities may result in insufficient flushing of the farm leading to an accumulation of potentially toxic compounds such as ammonium or nitrite and a critical decrease in dissolved oxygen levels due to an inadequate oxygen supply which does not cope with the intense respiration rates of the fish culture (Beverige, 2004). The magnitude of these phenomena is, however, not only driven by the environmental characteristics but also by the stocking density and the farm characteristics such as size, net type, shape etc. It therefore may be possible that the chosen criteria for current velocities with respect to cage flushing are taken too conservative, since from the existing farm practice at the time of this study, no adverse effects are known. Alternative criteria used for comparable studies define mean currents exceeding 1 cm s^{-1} (Halide et. al., 2009) to maximum currents exceeding 10 cm s^{-1} as described by the FAO (1988; 1989). The variability of these criteria does indicate that an absolute value for such criteria is difficult to define. Also, the adopted suitability criteria were only specified for key physical parameters and ignored additional parameters which were taken into account by Windupranata & Mayerle (2009) because they were deemed irrelevant for main objectives of this study. Examples of additional criteria are the variability of salinity, temperature, turbidity and water quality parameters such as natural oxygen levels, nitrite and ammonium concentrations, contaminants and pathogens; the occupation of available perimeter for other coastal uses such as traffic lanes, conservation areas, tourism; anthropogenic influences such as waste water discharges from industries and settlements.

9 A best practice strategy to optimize the arrangement of multiple floating net cage farms to efficiently accommodate dissolved nitrogenous wastes

9.1 Introduction

In chapter 7, water quality simulations have shown that due to the semi-enclosed nature of Pegametan Bay ammonium concentrations are enhanced locally but are subsequently dispersed throughout the domain. Because of the relatively small time scale at which ammonium is biologically converted into nitrate, it is nitrate which is spread through the domain. It accumulates in the bay during neap tides and is largely flushed away during spring tides by a residual flow in eastern direction. Persistently enhanced TAN and nitrate concentrations occur in the less flushed confinements where farm effluents cannot be well dispersed. Correspondingly some of the existing farms are situated in regions where current velocities were insufficient according to the adopted criteria for site suitability. Alternative placement of the floating net cage farms thus provides leverage to reduce the enhancement of TAN and nitrate concentrations.

In the present chapter, the water quality model will be used to simulate the fate of floating net cage discharges with respect to TAN and nitrate enhancement for alternative arrangements with respect to farm placement, farm densities and individual farm sizes. From the model simulations, indicators will be analyzed which may contribute to the planning and practice of more sustainable floating net cage mariculture practice.

9.2 Farm placement scenarios

Alternative farm locations are selected by taking in consideration the physical carrying capacity as described in chapter 8, the minimum spacing between individual farms and alternative distribution of a given, constant, holding capacity according to flow characteristics. Current legislation for floating net cage mariculture in Pegametan Bay is regulated by the local authorities of the Buleleng district which harbours Pegametan Bay stating that the regionally permitted farm surface area may not exceed 1% of the total perimeter available for floating net

cage farms (Hanafi, 2008). Currently the available perimeter is only based on the water depth. According to the identified suited area based on the criteria for depth and waves, as described in chapter 8, a total of 1% of the total available area equivalent to 21365 m² is available for floating net cage farms. For cages measuring 3 × 3 × 3 m, an equivalent of 2374 cages can be held with a total volume of 64095 m³. At a stocking density of 7 kg m⁻³ at the end of a grow-out period, the maximum allowable standing stock for the total farm volume would correspond to 448.7 tons with a maximum daily TAN flux in the order of 259.6 kg TAN d⁻¹. Individual farm locations were selected prioritizing the highest suitability. The standing stock of 448.7 tons, corresponding to the permitted regional farm surface area, was distributed over the farms according to three principles. At first, all individual farms were given equal sizes, where each farm had the same standing stock and corresponding TAN discharges. Second, farm sizes were normalized according to the tide averaged current velocity (Figure 9.1a). Third, farm sizes were normalized according to the Reynolds number (Figure 9.1b), an expression to classify the turbulence of a water body based on current velocity (u), water depth (d) and the kinematic viscosity (ν) of water (Equation 9.1).

Equation 9.1
$$Re = \frac{ud}{\nu}$$

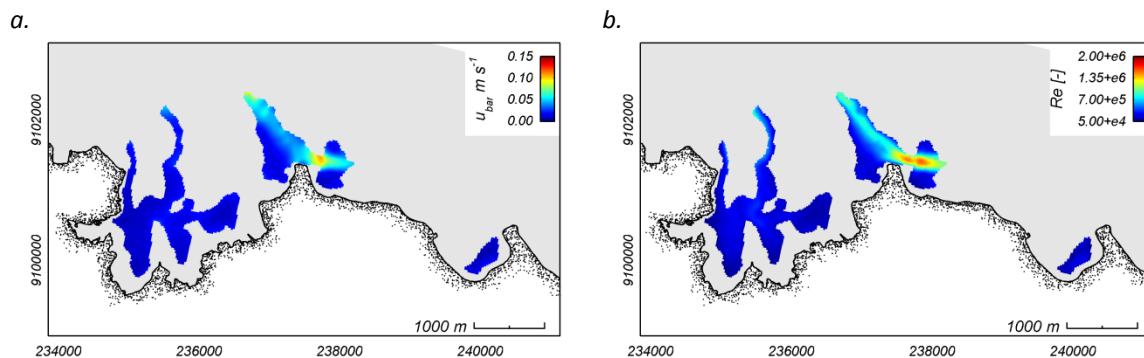


Figure 9.1: Spatial overviews of tide averaged and depth averaged current velocities (a) and tide averaged Reynolds numbers.

a. b.

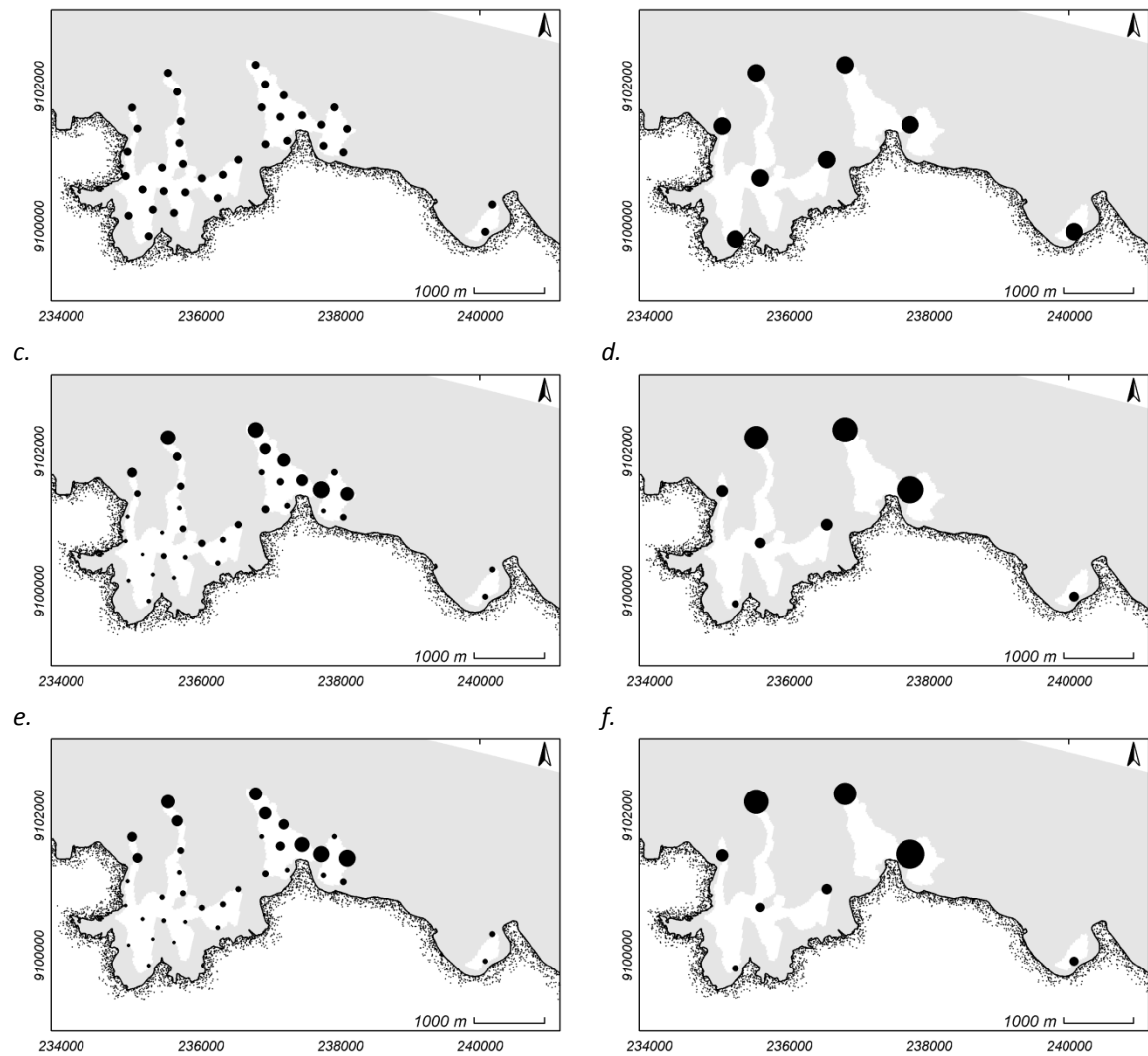


Figure 9.2. Scenarios for alternative farm arrangements within the suited domain.

Two scenarios with minimum separation distances of 300 meters (left) and 900 meters (right). Relative farm sizes are indicated through varying marker sizes for equally sized farms (a + b), farm sizes normalized according to velocity (c + d) and farm sizes normalized according to the Reynolds number (e + f).

In order to account for accumulative effects of discharges, high and low farm density scenarios were defined by keeping a larger and smaller minimum distance between individual farms. Considering the available physical carrying capacity, a clearing between individual farms of 300 and 900 meters were chosen to provide a contrast in farm density for the scenarios. Resulting farm arrangements held 36 and 8 farms, respectively (Figure 9.2) and are described in detail in appendix E.

9.3 Results

9.3.1 Equal farm sizes

For a scenario with high farm density and equally sized farms, i.e. 36 farms distributed over the suitable area with an individual distance of 300 meters (Figure 9.2 a), the model simulation indicates that enhancement of TAN levels occurs in those areas where the aggregation of farms is highest. Since all farms have equal discharges, the relatively high accumulation of TAN in the western embayment is likely caused by lacking current velocities (Figure 9.3 a). For the low density scenario with 8 farms spaced 900 meters apart (Figure 9.2 b), TAN enhancement occurred more localized in the vicinity of the farms because individual farm sizes and corresponding discharges were larger (Figure 9.3 b). Accumulation of TAN in between farms was not as apparent because of the increased spacing. The localized “hot spots” in the western embayment confirm the lack of substantial dispersion in this area whereas equally sized farms elsewhere in the domain show lower impacts (Figure 9.3 b). According to model results, ammonium is nitrified to nitrate at a rate of approximately 0.3 d^{-1} . During the time ammonium is nitrified, it is dispersed away from the farms leaving a dimmed signal of its original source. Nonetheless, nitrate concentrations are elevated at sites where an abundance of ammonium prevails. Nitrate was accumulated in the western embayment for both high- and low farm density arrangements which indicate the importance of the dispersive character of a site (Figure 9.3 c and d).

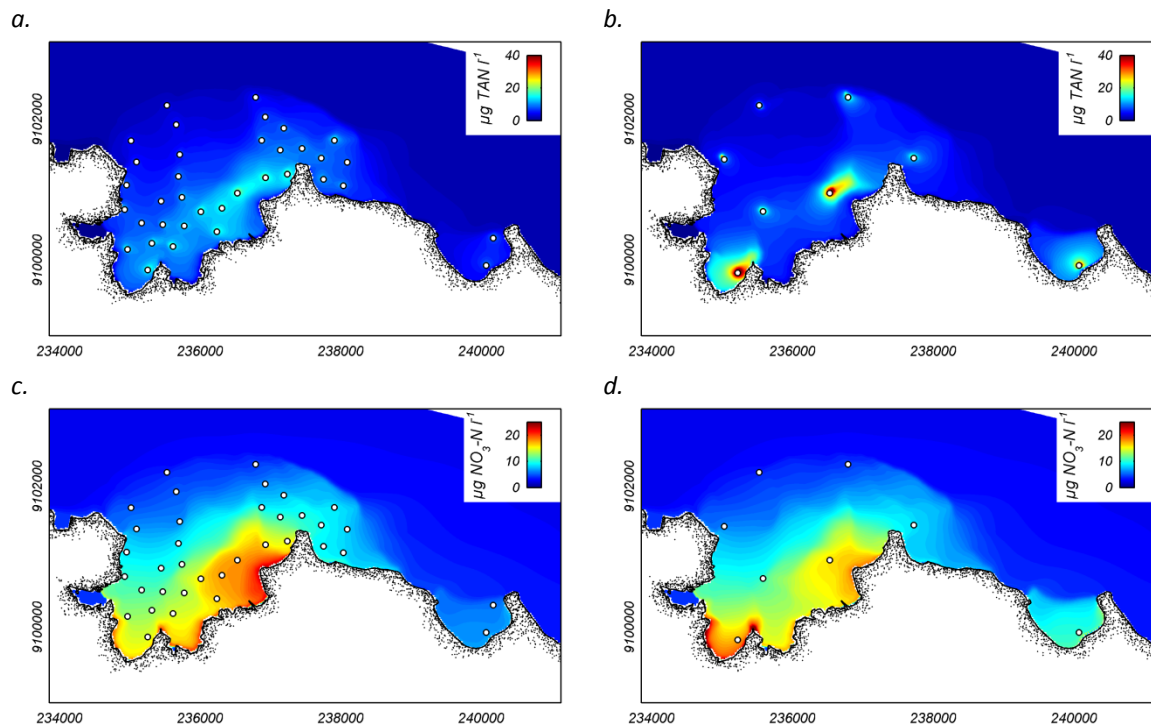


Figure 9.3. Distribution patterns of time averaged vertical TAN and nitrate maxima in Pegametetan Bay for model scenarios with equal farm sizes but different farm densities
 a. High farm density TAN distribution; b. TAN distribution at low farm density; c. High farm density nitrate distribution; and d. nitrate distribution at low farm density. The total standing stock for each scenario is 448.7 tons.

9.3.2 Farm sizes scaled according to current velocities

By scaling farm sizes according to current velocities at each farm site, the weight of the total ammonium discharge was shifted towards the center of the domain. Model results show that by reducing farm sizes in the poorly flushed areas the pressure with respect to TAN enrichment is relieved. The better flushed regions on their turn assimilated the bulk of the ammonium (Figure 9.4 a and b). Similar to the equal farm size scenario, the scaled low density scenario, i.e. placing fewer but larger farms led to an increase in localized TAN concentrations in the direct vicinity of the farms.

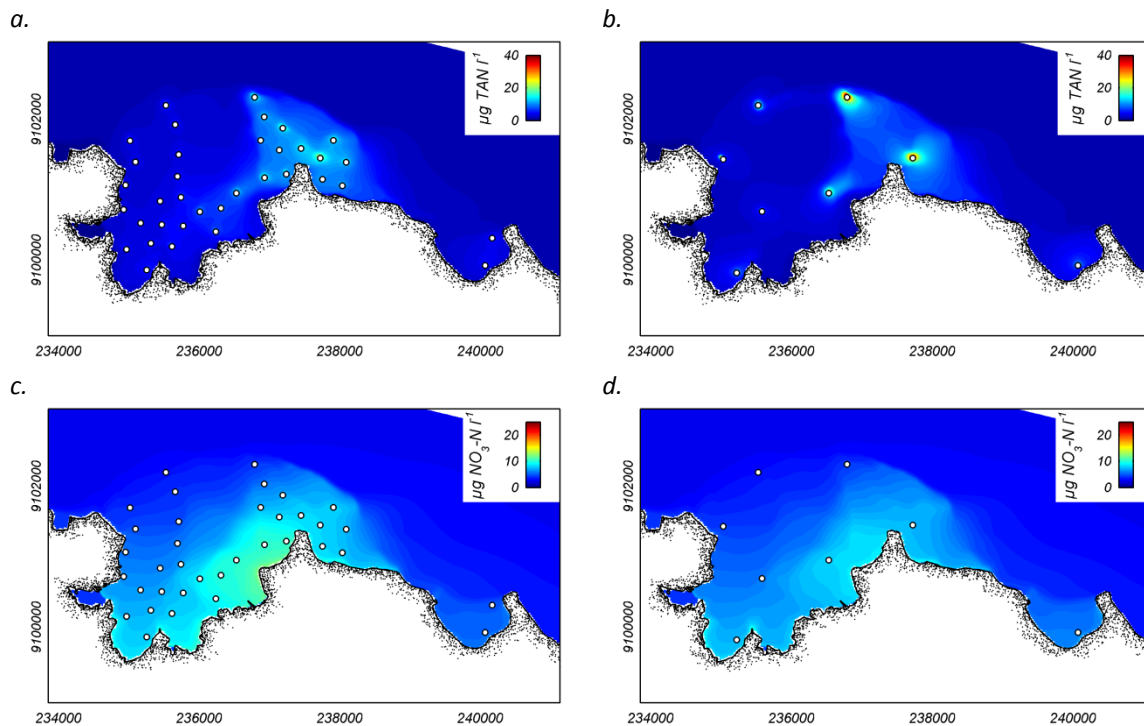


Figure 9.4. Distribution patterns of time averaged vertical TAN and nitrate maxima in Pegamet Bay for model scenarios with farm sizes normalized according to current velocities at different farm densities a. High farm density TAN distribution; b. TAN distribution at low farm density; c. High farm density nitrate distribution; and d. nitrate distribution at low farm density. The total standing stock of each scenario is 448.7 tons.

The pattern of nitrate is strongly governed by the dispersion of ammonium and the quantitative relation between nitrification and nitrate dispersion. This can be drawn from the phenomena that nitrate is abundantly found in the poorly flushed western embayment, even though the bulk of total ammonium discharges was transported away from the bay (Figure 9.4 c and d). This accumulation was primarily caused by the discharges of the downsized farms present in this poorly flushed area, which allocates over time to nitrification of ammonium. The relatively low nitrate concentrations in the well flushed regions indicate the effective transport of ammonium and nitrate away from the domain by the predominantly eastern residual flows.

9.3.3 Farm sizes scaled according to Reynolds numbers

Normalization of the farm sizes according to the local Reynolds number resulted in minor changes when compared to the scenarios where current velocities were used as a criterion for the distribution of the standing stock (Figure 9.5). Some farms at sites holding favorable current velocities were decreased in size because of their shallow water depth while other locations with lower current velocities gained in farm size because of their larger depths. Model simulation of

both high and low farm density scenarios indicated only minor differences in the resulting patterns of TAN and nitrate concentrations.

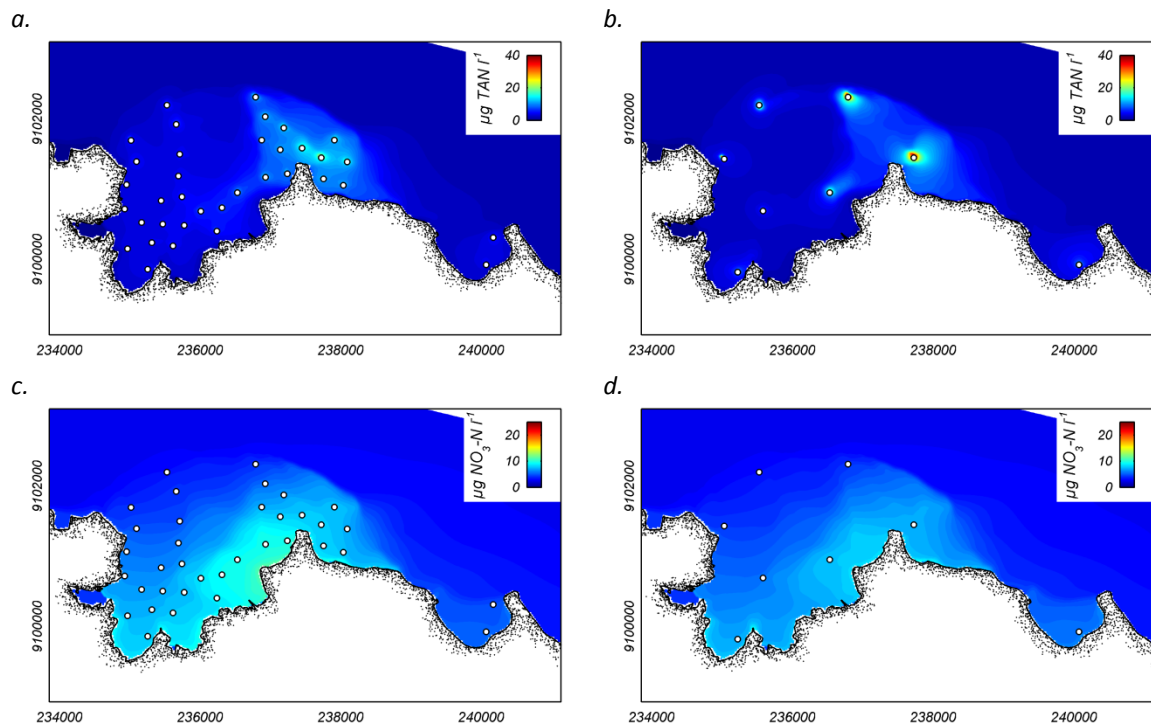
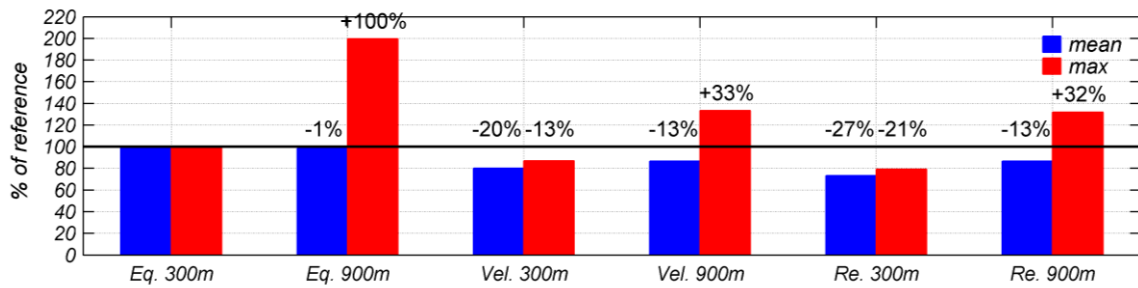


Figure 9.5. Distribution patterns of time averaged vertical TAN and nitrate maxima in Pegametan Bay for model scenarios with farm sizes normalized according to Reynolds numbers at different farm densities a. High farm density TAN distribution; b. TAN distribution at low farm density; c. High farm density nitrate distribution; and d. nitrate distribution at low farm density. The total standing stock of each scenario is 448.7 tons.

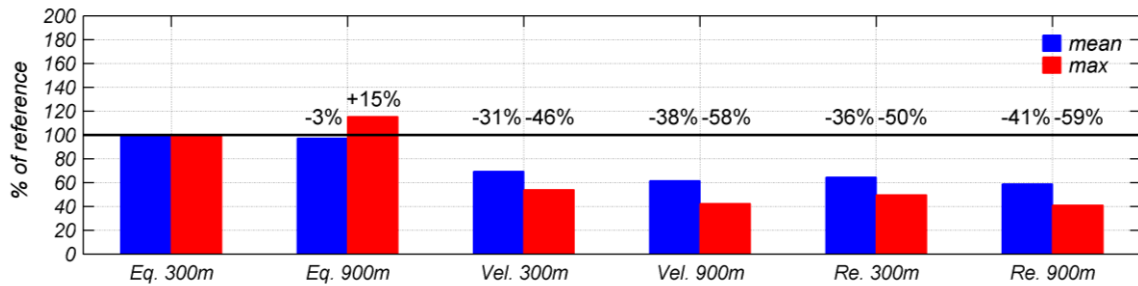
9.3.4 Comparing the overall impacts

In order to compare the overall impacts results from farm arrangements of the different scenarios, time averaged concentrations of TAN and nitrate in the domain were taken. The affected area was defined as the area where both ammonium and nitrate concentrations exceed background concentrations by 50%, representing thresholds of 2.1 g TAN l^{-1} and $1.99 \text{ g NO}_3\text{-N l}^{-1}$. Within the affected area, average TAN and nitrate concentrations were assumed to characterize the overall impact on the domain. In addition the maximum concentrations for both TAN and nitrate within the domain were compared (Figure 9.6 & Appendix F).

a. Ammonium



b. Nitrate



c. Affected area

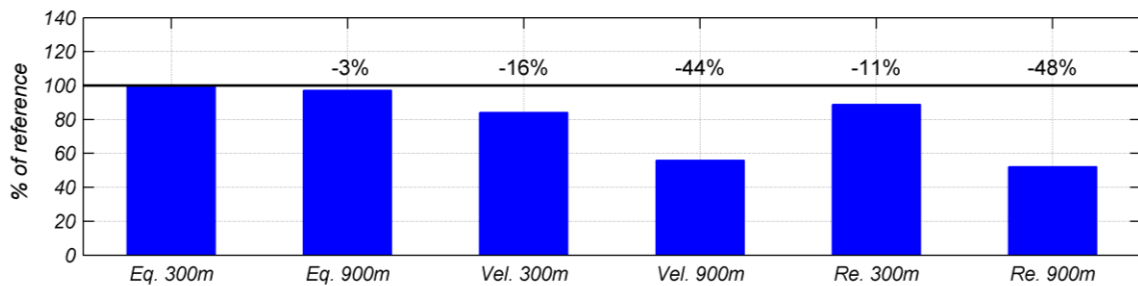


Figure 9.6. Comparison of the overall impact of results from the different farm arrangements.

Mean and maximum TAN (a) and nitrate (b) levels within the affected area (c) relative to the reference scenario.

Compared to the equal farm sizes / high farm density (i.e. 300 separation distance) scenario as a reference, localized TAN and nitrate enhancement was twice as high for the scenario with equal farm sizes at a low farm density (i.e. 900 m separation distance) scenario. By contrast, the extension of the affected area and the overall impact on the area in terms of average TAN and nitrate concentrations was not significantly different. For the equal farm size scenarios, it can be thus stated that many small farms are preferable over few larger farms in order to mitigate local TAN enhancement.

Scaling of the individual farm sizes according to the local current velocities yielded a substantial reduction of TAN and nitrate levels especially in the high farm density scenario since the bulk of the discharges was released in a relatively well flushed region and poorly flushed regions received a relatively small share of the farm effluents. The average TAN concentrations within

the impacted area showed a decrease of 20% and local maximum concentrations were reduced by 13% when compared to the reference scenario. Instead of being accumulated, nitrate was transported away by the predominantly eastern residual flow resulting in an overall reduction of mean nitrate levels of 31%, where the peak concentration was even reduced by 46%. The affected area was decreased by 16%. By contrast, when dividing the total standing stock over a reduced number of scaled farms, the maximum TAN concentration increased by 33% when compared to the reference scenario, whereas the mean TAN levels decreased by only 13%. However, placement of few larger farms at better flushed locations enhanced mass transport, minimized retention time and led to a substantial decrease in mean and maximum nitrate concentrations, accounting for 38% and 58%, respectively. Also, the affected area of the low farm density scenario scaled according to current velocities established a significant reduction of 44%.

For a farm sizes scales according to the Reynolds number arranged at a high farm density, maximum TAN concentrations were reduced by 21% while overall impacted ammonium levels decreased by 27%. The reduction in maximum and mean nitrate concentrations accounted for 50% and 36%, respectively. The impacted area, however, was reduced by only 11%.

Compared to the reference scenario, the most effective reduction was observed for the low farm density scenario with scaling of farm sizes according to the Reynolds numbers. Even though maximum localized TAN concentrations were increased by 32%, a 13% reduction in overall TAN levels was achieved. Maximum and overall nitrate concentrations even decreased by 59% and 41%. The affected domain was reduced by 48%, thus yielding the lowest impact of all scenarios tested.

Considering the high degree of reduction in average dissolved nitrogen levels (TAN and nitrate), i.e. 59%, and the considerable decrease of the impacted area, a farm arrangement with low farm density and a scaling of farm sizes according to the Reynolds numbers prove to be the best practice to minimize the impact of dissolved nitrogenous fish farm wastes in the area.

9.4 Discussion

A number of scenarios with different farm arrangements were simulated using the water quality model for Pegametan Bay. Within the current legislative boundaries of Pegametan Bay, a maximum permitted standing stock of 448.7 tons was distributed over a high and low farm density arrangement containing 37 and 8 farms, respectively. The distribution of the maximum standing stock over the available farms was tested according to three principles: equally sized

farms, normalization of farm sizes according to locally occurring current velocities and normalization of farm sizes according to locally occurring Reynolds numbers.

Model results show that the consideration of the dispersive character and the distribution of the defined standing stock towards better flushed areas provide a significant reduction of nitrogen levels compared to scenarios where the total standing stock is distributed equally over the available farms.

Within Pegametan Bay, distinct pockets are sensitive to accumulation of discharged nitrogen from farm effluents, which due to nitrification of ammonium, is most abundant in the form of nitrate. Allocation of the total standing stock towards the better flushed regions results in an optimized usage of the area's specific dispersive character. Vice versa, avoiding nutrient discharges into poorly flushed regions minimizes accumulation, thus resulting in an overall lower impact. Relative to scenarios with equal farm sizes, the shift towards better flushed areas resulted in a reduction of the impacted area by 16% to 44% when scaling farm sizes according to current velocities, and 13% to 48% when scaling farm sizes according to the Reynolds numbers.

Since high farm densities allow small sized farms distributed over the available perimeter, maximum local TAN concentrations could be reduced by 21%. By contrast, few but bigger farms at optimally flushed sites allow the bulk of the emission to be dispersed from few "hotspots" with the disadvantage of locally increased TAN levels by 32% within the direct vicinity of the farms.

10 Environmental carrying capacity

10.1 Introduction

So far, the physical carrying capacity for floating net cages and the relative farm sizes have been addresses. The actual size of each individual farm is based on the relative farm sizes and the environmental carrying capacity, which is defined as the maximum allowable standing stock within a region with no degradation beyond the resilience capacity of the environment. (Soto et al. 2008). The environmental capacity is in this case considered with respect to the amount of dissolved nitrogen that an environment can assimilate.

10.2 Determining the environmental carrying capacity

The environmental carrying capacity with respect to dissolved nitrogenous farm effluents was determined using a modified approach as proposed by (Weston, 1986) applied to the Pudget Sound, Washington State. Weston's method determines the environmental capacity based on the natural dissolved nitrogen flux defined for individual embayments. The environmental capacity is defined as the standing stock who's corresponding dissolved nitrogen discharge does not exceed 1% of the natural nitrogen flux (N_{flux}) of a predefined area, calculated from the cross-boundary flows (Q) and total dissolved nitrogen reference concentration (C_{TDN}) as shown in Equation 10.1.

Equation 10.1.
$$N_{flux} = QC_{TDN}$$

In contrast to the original approach, this study used the physical carrying capacity as spatial boundaries for the determination of the natural nitrogen flux and environmental capacity.

Cross-boundary flows were extracted from the flow model for each individual domain of the physical carrying capacity of two scenarios: Consideration of waves, water depth and current velocities (Figure 10.1a); and consideration of waves and water depth (Figure 10.1b). The latter, excluding current velocities was chosen since lacking current velocities are critical for the well

being of cultured fish but is strongly dependent on the size of the farm and amount of cultured fish.

Natural total nitrogen fluxes were calculated based on a natural total dissolved nitrogen background concentration of $133.7 \pm 4.22 \mu\text{g TDN l}^{-1}$ as defined in chapter 4. The environmental carrying capacities were determined based on discharges of 0.58 kg TAN per ton of fish corresponding to a stocking density of 7 kg m^3 at the end of a grow out period as described in Chapter 6.

For the first scenario, averaged daily inflows for each selected perimeter were in the order of $3.2 \cdot 10^{+7}$, $1.29 \cdot 10^{+7}$ and $5.4 \cdot 10^{+6} \text{ m}^3 \text{ d}^{-1}$. The resulting nitrogen flux was in the order of 4288 ± 1353 , 1722 ± 544 , and $724 \pm 228 \text{ kg N d}^{-1}$. Environmental carrying capacities of 74 ± 23 , 30 ± 9 , 13 ± 4 tons were found summing up to a total of 116 ± 37 tons when physical carrying capacities were determined based on current velocities, water depth and waves (Figure 10.1a).

Similarly, for the second scenario, averaged daily inflows for each selected perimeter were in the order of $3.44 \cdot 10^{+7}$, $3.28 \cdot 10^{+7}$ and $2.5 \cdot 10^{+6} \text{ m}^3 \text{ d}^{-1}$. Nitrogen fluxes were in the order of 4596 ± 1451 , 4384 ± 1384 and $331 \pm 105 \text{ kg N d}^{-1}$. Environmental carrying capacities of 79 ± 25 , 76 ± 24 , 6 ± 2 tons were found with a total of 161 ± 51 tons when the considered areas correspond to physical carrying capacities, determined based on water depth and waves only (Figure 10.1b).

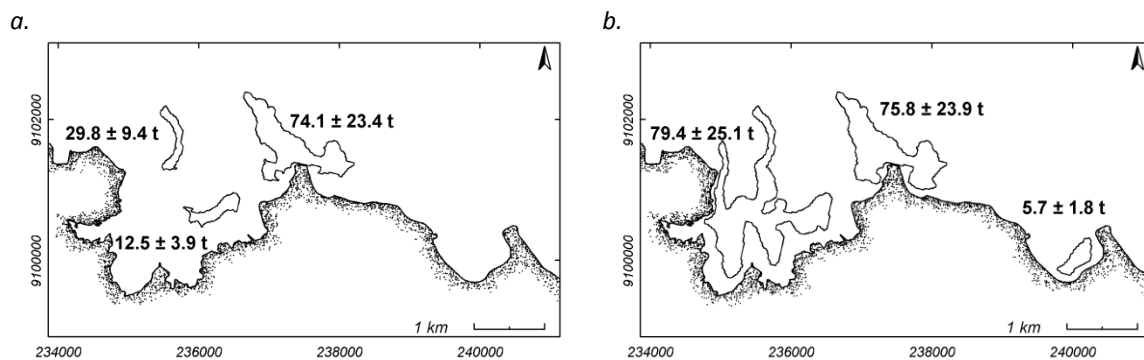


Figure 10.1. Carrying capacities for each suited domain according to the 1% nitrogen flux method (Weston, 1986). An environmental carrying capacity of 116 tons was found when physical carrying capacities were determined based on current velocities, water depth and waves (a) and an environmental carrying capacity of 161 tons was found when physical carrying capacities were determined based on water depth and waves only (b).

10.3 Model simulations

As outlined in chapter 9, using the distribution of Reynolds numbers to determine the relative scaling farm sizes resulted in the highest reduction of affected area and domain averaged concentrations. Accordingly, optimized farm arrangements were proposed for Pegametan Bay where carrying capacities, determined by the 1% flux method, were distributed over the

corresponding suited areas. Taking into consideration the suitable area based on the analysis of water depth waves and current velocities (Figure 10.1a), a total of 116.4 tons standing stock was distributed over the farms assuming a high and a low farm density scenario with 16 and 4 farms, respectively, as indicated in Figure 10.2 a and b.

Model results indicate that, at a high farm density, the average concentrations within an affected domain of 97.1 hectares were in the order of $3.7 \pm 1.1 \mu\text{g TAN l}^{-1}$ and $4.2 \pm 1.3 \mu\text{g NO}_3\text{-N l}^{-1}$. Such concentrations imply that within the affected area the background concentrations are exceeded by 80 and 111% for TAN and nitrate, respectively. Fewer but larger farms experienced domain averaged concentrations of $4.1 \pm 1.5 \mu\text{g TAN l}^{-1}$ and $4.1 \pm 1.1 \mu\text{g NO}_3\text{-N l}^{-1}$ within an affected area of 82.5 hectares. Domain averaged impacts were in the order of 100% and 106% above background levels for TAN and nitrate.

Similarly, taking into consideration the physical carrying capacity based on the analysis of water depth and waves (Figure 10.1 b), a total of 160.9 tons standing stock was distributed over the farms assuming a high and a low farm density scenario with 36 and 8 farms, respectively, as indicated in Figure 10.3 a and b.

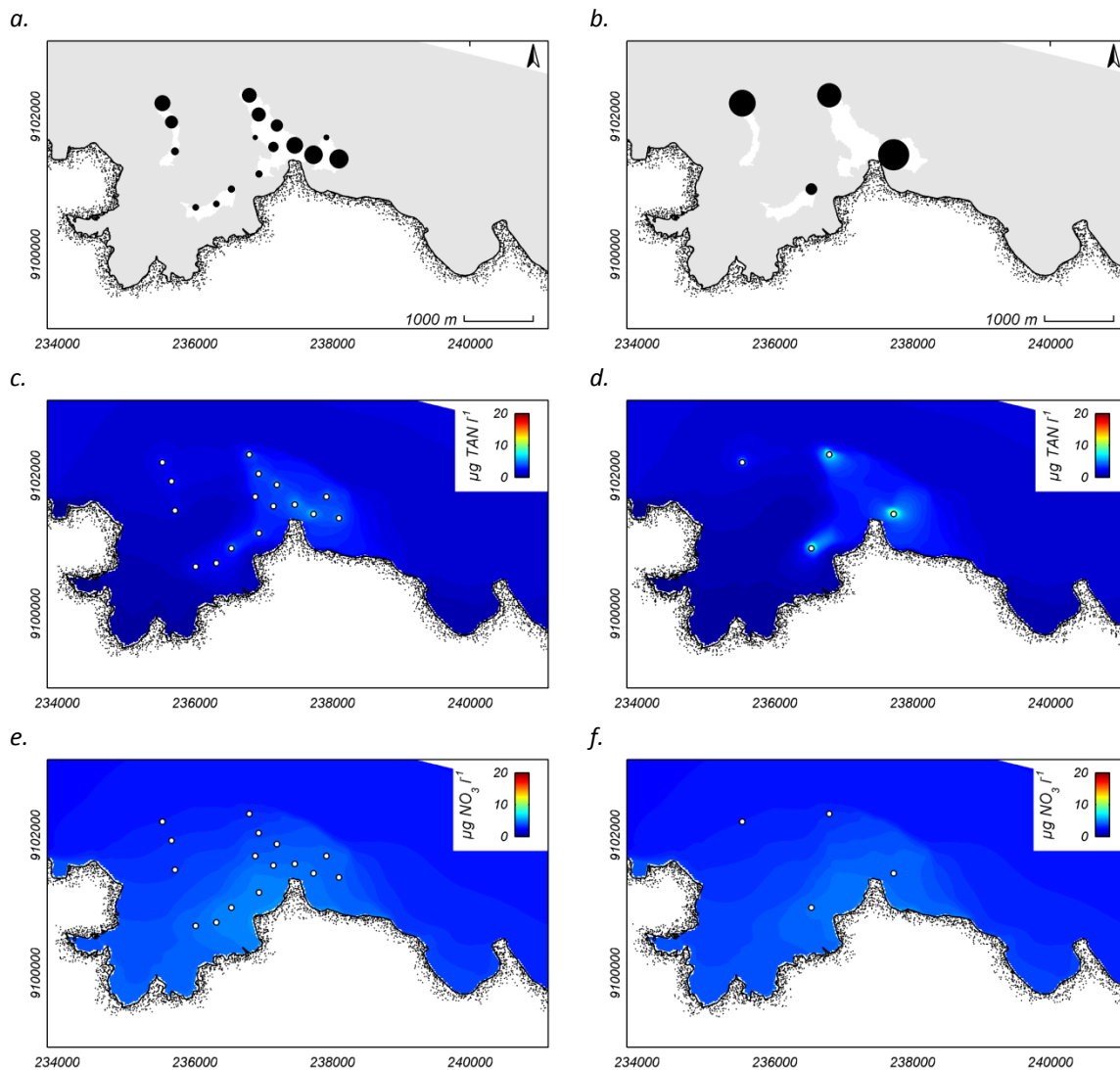


Figure 10.2. Farm distributions and simulated nutrient gradients for an environmental capacity of 116 tons. Two scenarios with minimum distances of 300 meters (a) and 900 meters (b) hold individual farm situated in a perimeter equal to the physical carrying capacity determined based on current velocities, water depth and waves and normalized according to the Reynolds number. Ammonium concentrations of both scenarios (c and d) and nitrate concentrations (e and f).

Water quality model results indicate that, at a high farm density, the average concentrations within an affected domain of 137.9 hectares were in the order of $3.7 \pm 0.9 \mu\text{g TAN l}^{-1}$ and $4.4 \pm 0.75 \mu\text{g NO}_3\text{-N l}^{-1}$. Such concentrations imply that within the affected area the background concentrations are exceeded by 76 and 121% for TAN and nitrate, respectively. Fewer but larger farms experienced domain averaged concentrations of $4.1 \pm 1.4 \mu\text{g TAN l}^{-1}$ and $3.9 \pm 0.6 \mu\text{g NO}_3\text{-N l}^{-1}$ within an affected area of 88 hectares. Domain averaged impacts were in the order of 95% and 96% above background levels for ammonium and nitrate.

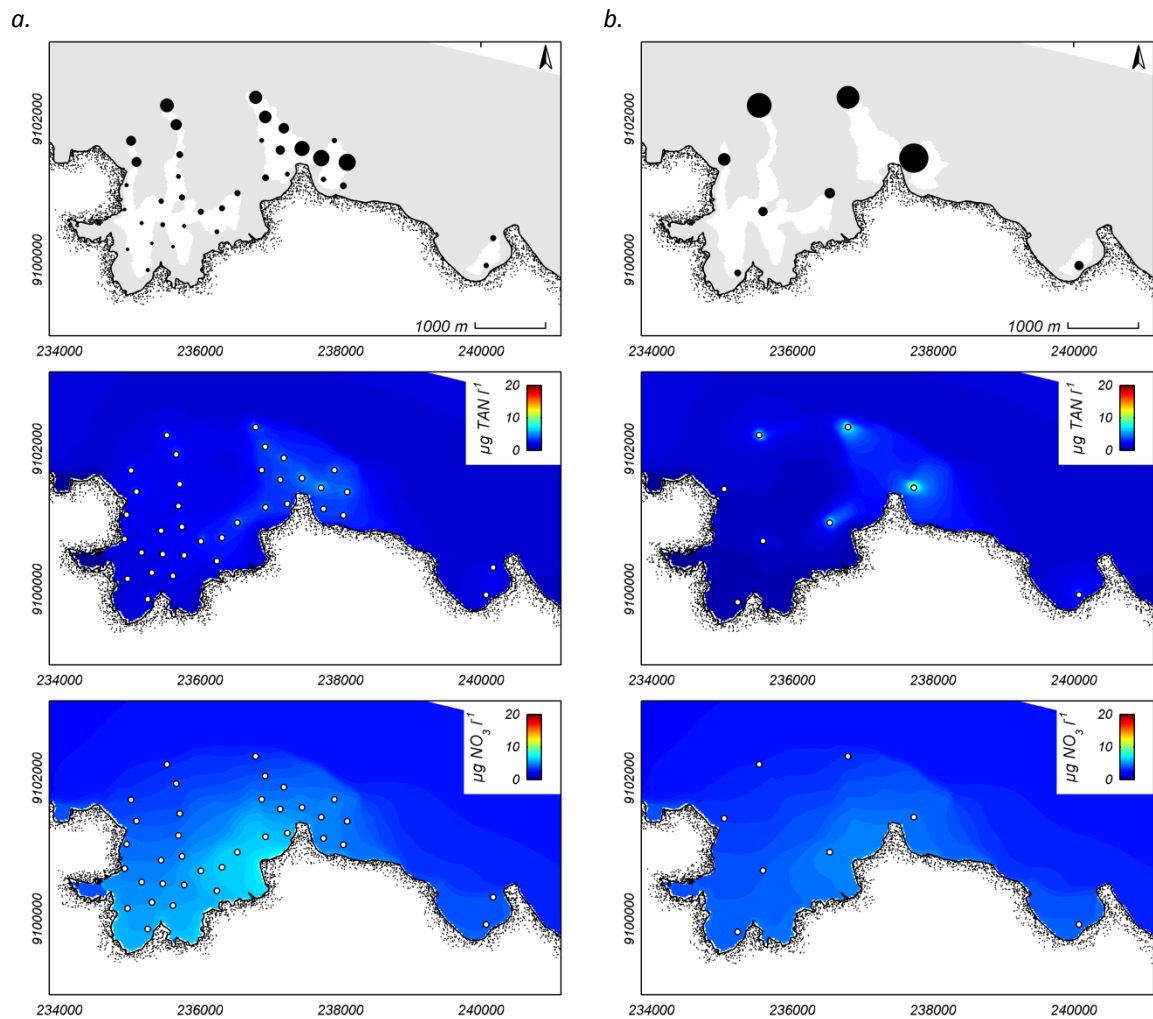


Figure 10.3. Farm distributions and simulated nutrient gradients for an environmental capacity of 161 tons. Two scenarios with minimum distances of 300 meters (a) and 900 meters (b) hold individual farm situated in a perimeter equal to the physical carrying capacity determined based on water depth and waves and normalized according to the Reynolds number. Ammonium concentrations of both scenarios (c and d) and nitrate concentrations (e and f).

A comparison between modelled optimized arrangements for different standing stocks indicate that the differences between resulting ammonium concentrations are similar and overall nitrate concentrations was even 5% lower even though a larger standing stock was defined. Impacts however were not lower with respect to the affected area. A larger standing stock does result in a 7 to 42% increase of the affected area for low and high farm density scenarios, respectively.

10.4 Discussion

With the chosen method to determine the environmental carrying capacity, the size of the considered domains showed that larger physical carrying capacities are likely to provide a larger flow rate and hence a higher nitrogen flux and environmental carrying capacity. Model results showed minor difference between resulting ammonium or nitrate concentrations for standing

stocks of 116 and 161 tons. This indicates that farm the distribution of standing stock over the optimized farm arrangements using the Reynolds number as an indicator managed to assimilate the arising dissolved nutrient loads.

Coupling the determination of the environmental carrying capacity to the physical carrying capacity provides a proportional impact with respect to the impacted area.

11 Discussion

In the present study it was shown how numerical flow, wave and water quality modelling techniques were used to define a strategy to optimize the farm arrangement to minimize the impact of dissolved nitrogenous emission from floating net cage farms. Illustratively, Pegametan Bay was used as a pilot study site. To do so, the set up of the models and different aspects of floating net cage farm including the determination of the physical carrying capacity, optimizing farm arrangements and determination of the environmental carrying capacity were and will be discussed in the following section.

11.1 The physical carrying capacity for floating net cage farms

Flow and wave model results provided the basis for a suitability analysis to determine the physical carrying capacity. This technique already proved to be very effective to reduce a region of interest to those perimeters which are actually suited for the intended type of floating net cage cultures (Windupranata & Mayerle, 2009). For the study area, most of the physical carrying capacity lies in the confined areas of Pegametan Bay. This is mostly due to the considerations taken to account for wave exposure for those areas that are exposed to the open sea and wave fields approaching the north Bali shoreline. The present reefs provide protection to the inner perimeter of Pegametan Bay. Within the bay itself, it is a combination of the shallow reef and the consideration of current velocities which mostly affect the physical carrying capacity. By taking into account more parameters and corresponding criteria, a more conservative approximation will follow with a reduced risk of mishaps but at cost of physical carrying capacity. When considering water depth and wave impact, the identified suited areas match with the placement of existing farms, which were positioned by trial and error experience of the farmers (Hanafi, 2008). Additional incorporation of current velocities resulted in a more conservative selection of available perimeter and indicated a sub-optimal placement of some of the existing farms which were not identified by current planning practices.

Adequate local current velocities provide better water exchange of the floating net cages allowing a higher supply of oxygen and more effective removal of effluents at farm level and reduce the risk of disease to the farmed standing stock (Beveridge, 2004). Current velocities are

considered as an important prerequisite for a farm site (Halide, 2009). However, risks caused by insufficient flow of water through a fish farm is not only dependent on the local current velocities but also on the farm size and layout of a floating net cage farm and the resulting drag acting on the local water movement. Site selection criteria with respect to required current velocity should therefore be specified for each individual farm layout which is left out of consideration in this study.

The adopted criteria for key physical parameters are common for traditional South East Asian semi-intensive cultures (FAO, 1989) but have to be redefined when dealing with other cage types with different dimensions and characteristics with respect to allowable exposure to currents and waves. The choice of different cage types will result in a different physical carrying capacity of the considered region.

Apart from physical parameters used for this study, other coastal planning related parameters are mostly region specific. Additional criteria (FAO, 1989; Windupranata & Mayerle, 2009; Halide, 2009) took the interests of other coastal uses into consideration. Examples are the presence of traffic lanes, marine protected areas or fishing grounds. The presence of fish farms may be undesired on an aesthetic level. Touristic areas, as found along the North Bali coast, have a major importance to the local economy and may conflict with floating net cages. Also, natural or anthropogenic discharges are of importance for critical factors such as turbidity, pollutants or pathogens, which affect the stock and food safety when fish farms are placed in the vicinity of urban areas or estuaries (FAO, 1989). Each considered criteria will affect the resulting potential fish farming area and thus the possibilities for development of fish farms. A suitability study considering an extended list of criteria should comply with the regional interest of the various actors to safeguard environmental and socio-economic sustainable coastal usage. To test various arrangements of floating net cage farms, the physical carrying capacity was determined based on allowable water depth and wave impact only.

11.2 Optimizing farm arrangements

Water quality simulations were done for the pilot study area Pegametan Bay to illustrate the behaviour and fate of dissolved nitrogenous wastes from floating net cage fish farms.

Flow model results provided the backbone of the water quality model with definitions of water depths and current velocities in both space and time. Uniform stocking densities and idealized farm operation resulted in dissolved nitrogen fluxes which accounted for the nitrogen discharges released in the model. In reality, every floating net cage farm is managed differently and differences in emissions, due to amongst others: varying stocking densities, food quality of

farmer skills, may occur. Nonetheless, quantified nitrogen flux were approximated based on the fish culture information of Tiger grouper (*Epinephelus fuscoguttatus*) the most common fish species from the study site and show a resemblance within the wide range of nitrogen flux from existing literature.

Considering the relatively short time scale of the simulated period, potential biological responses regarding the nitrogen uptake by primary producers, remineralisation and denitrification were neglected. Ammonium and nitrate were taken as indicators for environmental impact under the assumption that nitrogen in tropical coastal systems is mostly considered to be the limiting nutrient for eutrophication (Howarth & Marion, 2006).

The water quality model was calibrated based on measurements taken during a dry period, minimizing disturbance from natural and anthropogenic land based sources. A clear signal with respect to dissolved nutrients from the existing floating net cages was not captured since there was no statistically significant difference between concentrations of ammonium or nitrate in the domain centre and offshore reference concentrations. Nonetheless, averaged nitrate concentrations within the bay were slightly higher than those found at the reference stations.

The measured nutrient concentrations were generally low which could indicate little impact of existing floating net cages but also land based sources such as the existing shrimp farms. This view may change during wet seasons where land based discharges may surpass the nutrient enhancement as a result of fish farm activities (Sulawestian, 2008). The land based discharges are specific for Pegametan Bay and their influence are beyond the scope of this study.

The water quality model reproduces ammonium and nitrate concentrations which are within the order of magnitude of those concentrations measured. Simulations of the existing farm arrangement showed a tendency of accumulation of ammonium and nitrate around those fish farms situated in poorly flushed pockets.

From various simulated farm arrangement scenarios where individual farm sizes were scaled according to local dispersive characteristics with the Reynolds Number as an indicator, the impacted area, defined as the area where background concentrations are exceeded by 50%, was reduced by up to 48% and the average ammonium and nitrate concentrations within the affected domain were reduced by 27% and 41%, respectively, relative to a non-optimized farm arrangement with the same total standing stock. Applying the same scaling, using current velocities produced similar results with slightly less mitigation of ammonium, nitrate and affected area. Based on this result, the Reynolds number is adopted to be the best indicator for the scaling of relative farm sizes within an area.

The farm density was determined based on the physical carrying capacity and a uniform spacing between individual farms, for the scenarios illustratively taken to be 300 and 900 meters.

Maximum impact reduction in terms of impacted area and nitrate concentrations were achieved using a low farm density i.e. a large spacing between farms situated in the suited perimeter. Larger farms however will face a higher localized impact of ammonium which may become toxic to cultured fish when concentrations reach $500 \mu\text{g l}^{-1}$ (FAO, 1989). By contrast, a larger number of smaller farms result in lower localized ammonium concentrations, slightly higher nitrate concentrations but affect a much larger area.

11.3 Environmental carrying capacity

The maximum allowable standing stock for Pegametan Bay was determined according to the local legislative procedure and constitutes an effective farm surface equal to 1% of the physical carrying capacity (Hanafi, 2008). The corresponding standing stock accounts of 448.7 tons and was calculated assuming a cage depth of three meters and a stocking density 7 kg m^{-3} . When different stock properties or site suitability criteria apply, the resulting maximum standing stock will differ accordingly. This method lacks a constructive basis which does not consider potential environmental impacts.

Instead, a maximum standing stock was determined based on the 1% nitrogen flux method as modified from Weston (1986). This method has been applied to Pegametan Bay considering the bay as a whole, yielding an environmental capacity of approximately 700 tons per year (Wulp, et. al., 2010).

By contrast, this study has determined the nitrogen flux on the basis of the available physical carrying capacity and resulted in a total allowable standing stock of 116.4 tons when the physical carrying capacity is determined based on water depth, wave impacts and current velocities; and 161 tons for a physical carrying capacity which is determined by water depth and waves only. These standing stocks would correspond to annual production rates of 137 and 190 tons per year when a grow-out period of 310 days is considered. The same analysis is shown in Mayerle et. al. (2011) using similar considerations to determine the physical carrying capacity.

The discrepancy between the outcome of Wulp et. al. (2010) and this study indicates the sensitivity of this method on how the spatial boundaries are defined. In contrast to confined marine systems such as estuaries, sounds or lagoons, semi-confined and open embayments do not have clear physical boundaries separating them from the sea. Assumable, larger domains have higher cross boundary flows. Increasing cross-boundary flows increase the natural nitrogen flux and thus the derived environmental carrying capacity. Since only part of an embayment

such as Pegametan Bay is suited for floating net cage farms, defining a larger domain, would result in a high environmental carrying capacity, a production intensity which has to be fit in the perimeter which provides favourable conditions for floating net cage farms, equal to the physical carrying capacity. This may result in higher fish production rates within a relatively small perimeter which on its turn will cause a stronger localized dissolved nitrogen concentration enhancement.

By linking the determination of the environmental carrying capacity to both the water exchange and natural background concentrations of the region, adaptation to physical and biochemical properties of an area are considered, making this method applicable to any region. When the physical carrying capacity is included and the considered perimeter of the spatial boundaries become smaller, a more conservative environmental carrying capacity is found.

The 1% nutrient-flux assumption lacks a constructive scientific explanation and is defined as: "an increase of small enough magnitude that it should be adequately protective" (Weston, 1986). It is therefore necessary to set quality targets to allow a quantification of the total allowable nitrogen flux for each specific region.

In this study, the OSPAR recommendations, where nutrient enhancement should not exceed natural background concentrations by 50% (OSPAR, 2008), were so far adopted to define an "impact" which were exceeded for all simulated scenarios including those where the determined environmental carrying capacity of 116 and 161 tons were modelled.

OSPAR (2008) stated that the 50% above background threshold is site specific and accounts for the natural variability. An ongoing discussion deals with the OSPAR recommendations of the 50% threshold to be reduced to 25% as an acceptable deviation from the reference concentrations as discussed for the Danish implementation (OSPAR, 2003). Similarly, it can be argued that with regards of the low background concentrations of Pegametan Bay, the area would be oversensitive to such a threshold. This leads to the question what threshold would be suited for tropical coral reef systems. From studies in other coral reef systems including the Caribbean, Indian Ocean, the Great Barrier Reef and Red Sea it has been concluded that nitrogen concentrations exceeding the range of $14 \mu\text{g DIN l}^{-1}$ which may lead to increased algal dominance (Lapointe, 1997). For the study area, such threshold would imply that DIN background levels may be exceeded by 230% for an observed background level $4.23 \pm 1.23 \mu\text{g DIN l}^{-1}$. The sum of domain averaged DIN concentrations for simulations using the environmental carrying capacities of 116 and 161 tons remained below a threshold of $14 \mu\text{g DIN l}^{-1}$ (maxima of 9.8 and $10.19 \mu\text{g DIN l}^{-1}$, respectively) for coral reef ecosystems as defined by Lapointe (1997) indicating that the 1% percent nitrogen flux may be too conservative. This extends the

discussion to a broader level where the definitions of "acceptable environmental change" are sought. The definition of acceptable change is subject to natural sciences but also social cultural and political factors (Hambrey and Senior, 2007; White and Beveridge, 2013).

On a natural science level, intensive monitoring and observation of biological responses can provide an improved understanding in the environmental resilience capacity for each site. Thus, thresholds should be defined based on a clear definition of the allowable impact and monitoring to verify the assimilative capacity of the environment.

11.4 Not only dissolved nitrogen

This study only addressed the behaviour and accommodation of dissolved nitrogenous wastes which are directly emitted from floating net cage farms. To my opinion a separation between: localized impacts and so called production capacities (Byron & Pierce, 2013) which determine the limit of one individual fish farm, mostly based on deposition of organic matter to the seabed and reaches as far as the footprint it leaves. Spacing between individual farms should therefore be determined based localized impacts. On the other hand the impact of dissolved substances, including dissolved nitrogen, which affect a wider area and should consider individual farms acting as individual components contributing to the overall impact.

12 Conclusions and recommendations

- ✓ The alternative arrangements of floating net cage farm sizes which are scaled according to physical, dispersion enhancing properties described by the spatial current velocity or Reynolds number distribution achieved a clear reduction of the affected area and concentration enhancement of nitrate. The use of Reynolds numbers as an indicator for the relative farm size provided an arrangement of floating net cage farms with a slightly better accommodation of dissolved nitrogenous wastes.
- ✓ While using Reynolds numbers as an indicator for the relative farm size, fewer larger farms have higher localized enhancement of ammonium but allow a better accommodation of nitrate as a conversion product of ammonium. By contrast, many smaller farms have only limited local impact in terms of ammonium enhancement, a slightly higher overall nitrate concentration, but a clearly more widespread impact of nitrate in terms of affected area with a tendency to accumulate in the poorly flushed sections of the domain.

The accommodation of dissolved nitrogen flux from floating net cage farms, its behaviour and the resulting concentrations therefore behave as a function of:

- The physical carrying capacity expressed as the perimeter available for floating net cage farms within a domain;
 - The number of farms distributed within the available perimeter which results in a generic spacing in between individual farms;
 - The relative farm size of each individual farm, which are scaled by the spatial distribution of Reynolds numbers;
 - The environmental carrying capacity in terms of the total production and corresponding dissolved nitrogen flux, distributed over the individual farms accordingly.
- ✓ Environmental carrying capacity, i.e. the total allowable standing stock from which dissolved nitrogen can be assimilated, can be determined considering water exchange and natural background concentrations where the allowable nitrogen flux from floating net cage fish farms constitutes a given percentage of the natural nitrogen flux.

-
- ✓ The definition of the spatial boundaries to determine the environmental carrying capacity is subject to various interpretations where consideration of the physical carrying capacity yields a conservative approach.
 - ✓ The assimilative capacity of an environment and the acceptable change is site specific and should be defined for each individual region of interest.

A recommendation on how to address dissolved nitrogenous wastes and the arrangement of individual farms would involve a chain of actions as illustrated in Figure 12.1. Three components were addressed in this study including the determination of the physical carrying capacity and determination of the relative farm sizes based on the Reynolds number. Assigning an initial environmental capacity would result in a given impact. Further study on impacts through monitoring will allow an adjustment of the environmental carrying capacity. As mentioned in the discussion, these actions do not stand alone and should be considered in conjunction with localized impacts of particulate organic wastes.

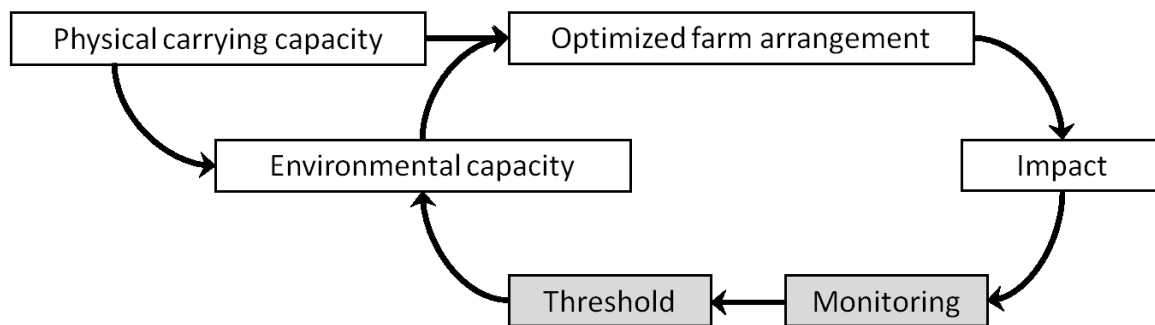


Figure 12.1: Assessment diagram to deal with efficiently accommodate dissolved nitrogenous wastes from floating net cage fish farms.

References

- Alongi, D. M., V. C. Chong, Dixon, P., Sasekumar, A. (2003). "The influence of fish cage aquaculture on pelagic carbon flow and water chemistry in tidally dominated mangrove estuaries of peninsular Malaysia." *Marine Environmental Research* 55(4): 313-333.
- Alongi, D. M., McKinnon, A. D., Brinkman, R., Trott, L. A., Undu, M. C., Muawanah, Rachmansyah (2009). "The fate of organic matter derived from small-scale fish cage aquaculture in coastal waters of Sulawesi and Sumatra, Indonesia." *Aquaculture* 295(1-2): 60-75.
- Angel, D. L., Krost, P., Silvert, W. (1995). "Benthic effects of fish cage farming in the Gulf of Aqaba, Red Sea." *International Workshop on Environmental Interactions of Mariculture*. ICES. Dartmouth, Nova Scotia, Canada, ICES.
- Aure, J. and Stigebrandt, A. (1990). "Quantitative estimates of the eutrophication effects of fish farming on fjords." *Aquaculture* 90(2): 135-156.
- Bakorsutanal (2008). "Bathymetric echo-soundings of the North Bali shoreline." *Badan Koordinasi Survey dan Pemetaan Nasional, National Geo-surveying and Mapping agency, Indonesia*.
- Bermudez, J. (2013). "Legal and policy components of the application of the ecosystem approach to aquaculture to site selection and carrying capacity." In L.G. Ross, T.C. Telfer, L. Falconer, D. Soto & J. Aguilar-Manjarrez, eds. *Site selection and carrying capacities for inland and coastal aquaculture*, pp. 117–127. FAO/Institute of Aquaculture, University of Stirling, Expert Workshop, 6–8 December 2010. Stirling, the United Kingdom of Great Britain and Northern Ireland. FAO Fisheries and Aquaculture Proceedings No. 21. Rome, FAO. 282 p.
- Beveridge, M. C. M. (2004). "Cage Aquaculture", Blackwell Publishing. 368 p.
- Boderie, P.M.A., Ouboter, M.R.L. (1997). "Operationalisering van het water- kwaliteitsmodel Schelde-estuarium", *Waterloopkundig laboratorium, Delft, The Netherlands*, 28 p.
- Booij, N. (1989). "User Manual for the program DUCHESS, Delft University computer program for 2D horizontal estuary and sea surges." *Department of Civil Engineering, Delft University of Technology, Delft, The Netherlands*.
- Byron, C.J. & Costa-Pierce, B.A. (2013). "Carrying capacity tools for use in the implementation of an ecosystems approach to aquaculture." In L.G. Ross, T.C. Telfer, L. Falconer, D. Soto & J. Aguilar-Manjarrez, eds. *Site selection and carrying capacities for inland and coastal*

-
- aquaculture, pp. 87–101. FAO/Institute of Aquaculture, University of Stirling, Expert Workshop, 6–8 December 2010. Stirling, the United Kingdom of Great Britain and Northern Ireland. FAO Fisheries and Aquaculture Proceedings No. 21. Rome, FAO. 282 p.
- Chow, V.T. (1959). "Open-channel hydraulics", New York, McGraw-Hill, 680 p.
- Deltares (2011a). "User manual Delft3D-FLOW, Simulation of multidimensional hydrodynamic and transport phenomena, including sediments." Deltares, Delft, the Netherlands, 688 pp.
- Deltares (2011b). "User manual Delft3D-WAVE, Simulation of short-crested waves with SWAN." Deltares, Delft, the Netherlands, 214 pp.
- Deltares (2011c). "User manual Delft3D-WAQ, Versatile water quality modelling in 1D, 2D or 3D systems including physical, (bio)chemical and biological processes." Deltares, Delft, the Netherlands, 320 pp.
- Directorate General of Aquaculture (2006). "Masterplan of Mariculture Area Development Program 2006." Jakarta, Indonesia, 137 pp.
- Dosdat, A., Servais, F., Métailler, R. Huelvan, C. Desbroyères, E. (1996). "Comparison of nitrogenous losses in five teleost fish species." *Aquaculture* 141(1-2): 107-127.
- Egbert, G. D. and Erofeeva, S. Y. (2002). "Efficient Inverse Modeling of Barotropic Ocean Tides." *Journal of Atmospheric and Oceanic Technology* 19(2).
- Food and Agriculture Organization of the United Nations (FAO). (1988). "Training manual on marine finfish netcage culture in Singapore.", Regional Seafarming Development and Demonstration Project. Project Reports, FAO.
- Food and Agriculture Organization of the United Nations (FAO). (1989). "Site Selection Criteria for Marine Finfish Netcage Culture in Asia, UNDP/FAO Regional Seafarming Development and Demonstration Project", Network of Aquaculture Centers in Asia. FAO Doc. NACA-SF/WP/89/13.
- Food and Agriculture Organization of the United Nations (FAO). (2014). FIGIS. FishStat (Database). (Latest update: 31 Jan 2014) Accessed (15 Feb 2014). URI: <http://data.fao.org/ref/babf3346-ff2d-4e6c-9a40-ef6a50fcd422.html?version=1.0>
- GESAMP (2001). "Planning and management for sustainable coastal aquaculture development. ", GESAMP Reports and Studies No. 68, FAO: 90 pp.
- Gillibrand, P. A. and W. R. Turrell (1997). "The use of simple models in the regulation of the impact of fish farms on water quality in Scottish sea lochs." *Aquaculture* 159(1-2): 33-46.

-
- Gowen, R. J. and N. B. Bradbury (1987). "The ecological impact of salmon farming in coastal waters: A review." *Oceanogr. Mar. Biol. Ann. Rev.* 25: 563-575.
- Gowen, R.J., Bradbury, N.B., Brown, J.R. (1989). "The use of simple models in assessing two of the interactions between fish farming and the marine environment." *Aquaculture - A Biotechnology in Progress*. N. DePau, Jaspers, E., Ackefors, H. & Wilkins, N. European Aquaculture Society. Bredene, Belgium.
- Grasshoff, K., Kremling, K., Ehrhardt, M. (2009). "Methods of Seawater Analysis." Wiley.
- Halide, H., Stigebrandt, A., Rehbein, M., McKinnon, A. D. (2009). "Developing a decision support system for sustainable cage aquaculture." *Environmental Modelling & Software* 24(6): 694-702.
- Hall, P.O.J., Anderson, L.G., Holby, O., Kollberg, S., Samuelsson, M. O. (1990). "Chemical fluxes and mass balances in a marine fish cage farm. I. Carbon." *Marine Ecology Progress Series* 61: 61-73.
- Hall, P.O.J., Holby, O., Kollberg, S., Samuelsson, M. O. (1992). "Chemical fluxes and mass balances in a marine fish cage farm. IV. Nitrogen." *Marine Ecology Progress Series* 89: 81-91.
- Hambrey, J. & Senior, B. (2007) "Taking forward environmental carrying capacity and ecosystem services. Recommendations for CCW." CCW Policy Research Report No. 07/22.
- Hanafi, A. (2008). "Personal communication", Gondol Research Institute for Mariculture, Bali, Indonesia.
- Handy, R. D. and M. G. Poxton (1993). "Nitrogen pollution in mariculture: toxicity and excretion of nitrogenous compounds by marine fish." *Rev. Fish Biol. Fish.* 3: 205–241.
- Hargrave, B. T. (2002). "A traffic light decision system for marine finfish aquaculture siting." *Ocean & Coastal Management* 45(4-5): 215-235.
- HELCOM. (2004). "HELCOM RECOMMENDATION 25/4, measures aimed at the reduction of discharges from freshwater and marine fish farming.", Helsinki Commission. www.helcom.fi/Recommendations/en_GB/rec25_4/.
- Hevia, M., Rosenthal, H., Gowen, R.J. (1996). "Modelling benthic deposition under fish cages." *J. Appl. Ichthyol.* 12(1996): 71-74.
- Holby, O. and P. O. J. Hall (1991). "Chemical fluxes and mass balances in a marine fish cage farm. II. Phosphorus." *Marine Ecology Progress Series* 70: 263-272.

-
- Howarth, R. W., Marino, R. (2006). "Nitrogen as the limiting nutrient for eutrophication in coastal marine ecosystems: Evolving views over three decades." *Limnology and Oceanography* 51(2006): 364-376
- IOC, IHO and BODC (2003), "Centenary Edition of the GEBCO Digital Atlas", published on CD-ROM on behalf of the Intergovernmental Oceanographic Commission and the International Hydrographic Organization as part of the General Bathymetric Chart of the Oceans; British Oceanographic Data Centre, Liverpool.
- Kalnay, E. (1996). "The NCEP/NCAR 40-year reanalysis project." *Bull. Amer. Meteor. Soc.*, 77, 437-470. NCEP Reanalysis data provided by the NOAA/OAR/ESRL PSD at www.esrl.noaa.gov/psd/.
- Karakassis, I., Pitta, P., Krom, M. D. (2005). "Contribution of fish farming to the nutrient loading of the Mediterranean." *Scientia Marina* 69: 313–321.
- Lapointe, B. E. (1997). "Nutrient thresholds for bottom-up control of macroalgal blooms on coral reefs in Jamaica and southeast Florida." *Limnology and Oceanography*, 42(5): 1119-1131.
- Leung, K. M. Y., Chu, J. C. W., Wu, R. S. S. (1999). "Nitrogen budgets for the areolated grouper *Epinephelus areolatus* cultured under laboratory conditions and in open sea cages." *Marine Ecology Progress Series* 186: 271-281 pp.
- Mayerle, R., Windupranata, W. & Hesse, K.J. (2009). "A Decision Support System for a Sustainable Environmental Management of Marine Fish Farming." Yang, Y., Wu, X.Z. & Zhou, Y.Q. (eds.) (2009): *Cage Aquaculture in Asia: Proceedings of the Second International Symposium on Cage Aquaculture in Asia, 3-8 July 2006, Hangzhou, China (Vol. 2)*: pp 370-383. Asian Fisheries Society, Manila, Philippines, and Zhejiang University, Hangzhou, China.
- Mayerle, R., Hanafi, A., Hesse, K.-J., van der Wulp, S. A., Niederndorfer, K., Runte, K.-H., Ladwig, N., Giri, a., Kleinfeld, F., Sugama, K. (2011). "Integriertes System für das Management einer ökologisch und sozioökonomisch nachhaltigen Marikultur in Indonesien." Bundesministerium für Bildung und Forschung, Project FKZ03F0469A Subproject 1, Final report: 83 pp (partly in German).
- OSPAR (2003). "OSPAR Integrated Report 2003 on the Eutrophication Status of the OSPAR Maritime Area Based Upon the First Application of the Comprehensive Procedure.", *Eutrophication Series*, OSPAR Commission: 59 pp.
- OSPAR (2008). "Second OSPAR Integrated Report on the Eutrophication Status of the OSPAR Maritime Area. ", *Eutrophication Series*, OSPAR Commission: 107 pp.

-
- OSPAR (2009). "Assessment of Impacts of Mariculture", Biodiversity Series, OSPAR Commission: 64 pp.
- Pérez Martinez, O., Telfer, T. C., Ross, L. G. (2002). "GIS-based models for optimisation fo marine cage aquaculture in Tenerife, Canary Islands. ", Institute of Aquaculture. Stirling, University of Stirling, Scotland. PhD: 336.
- Petihakis, G., Tsiaras, K., Triantafyllou, G., Korres, G., Tsagaraki, T. M., Tsapakis, M., Vavillis, P., Pollani, A., Frangoulis, C. (2012). "Application of a complex ecosystem model to evaluate effects of finfish culture in Pagasitikos Gulf, Greece." *Journal of Marine Systems* 94, Supplement(0): S65-S77.
- Pitta, P., Karakassis, I., Tsapakis, M., Zivanovic, S. (1998). "Natural vs. mariculture induced variability in nutrients and plankton in the eastern Mediterranean." *Hydrobiologia* 391(1): 179-192.
- Sara, G. (2007). "A meta-analysis on the ecological effects of aquaculture on the water column: Dissolved nutrients." *Marine Environmental Research* 63(4): 390-408.
- Schlumberger water services (2010). "Cera-diver Product Manual" Schlumberger Water Services, Delft, the Netherlands 34pp, www.swstechnology.com.
- Silvert, W. (1994). "A decision support system for regulating finfish aquaculture." *Ecological Modelling* 75/76: 609-615.
- Skogen, M. D., Eknes, M., Asplin, L. C., Sandvik, A. D. (2009). "Modelling the environmental effects of fish farming in a Norwegian fjord." *Aquaculture* 298(1-2): 70-75.
- Soto, D., Aguilar-Manjarrez, J., Brugère, C., Angel, D., Bailey, C., Black, K., Edwards, P., Costa-Pierce, B., Chopin, T., Deudero, S., Freeman, S., Hambrey, J., Hishamunda, N., Knowler, D., Silvert, W., Marba, N., Mathe, S., Norambuena, R., Simard, F., Tett, P., Troell, M. & Wainberg, A. (2008) "Applying an ecosystembased approach to aquaculture: principles, scales and some management measures. " In Soto, D., Aguilar-Manjarrez, J. & Hishamunda, N., eds. *Building an ecosystem approach to aquaculture*. FAO/Universitat de les Illes Balears Expert Workshop. 7–11 May 2007, Palma de Mallorca, Spain. FAO Fisheries and Aquaculture Proceedings. No. 14. Rome, FAO. pp. 15–35.
- Sparre, P. and Venema, S. (1998). "Introduction to tropical fish stock assessment - Part 1: Manual FAO Fisheries Technical Papers" Rome, FAO. T306/1Rev.2: 407.
- Stigebrandt, A. (1999). "Turnover of Energy and matter by fish - a General Model with application to Salmon." *Fisken Og Havet*. Bergen, Havforskningsinstituttet. 5: 26.

-
- Stigebrandt, A., J. Aure, Ervik, A., Hansen, P. K. (2004). "Regulating the local environmental impact of intensive marine fish farming: III. A model for estimation of the holding capacity in the Modelling-Ongrowing fish farm-Monitoring system." *Aquaculture* 234(1-4): 239-261.
- Sulawestian, H.P. (2008) "Study of nutrient distribution in Pegametan Bay, Bali, Indonesia.", Master's thesis, Kiel University, 66 pages.
- Sumagaysay-Chavoso, N. S. (2003). "Nitrogen and phosphorus digestibility and excretion of different-sized groups of milkfish (*Chanos chanos* Forsskal) fed formulated and natural food-based diets." *Aquaculture Research* 34(5): 407-418.
- US Army Corps of Engineers (1984). "Shore Protection Manual. ", Volume I and II. US Government Printing Office, Washington DC.
- Weston, D. P. (1986). "Recommended Interim guidelines for management of Salmon net-pen culture in Pudget Sound.", Washington department of Ecology.
- White, P., Phillips, M.J. & Beveridge, M.C.M. (2013). "Environmental impact, site selection and carrying capacity estimation for small-scale aquaculture in Asia." In L.G. Ross, T.C. Telfer, L. Falconer, D. Soto & J. Aguilar-Manjarrez, eds. *Site selection and carrying capacities for inland and coastal aquaculture*, pp. 231–251. FAO/Institute of Aquaculture, University of Stirling, Expert Workshop, 6–8 December 2010. Stirling, the United Kingdom of Great Britain and Northern Ireland. FAO Fisheries and Aquaculture Proceedings No. 21. Rome, FAO. 282 pp.
- Windupranata, W. and R. Mayerle (2009). "A Decision Support System for Selection of Suitable Mariculture Site in the Western Part of Java Sea, Indonesia." *ITB Journal of Engineering Science* 41(1): 77-96.
- Wu, R. S. S. (1995). "The environmental impact of marine fish culture: Towards a sustainable future." *Marine Pollution Bulletin* 31(4-12): 159-166.
- Wu, R. S. S., Lam, K. S., MacKay, D. W., Lau, T. C., Yam, V. (1994). "Impact of marine fish farming on water quality and bottom sediment: A case study in the sub-tropical environment." *Marine Environmental Research* 38(2): 115-145.
- Wu, R. S. S., Shin, P. K. S., MacKay, D. W., Mollowney, M., Johnson, D. (1999). "Management of marine fish farming in the sub-tropical environment: a modelling approach." *Aquaculture* 174(3-4): 279-298.

-
- Wulp, van der, S. A., K. R. Niederndorfer, Hesse, K-J., Runte, K-H., Mayerle, R., Hanafi, A. (2010). "Sustainable Environmental Management for Tropical Floating Net Cage Mariculture, a Modelling Approach." XVIIth World Congress of the International Commission of Agricultural and Biosystems Engineering (CIGR). Québec City, Canada, Canadian Society for Bioengineering (CSBE/SCGAB).
- Yokoyama, H., Inoue, M., Abo, K. (2004). "Estimation of the assimilative capacity of fish-farm environments based on the current velocity measured by plaster balls." *Aquaculture* 240(1): 233-247.

Appendices

Appendix A: Existing farms and number of cages

<i>Farm number</i>	<i>Total number of cages</i>	<i>Stocked cages</i>
1	750	350
2	140	40
3	136	132
4	97	67
5	70	2
6	55	55
7	54	35
8	40	4
9	33	4
10	28	21
11	20	0
12	11	0
13	9	9
14	8	1
15	8	0
16	8	0
17	7	7
18	4	2
Σ	1478	729

Appendix B: Flow model settings

<i>Parameter</i>	<i>Settings</i>
<i>Bottom roughness</i>	$0.03 \text{ m}^{\frac{1}{2}} \text{ s}^{-1}$
<i>Water density</i>	1018 kg m^{-3}
<i>Water temperature</i>	30°C
<i>Salinity</i>	30 ‰
<i>Horizontal eddy viscosity</i>	$1 \text{ m}^2 \text{ s}^{-1}$
<i>Wind</i>	<i>NCEP wind data</i>
<i>Computational time step</i>	3 s
<i>Coupling interval</i>	15 min

Appendix C: Wave model settings

<i>Parameter</i>	<i>Settings</i>
<i>Fetch Length</i>	<i>100 km</i>
<i>Wind speed</i>	<i>11.88m s⁻¹</i>
<i>Wind direction</i>	<i>35°</i>
<i>Duration</i>	<i>6 hrs</i>
<i>Significant wave height (H_s)</i>	<i>1.9 m</i>
<i>Wave period (T_p)</i>	<i>6.25 s</i>

Appendix D: Water quality model settings

Parameter	Setting
<i>Computational time step</i>	15 s
<i>Coupling interval</i>	15 min
<i>Water temperature</i>	30°C
<i>Constant oxygen concentration</i>	7 mg l ⁻¹
<i>Background diffusion</i>	1×10 ⁻⁷ m ² s ⁻¹
<i>Horizontal diffusion coefficient</i>	
<i>a</i>	1
<i>b</i>	0.6
<i>c</i>	1.4
<i>Vertical diffusion coefficient</i>	1×10 ⁻⁷ m ² s ⁻¹
<i>Michaelis –Menten nitrification rate at 20°C</i>	0.1 g N m ⁻³ d ⁻¹
<i>Temperature coefficient for nitrification</i>	1.07
<i>Half saturation constant for dissolved oxygen limitation</i>	1.0 g m ⁻³
<i>Half saturation constant for ammonium limitation</i>	0.5 gNm ⁻³
<i>Average fish weight (170 g) stocking density</i>	3 kg m ⁻³
<i>Average fish weight (170 g) ammonium discharge</i>	2.91 g N m ⁻³ d ⁻¹
<i>Maximum fish weight (500 g) stocking density</i>	7 kg m ⁻³
<i>Maximum fish weight (500 g) ammonium discharge</i>	4.05 g N m ⁻³ d ⁻¹

Appendix E1: High density farm arrangement (300m) with equal farm sizes

Farms	Fraction	Fraction %	Standing stock (tons)	# Cages
1	1/36	2.8%	12.46	66
2	1/36	2.8%	12.46	66
3	1/36	2.8%	12.46	66
4	1/36	2.8%	12.46	66
5	1/36	2.8%	12.46	66
6	1/36	2.8%	12.46	66
7	1/36	2.8%	12.46	66
8	1/36	2.8%	12.46	66
9	1/36	2.8%	12.46	66
10	1/36	2.8%	12.46	66
11	1/36	2.8%	12.46	66
12	1/36	2.8%	12.46	66
13	1/36	2.8%	12.46	66
14	1/36	2.8%	12.46	66
15	1/36	2.8%	12.46	66
16	1/36	2.8%	12.46	66
17	1/36	2.8%	12.46	66
18	1/36	2.8%	12.46	66
19	1/36	2.8%	12.46	66
20	1/36	2.8%	12.46	66
21	1/36	2.8%	12.46	66
22	1/36	2.8%	12.46	66
23	1/36	2.8%	12.46	66
24	1/36	2.8%	12.46	66
25	1/36	2.8%	12.46	66
26	1/36	2.8%	12.46	66
27	1/36	2.8%	12.46	66
28	1/36	2.8%	12.46	66
29	1/36	2.8%	12.46	66
30	1/36	2.8%	12.46	66
31	1/36	2.8%	12.46	66
32	1/36	2.8%	12.46	66
33	1/36	2.8%	12.46	66
34	1/36	2.8%	12.46	66
35	1/36	2.8%	12.46	66
36	1/36	2.8%	12.46	66
Σ	1	100.0%	448.70	2376

Appendix E2: High density farm arrangement (300m) with farm sizes normalized according to current velocity (\bar{u})

Farms	\bar{u} ($m s^{-1}$)	Normalized fraction $\bar{u}_{\%} = \frac{\bar{u}_i}{\sum_{i=1}^n \bar{u}_i}$	Standing stock (tons)	# Cages
1	0.39	11.9%	53.55	283
2	0.33	9.9%	44.50	235
3	0.29	8.9%	39.80	211
4	0.26	7.8%	34.94	185
5	0.22	6.6%	29.66	157
6	0.19	5.8%	26.01	138
7	0.17	5.3%	23.74	126
8	0.14	4.1%	18.51	98
9	0.10	3.0%	13.63	72
10	0.08	2.5%	11.35	60
11	0.07	2.2%	9.97	53
12	0.07	2.2%	9.72	51
13	0.07	2.0%	9.15	48
14	0.07	2.0%	9.06	48
15	0.07	2.0%	8.90	47
16	0.06	1.9%	8.42	45
17	0.06	1.8%	8.09	43
18	0.06	1.8%	7.95	42
19	0.05	1.5%	6.92	37
20	0.05	1.5%	6.72	36
21	0.05	1.4%	6.50	34
22	0.05	1.4%	6.41	34
23	0.04	1.3%	6.04	32
24	0.04	1.3%	6.02	32
25	0.04	1.3%	5.76	30
26	0.03	1.0%	4.30	23
27	0.03	0.9%	4.25	22
28	0.03	0.9%	4.11	22
29	0.03	0.9%	3.92	21
30	0.03	0.8%	3.59	19
31	0.02	0.8%	3.40	18
32	0.02	0.8%	3.37	18
33	0.02	0.7%	3.10	16
34	0.02	0.6%	2.82	15
35	0.02	0.6%	2.71	14
36	0.01	0.4%	1.85	11
Σ	3.29	100.0%	448.70	2376

Appendix E3: High density farm arrangement (300m) with farm sizes normalized according to the Reynolds number

Farms	Re (-)	Normalized fraction $Re_{\%} = \frac{Re}{\sum_{i=1}^n Re_i}$	Standing stock (tons)	# Cages
1	3.848E+06	10.8%	48.68	258
2	2.382E+06	6.7%	30.14	159
3	2.805E+06	7.9%	35.49	188
4	4.039E+06	11.4%	51.10	270
5	1.686E+06	4.8%	21.34	113
6	3.149E+06	8.9%	39.85	211
7	2.259E+06	6.4%	28.59	151
8	1.426E+06	4.0%	18.04	95
9	1.805E+06	5.1%	22.83	121
10	6.000E+05	1.7%	7.59	40
11	5.311E+05	1.5%	6.72	36
12	1.145E+06	3.2%	14.49	77
13	6.521E+05	1.8%	8.25	44
14	4.838E+05	1.4%	6.12	32
15	1.457E+06	4.1%	18.43	98
16	6.128E+05	1.7%	7.75	41
17	4.804E+05	1.4%	6.08	32
18	4.251E+05	1.2%	5.38	28
19	3.840E+05	1.1%	4.86	26
20	5.588E+05	1.6%	7.07	37
21	3.419E+05	1.0%	4.33	23
22	3.702E+05	1.0%	4.68	25
23	3.236E+05	0.9%	4.09	22
24	4.785E+05	1.3%	6.05	32
25	3.105E+05	0.9%	3.93	21
26	2.234E+05	0.6%	2.83	15
27	3.595E+05	1.0%	4.55	24
28	2.214E+05	0.6%	2.80	15
29	3.778E+05	1.1%	4.78	25
30	1.997E+05	0.6%	2.53	13
31	1.799E+05	0.5%	2.28	12
32	2.700E+05	0.8%	3.42	18
33	1.701E+05	0.5%	2.15	11
34	1.676E+05	0.5%	2.12	11
35	4.583E+05	1.3%	5.80	31
36	2.829E+05	0.8%	3.58	19
Σ	35463351.12	100.0%	448.70	2374.00

Appendix E4: Low density farm arrangement (900m) with equal farm sizes

Farms	Fraction	Fraction %	Standing stock (tons)	# Cages
1	1/8	12.5%	56.09	66
2	1/8	12.5%	56.09	66
3	1/8	12.5%	56.09	66
4	1/8	12.5%	56.09	66
5	1/8	12.5%	56.09	66
6	1/8	12.5%	56.09	66
7	1/8	12.5%	56.09	66
8	1/8	12.5%	56.09	66
Σ	1	100.0%	448.70	2374

Appendix E-5: Low density farm arrangement (900m) with farm sizes normalized according to current velocity (\bar{u})

Farms	\bar{u} ($m\ s^{-1}$)	Normalized fraction $\bar{u}_{\%} = \frac{\bar{u}_i}{\sum_{i=1}^n \bar{u}_i}$	Standing stock (tons)	# Cages
1	0.39	30.3%	136.16	720
2	0.33	25.2%	113.14	599
3	0.29	22.5%	101.18	535
4	0.08	5.9%	26.37	140
5	0.07	5.6%	25.35	134
6	0.06	4.3%	19.15	101
7	0.05	3.9%	17.59	93
8	0.03	2.2%	9.77	52
Σ	1.29	100%	448.70	2374

Appendix E-6: Low density farm arrangement (900m) with farm sizes normalized according to the Reynolds number.

Farms	Re (-)	Normalized fraction $Re_{\%} = \frac{Re}{\sum_{i=1}^n Re_i}$	Standing stock (tons)	# Cages
1	3.848E+06	34.3%	153.74	813
2	2.382E+06	21.2%	95.18	504
3	2.805E+06	25.0%	112.07	593
4	6.725E+05	6.0%	26.87	142
5	5.311E+05	4.7%	21.22	112
6	3.952E+05	3.5%	15.79	84
7	3.840E+05	3.4%	15.34	81
8	2.124E+05	1.9%	8.49	45
Σ	1.123E+07	100.0%	448.70	2374

Appendix F: Impact of the various scenarios

		<i>mean</i> $\mu\text{g TAN l}^{-1}$	<i>mean</i> $\mu\text{g NO}_3\text{-N l}^{-1}$	<i>Affected</i> <i>area (ha)</i>	<i>max.</i> $\mu\text{g TAN l}^{-1}$	<i>max.</i> $\mu\text{g NO}_3\text{-N l}^{-1}$
<i>Equal farm sizes</i>	300 m*	7.5 ± 1.6	10.4 ± 2.6	684.0	20.7	23
	900 m**	7.4 ± 1.9	10.1 ± 2.4	664.5	41.3	26.5
<i>Scaling by velocity</i>	300 m*	6.0 ± 1.9	7.2 ± 2.1	575.3	18.0	12.4
	900 m**	6.5 ± 2.7	6.4 ± 2.2	382.3	27.6	9.7
<i>Scaling by Reynolds</i>	300 m*	5.5 ± 1.7	6.7 ± 1.9	608.2	16.4	11.4
	900 m**	6.5 ± 2.7	6.1 ± 2.1	355.9	27.3	9.4

* High farm density

** Low farm density

AppendixG-1: High density farm arrangement (300m) with farm sizes normalized according to the Reynolds number

Farms	Re (-)	Normalized fraction $Re_{\%} = \frac{Re}{\sum_{i=1}^n Re_i}$	Standing stock (tons)	# Cages
1	2.805E+06	53.3%	15.89	84
2	1.805E+06	34.3%	10.22	54
3	6.521E+05	12.4%	3.69	20
4	4.838E+05	32.4%	4.05	21
5	4.785E+05	32.0%	4.01	21
6	5.311E+05	35.6%	4.45	24
7	2.382E+06	12.0%	8.89	47
8	3.236E+05	1.6%	1.21	6
9	2.259E+06	11.4%	8.43	45
10	6.000E+05	3.0%	2.24	12
11	1.145E+06	5.8%	4.27	23
12	1.686E+06	8.5%	6.29	33
13	3.149E+06	15.9%	11.75	62
14	3.848E+06	19.4%	14.36	76
15	4.251E+05	2.1%	1.59	8
16	4.039E+06	20.3%	15.07	80
Σ			116.4	616

Appendix G-2: High density farm arrangement (900m) with farm sizes normalized according to the Reynolds number

Farms	Re (-)	Normalized fraction $Re_{\%} = \frac{Re}{\sum_{i=1}^n Re_i}$	Standing stock (tons)	# Cages
1	2804606	100%	29.8	158
2	531068	100%	12.5	66
3	2382050	38.2%	28.3	150
4	3847509	61.8%	45.8	242
Σ			116.4	616

Erklärung

Hiermit erkläre ich, dass die Abhandlung, abgesehen von der Beratung durch meine akademischen Lehrer, nach Inhalt und Form meine eigene Arbeit ist. Diese Arbeit hat an keiner anderen Stelle im Rahmen eines Prüfungsverfahrens vorgelegen. Außerdem erkläre ich, dass diese mein erster Promotionsversuch ist.

Kiel, den 26.November 2013

Simon Adriaan van der Wulp